2-26-2013

Role of the Cytoplasmic Polyadenylation Element Binding Proteins in Neuron: A Dissertation

Aparna Oruganty
University of Massachusetts Medical School

ROLE OF THE CYTOPLASMIC POLYADENYLATION ELEMENT BINDING PROTEINS IN NEURON

A Dissertation Presented

By

APARNA ORUGANTY

Submitted to the faculty of the

University of Massachusetts Graduate School of Biomedical Sciences, Worcester

in partial fulfillment of the requirements for the degree of

DOCTOR OF PHILOSOPHY

26 February, 2013

INTERDISCIPLINARY GRADUATE PROGRAM

ROLE OF THE CYTOPLASMIC POLYADENYLATION ELEMENT BINDING PROTEINS IN NEURON

A Dissertation Presented By

Aparna Oruganty

The signatures of the Dissertation Defense Committee signifies completion and approval as to style and content of the Dissertation

Joel Richter, Ph.D., Thesis Advisor

Silvia Corvera, M.D., Member of Committee

Jason Kim, Ph.D., Member of Committee

Eric Klann, Ph.D., Member of Committee

Zuoshang Xu, Ph.D., Member of Committee

The signature of the Chair of the Committee signifies that the written dissertation meets the requirements of the Dissertation Committee

Leslie Shaw, Ph.D., Chair of Committee

The signature of the Dean of the Graduate School of Biomedical Sciences signifies that the student has met all graduation requirements of the School

Anthony Carruthers, Ph.D.
Dean of the Graduate School of Biomedical Sciences

Interdisciplinary Graduate Program
February 26, 2013

I WISH TO DEDICATE THIS THESIS TO MY MOM AND MY HUSBAND, MY PILLARS OF SUPPORT

ACKNOWLEDGEMENTS

I would like to express deep gratitude to my mentor and advisor, Joel Richter. He has been very encouraging, supportive and has taught me to do good science. He showed confidence in me even in situations when I had lost confidence in myself. He is an outstanding scientist and has taught me to be critical and always look at the bigger picture to try and understand the significance of any work in the larger perspective of biology. He gave me a lot of freedom to create my own scientific path, both in the lab work as well as regarding my career. His hard work, dedication and passion for science and willingness to explore and master new scientific fields will always be an inspiration for me. Thank you, Joel.

I have been very fortunate to have great scientists in my committee- Dr. Leslie Shaw (Chair of committee), Dr. Silvia Corvera, Dr. Jason Kim and Dr. Zuoshang Xu. I would like to thank them for their invaluable time, incredible suggestions and helpful comments which have been so valuable during my entire graduate training. I am extremely grateful to Dr. Eric Klann for agreeing to be my external examiner. I am especially thankful to him for taking time from his short trip to back to USA to attend my defense.

I am thankful to all my past and present labmates for giving me great scientific suggestions and for making my stay here so wonderful and full of fond memories- Jihae Shin, Maria Ivshina, Natalie Farny, Lori Lorenz, Ki-young Paek,

Tsuyoshi Udagawa, Rachel Groppo, Morris Nehama, Ilya Alexandrov, Ming chung Kan, Chien ling Lin, Andrea Dambrogio, Meghna Jani, Kentaro Nagaoka, Quiping Cao, David Burns, Amalene Cooper-Morgan. I would specially like to thank Rachel Groppo, Tsuyoshi Udagawa and Ming Chun Kan for teaching me various techniques and for being my initial mentors. I would like to thank Steve Doxsey lab for the fun times in the break room.

My experience in graduate school has been made so special by the friends I made here. Special thanks to Dipti for her help, support and all the fun times. A big thanks to my batchmates Sandhya, Sneha, Seemin and Samyabrata for always being there and sharing the ups and downs of graduate school together. Special thanks to my group of postdoc friends- Sunil, Sreenath, Anuradha, Parul, Ashish, Shreekant and Priti, for the numerous birthday celebrations, dancing and loads of fun. I will really miss the crazy parties with Sneha, Mayuri, Ankita, Vahbiz, Swapnil, Karthik and Arvind in Worcester downtown. Many thanks to Nidhi, Tina and Aagya for their friendship.

I would be nowhere today without the love and support of my family. Our skype and hangout sessions kept me in good spirits. I am really grateful to my husband Gautam, who has always loved and supported me through thick and thin.

ABSTRACT

Genome regulation is an extremely complex phenomenon. There are various mechanisms in place to ensure smooth performance of the organism. Post-transcriptional regulation of gene expression is one such mechanism. Many proteins bind to mRNAs and regulate their translation. In this thesis, I have focused on the Cytoplasmic Polyadenylation Element Binding family of proteins (CPEB1-4); a group of sequence specific RNA binding proteins important for cell cycle progression, senescence, neuronal function and plasticity. CPEB protein binds mRNAs containing a short Cytoplasmic Polyadenylation Element (CPE) in 3' untranslated Region (UTR) and regulates the polyadenylation of these mRNAs and thereby controls translation. In Chapter II, I have presented my work on the regulation of mitochondrial function by CPEB. CPEB knockout mice have brain specific defects in mitochondrial function owing to a reduction in Electron transport chain complex I component protein NDUFV2. CPEB controls the translation of this NDUFV2 mRNA and thus affects mitochondrial function. A consequence of this reduced bioenergetics is reduced growth and branching of neurons, again emphasizing the importance of this pathway. Chapter III focuses on the role of CPEB4 in neuronal survival and protection against apoptosis. CPEB4 shuttles between nucleus and cytoplasm and becomes nuclear in response to stimulation with ionotropic glutamate receptors, focal ischemia *in*

vivo and when cultured neurons are deprived of oxygen and glucose; nuclear CPEB4 affords protection against apoptosis in ischemia model. The underlying cause for nuclear translocation is reduction in Endoplasmic Reticulum calcium levels. These studies give an insight into the function and dynamics of these two RNA binding proteins and provide a better understanding of cellular biology.

TABLE OF CONTENTS

LIST OF FIGURES AND TABLES

CHAPTER I

CHAPTER II

CHAPTER III

LIST OF ABBREVIATIONS

Akt	Protein Kinase B
AMPA	2-amino-3-(3-hydroxy-5-methyl-isoxazol-4-yl)propanoic acid
ATP	Adenosine triphosphate
CamKII	Calcium/calmodulin dependent Protein Kinase II
CI	Complex I
CPE	Cytoplasmic Polyadenylation Element
CPEB	Cytoplasmic Polyadenylation Element Binding Portein
CPSF	Cleavage and polyadenylation specificity factor
CstF	Cleavage stimulation factor
EEG-1	embryonic epithelia gene 1
eIF	Eukaryotic initiation factor
eRF	Eukaryotic release factor
Fis1	Fission 1
Gld-2	germline deficient-2
GluR	Glutamate receptor

KO	Knockout
MAPK	Mitogen-activated protein kinase
miRNA	micro Ribonucleic acid
mTOR	mammalian target of rapamycin
NDUFV2	NADH dehydrogenase (ubiquinone) flavoprotein 2
Ngd	Neuroguidin
NMDA	N-methyl D-aspartate
OPA1	optic atrophy 1
PABP	Poly(A)-binding protein
PAP	Poly(A) polymerase
PARN	Poly(A) specific ribonuclease
PGC1α	Peroxisome proliferator-activated receptor gamma coactivator-1-alpha
PI3	Phosphatidyl inositide 3
ROS	Reactive oxygen species
SCP	synaptonemal complex protein
ZO-1	zona occludens protein 1

PREFACE

Parts of this Dissertation appear in:

Translational control of mitochondrial energy production mediates neuron morphogenesis. Oruganty-Das A, Ng T, Udagawa T, Goh EL, Richter JD. Cell Metab. 2012 Dec 5;16(6):789-800.

CPEB4 is a cell survival protein retained in the nucleus upon ischemia or endoplasmic reticulum calcium depletion. Kan MC*, Oruganty-Das A*, Cooper-Morgan A, Jin G, Swanger SA, Bassell GJ, Florman H, van Leyen K, Richter JD. Mol Cell Biol. 2010 Dec; 30(24):5658-71. * equal contributors

CHAPTER I

INTRODUCTION

Translation

DNA is the blueprint of almost all life forms. Its information is interpreted through its conversion into RNA molecules. Of special importance is a molecule in the RNA category –mRNA. DNA is transcribed into mRNA and the mRNA is co-transcriptionally modified by addition of a 7-methylguanosine cap at the 5' end, a poly (A) tail at the 3' end, removal of introns by splicing and deposition of RNA binding proteins on some mRNAs leading to formation of large mRNP complexes. This decorated mRNA is then exported from the nucleus and is ready to be translated into protein, which are the workhorses of the cell as they perform most of the functions in living systems. The process of mRNA translation occurs in the distinct steps of initiation, elongation and termination. Initiation occurs when the pre-initiation complex (containing ribosomal small 40S subunit, Met-tRNA, initiation factors such as eIF4E, eIF4G, eIF4A) binds to the cap structure on 5' end of mRNA and scans the mRNA to locate the AUG start codon. The large 60S ribosomal subunit then joins and elongation ensues (Sonenberg and Hinnebusch, 2009). The Ribosome has three sites important for peptide bond

formation- A (aminoacyl), P (peptidyl) and E (exit) sites. The process of elongation is much simpler. tRNAs charged with amino acids (also called aminoacyl-tRNAs) are delivered to the ribosomal A site by the elongation factor eEF1A. Only if the anticodon on the tRNA corresponds to the codon on the mRNA it is retained on the A site, the rest of the incorrect tRNAs are expelled from the ribosome. A peptide bond is then formed between the amino acid on the A site and the amino acid on the P site of the ribosome. The elongation factor eEF2 promotes translocation of the ribosome along mRNA and each codon is thus read and translated into amino acid by the ribosome. Termination of translation is mediated by the release factor eRF1, which recognizes one of the three stop codons (UAG, UAA, UGA) and binds to ribosome leading to GTP hydrolysis by eRF3 and release of the nascent polypeptide from the ribosome. This poises the ribosome for recycling to prepare it for another round of translation. The ribosome is a large ~3.3 megadalton ribonucleoprotein complex with a sedimentation coefficient of 80S and as detailed before is the site of all protein synthesis in the cell (Schmeing and Ramakrishnan, 2009).

Initiation of translation is the first step and is therefore also the rate-limiting step. Initiation requires at least nine initiation factors comprised of more than 30 polypeptide chains, thus introducing many opportunities for regulation (reviewed in (Groppo and Richter, 2009). Various mechanisms of initiation control have been described over the years. Some of them control general translation of all mRNAs (as happens in stress or starvation conditions) whereas others are more

sequence specific such as micro RNAs or RNA binding proteins. The most well characterized translation control factor is eIF4E-binding protein (4E-BP) family of proteins named after its founder member eIF4E-BP. These proteins bind eIF4E and prevent its binding to eIF4G, thereby shutting down cap-dependent translation. Phosphorylation of 4E-BPs disrupts their interactions with eIF4G and thus relieves the inhibition. PI3 kinase/Akt/mTOR and Ras/MAPK signaling pathways regulate the phophorylation of 4E-BP and affect translation thus controlling cell growth, metabolism, proliferation, development, learning and memory (Sonenberg and Hinnebusch, 2007) . Several other proteins such as maskin, neuroguidin and cup also act similar to 4E-BP but bind to mRNA in a sequence specific manner. The translation initiation factor eIF2 is also under intense control especially during stress and starvation. eIF2B is the guanine nucleotide exchange factor which converts its substrate, inactive eIF2-GDP, into active eIF2-GTP, which can then bind the methionine charged initiator tRNA and participate in translation initiation. Under conditions of stress or starvation, the α subunit of eIF2 is phosphorylated thereby preventing eIF2B from binding and recycling this important initiation factor, bringing translation to a halt (Merrick, 1992).

Initiation is a highly regulated step in translation. The steps of elongation and termination are less regulated. Once the message in the coding sequence of the mRNA is initiated the ribosome elongates the message and termination occurs at the termination codon. Apart from the coding sequence, mRNAs also

possess untranslated (UTR) regions in their 5' as well as 3' ends. These UTR sequences provide many options for regulating the mRNAs. Many RNA binding proteins bind to mRNAs at these sites and control the expression of the mRNA. The 3' UTR is a special focus of this thesis.

Polyadenylation

Virtually all mRNAs, with the exception of histone mRNAs, are decorated with a cotranscriptionally added long poly (A) tail at the 3' UTR. This process occurs in the nucleus. The poly (A) tail has been suggested to be important for transcription termination, mRNA stability, translation efficiency and mRNA transport. Most mRNAs contain a polyadenylation signal consisting of two elements- a hexanucleotide (hex) sequence AAUAAA which lies 10-30 bases upstream of the cleavage/polyadenylation site, the second signal is a GU rich sequence located 30-40 bases downstream of the cleavage site. 3' end of the mRNA is processed by 2 steps- first is cleavage of the mRNA between these two signal sequences by an endonucleolytic process; second is the addition of poly (A) tail. The hex sequence is recognized by the cleavage and polyadenylation specificity factor (CPSF). It has been known for some time that cleavage occurs by formation of a 3' end processing complex on the mRNA; this complex is composed of the four proteins CPSF, cleavage stimulation factor (CstF), cleavage factors I and II (Colgan and Manley, 1997; Zhao et al., 1999). Recently Shi et al dissected the molecular architecture of the 3' end processing complex

by performing large scale proteomic analysis (Shi et al., 2009). The 3' end processing complex is more composite than previously imagined and is composed of more than 80 proteins. Cleavage is accompanied by polyadenylation of the mRNA and the two processes occur simultaneously *in vivo*. Poly (A) polymerase (PAP) is the enzyme that adds the multiple adenosine (A) nucleotides to the 3' end of mRNA. The maximum number of residues in the poly (A) tail is limited to 200-300; this is maintained by the poly (A) binding protein (PABP), which has a high affinity to poly (A) tracts. PABP also supports translation initiation by binding to the initiation factor eIF4G and thus circularizing the mRNA by bringing the 5' and 3' ends of the mRNA in close proximity.

There is evidence of regulation of the mRNA at the polyadenylation stage. Many mRNAs possess multiple polyadenylation signals and alternate polyadenylation can lead to differential mRNA subsets of the same pre-mRNA and affect the protein length and other processing functions.

Cytoplasmic polyadenylation

Upon undergoing polyadenylation in the nucleus, mRNAs are exported out of the nucleus into the cytoplasm. In some cases, the polyadenylation status of the mRNAs alters in the cytoplasm as detailed below. This phenomenon of cytoplasmic polyadenylation was discovered in *Xenopus* oocytes and is used as a means of translation control by regulating the length of poly(A) tail. Cytoplasmic polyadenylation process is mediated by CPEB (Cytoplasmic Polyadenylation

Element Binding Protein), an RNA binding protein that associates with the U-rich (UUUUUAU) cytoplasmic polyadenylation element (CPE) in the 3'UTRs of responding mRNAs. By doing so, it regulates the polyadenylation-induced translation of target mRNAs through formation of a large RNA-protein complex that includes cleavage and polyadenylation specificity factor (CPSF), the non-canonical poly(A) polymerase germline development factor 2 (Gld2), the deadenylase poly (A) ribonuclease (PARN), Neuroguidin (Ngd), the scaffold protein symplekin, and other factors (Richter, 2007). CPEB was originally discovered in Xenopus during studies on the development of Xenopus oocytes which occurs through various stages. The full grown oocytes remain in their immature state until they receive the development cue of induction by steroid hormone progesterone whereupon the oocytes mature into fertilizable eggs. Molecularly, progesterone stimulation activates Mos/MEK/MAP kinase pathway, which leads to release of the oocytes from cell cycle arrest. These arrested oocytes contain many mRNAs in dormant/masked state, which undergo stimulation dependent translation. Several of these masked/dormant mRNAs have short poly(A) tails which get elongated upon stimulation leading to their polyadenylation-mediated translation. All the mRNAs are tagged with a long poly(A) tail when they emerge from the nucleus, but mRNAs containing CPE elements in their 3'UTR attract CPEB and its associated factors gld-2 and PARN (Mendez and Richter, 2001). Gld-2 is the poly(A) polymerase that adds adenosine moieties to the mRNAs and PARN is the deadenylase which removes

the adenosine moieties. Because PARN is a faster acting enzyme, the net effect is shortening of the poly(A) tail and entrance of the mRNA into a dormant state (Kim and Richter, 2006). Upon CPEB's phosphorylation at Ser174 by Aurora kinase, the deadenylase is dissociated from the mRNA-protein complex which facilitates the elongation of poly(A) tail. Phosphorylation of CPEB also promotes the recruitment of poly(A) binding protein (PABP) which stabilizes the poly(A) and further facilitates translation of the mRNA. One important mRNA whose translation is regulated using this mechanism is cyclin B1, a protein essential for cell cycle regulation (Groisman et al., 2000) (Figure 1.1).

In some mRNAs an additional regulation by the protein maskin also occurs. Maskin is a CPEB binding protein which also binds eIF4E at the site where eIF4G normally binds, thus creating competition between eIF4G and maskin for eIF4E binding. eIF4E is the cap binding translation initiation factor and eIF4G is the translation initiation factor required for recruitment of 40S ribosomal subunit to the 5' UTR of the mRNA. CPE-containing mRNAs are maintained in translational dormant state due to maskin binding and its sequestration of eIF4E, making it non-available for eIF4G binding and thus repressing translation. When poly(A) tail is elongated, poly(A) binding protein (PABP) binds to the poly(A) tail and recruits eIF4G which helps it to displace maskin from eIF4E. Thus, translation ensues (Stebbins-Boaz et al., 1999).

Figure 1.1 Translation control by CPEB in neurons

CPEB binds to CPE elements in the 3'UTR of mRNA and recruits several factors Gld2, PARN, Ngd on the scaffolding factor Symplekin resulting in shorter poly (A) tail of the mRNA and translation inhibition. Stimulation of the neuron leads to Aurora A catalyzed phosphorylation of CPEB and concomitant changes in the CPEB complex leading to expulsion of PARN and resumption of polyadenylation and translation of the mRNA (details in text).

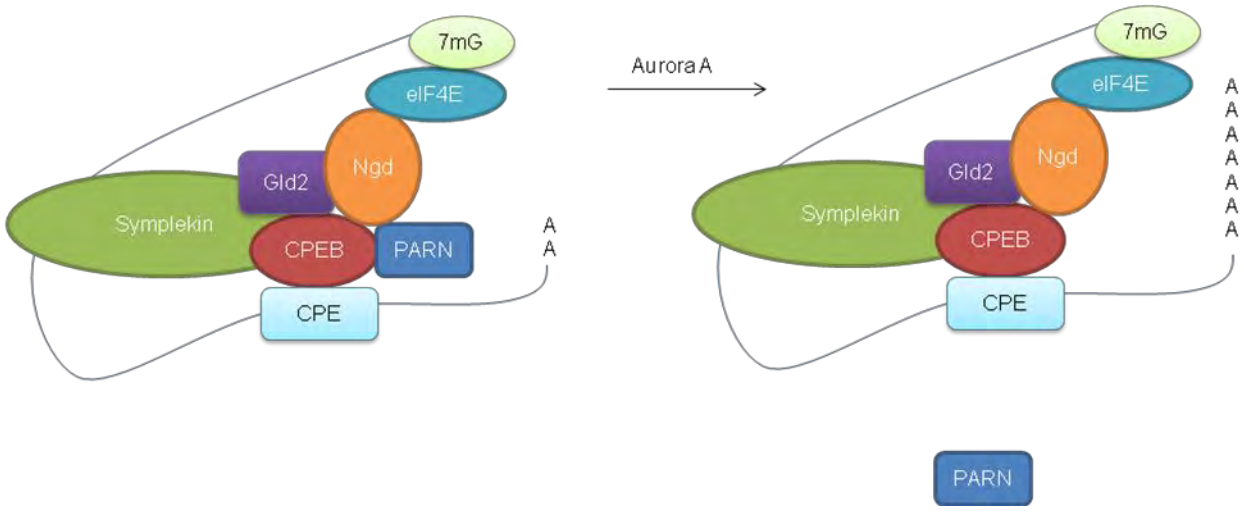
7mG
eIF4E
Ngd
Gld2
Symplekin
CPEB
PARN
CPE
A
A
Aurora A
7mG
eIF4E
Ngd
Gld2
Symplekin
CPEB
CPE
A
A
A
A
A
A
PARN

Figure 1.1

CPEB-mediated translation is required for several biological phenomena. CPEB is important for oocyte and sperm development as shown by studies in CPEB knockout mice; female CPEB KO mice have no detectable ovaries and the testis is 30% smaller in CPEB KO male mice (Tay and Richter, 2001). During meiosis in oocytes, CPEB plays a role in formation of synaptonemal complex through regulation of the mRNAs for synaptonemal complex proteins 1 (SCP1) and 3 (SCP3). In addition to its role in meiosis, CPEB also plays a role in regulating mitotic cell cycle progression (Novoa et al., 2010). CPEB has also been shown to shuttle between nucleus and cytoplasm; nuclear CPEB is important for regulating pre-mRNA splicing of a collagen 9a1 mRNA (Lin et al., 2010). CPEB also plays a role in regulating localization of ZO-1 mRNA and thereby regulating cellular tight junctions (Nagaoka et al., 2012). CPEB modulates hepatic insulin resistance by regulating translation of Phosphatase and Tensin homolog (PTEN) and Signal Transducer and Activator of Transcription 3 (STAT3) (Alexandrov et al.). Synaptic plasticity and learning and memory is also regulated by CPEB; neuronal CaMKII has CPE elements and is regulated by CPEB-mediated translational activation (Alarcon et al., 2004; Berger-Sweeney et al., 2006). CPEB regulates cell growth and senescence in human as well as mouse fibroblasts. Fibroblasts derived from CPEB knockout (KO) mice bypass senescence as do human skin fibroblasts depleted of CPEB (Burns and Richter, 2008; Groisman et al., 2006); in both cell types, reduced p53 mRNA translation is a key event causing the immortalization (Burns and Richter,

2008; Groppo and Richter). CPEB depletion, at least in human fibroblasts, results in the Warburg Effect, a cancer-related phenomenon in which ATP production by mitochondrial oxidative phosphorylation is impaired but compensated for by increased glycolysis (Burns and Richter, 2008; Levine and Puzio-Kuter; Vander Heiden et al., 2009).

CPEB in neurons

CPEB is highly abundant in the brain, kidney, lung and ovary (Theis et al., 2003; Wu et al., 1998). In the brain, CPEB is localized to the post-synaptic density (PSD) fraction of the synapse. Synapses are the structures where one neuron communicates with another and the PSD fraction is the electron dense region immediately below the postsynaptic membrane where a variety of signaling molecules are present. The PSD fraction also contains various translational machinery components suggesting that many mRNAs may undergo local translation in this compartment. Activation of the synapse by the neurotransmitter glutamate via activation of N-methyl D-aspartate (NMDA) receptors causes phosphorylation of CPEB at Thr 171 which activates CPEB and thus facilitates polyadenylation and translation of CPE-containing mRNAs (Huang et al., 2002). The polyadenylation-mediated activation by CPEB in neurons occurs in the same manner as in the Xenopus oocyte; activation of CPEB leads to expulsion of PARN and elongation of the poly(A) tail by Gld-2 (Udagawa et al., 2012). It has been shown that CPEB plays a role in

polyadenylation and thus local translation of calcium/calmodulin dependent protein kinase II (αCaMKII) mRNA at the synapse (Huang et al., 2002). αCaMKII plays a very important role in synaptic transmission and plasticity. CPEB knockout (KO) mice (Tay and Richter, 2001) show defects in hippocampus dependent memory, specifically in the form of memory known as extinction (Berger-Sweeney et al., 2006). Extinction is the process where conditioned responses diminish and gradually become extinct over time as the animal learns to uncouple a response from a stimulus. Improper extinction leads to impaired learning of new tasks. Synaptic plasticity is the ability of neurons to change their strength upon activation by a stimulus. Certain forms of synaptic plasticity known as long term potentiation (LTP) and long term depression (LTD) are affected in CPEB KO mice. CPEB KO mice show defects in LTP evoked by theta burst stimulation (Alarcon et al., 2004) and growth hormone stimulation (Zearfoss et al., 2008). In *Drosophila*, Orb2 is the homolog of CPEB and its reduction causes impairment specifically in long-term memory but not in short-term memory (Keleman et al., 2007). *Aplysia* CPEB has been shown to form amyloidogenic oligomers when over expressed and these oligomers increase in an activity-dependent manner in neurons (Si et al., 2003a; Si et al., 2003b). *Drosophila* Orb2 has also been shown to form such oligomers upon neuronal stimulation and *Drosophila* mutants defective in forming these oligomers have impaired long-term memory (Majumdar et al., 2012). CPEB also controls mRNA transport in neurons (Huang et al., 2003). CPEB binds CPE containing mRNAs and transports them to

dendrites from the cell body (soma). It is likely that these CPE containing mRNAs then get translationally activated upon synaptic stimulation. CPEB also has been shown to be important for experience-dependent dendritic morphogenesis in *Xenopus* optical tectal neurons (Bestman and Cline, 2008, 2009). Taken together, these studies reveal the importance of CPEB in neuronal activity, neuronal mRNA transport and memory consolidation.

CPEB family proteins

Invertebrates such as *Drosophila* have 2 CPEB-like proteins (Orb1 and Orb2), but vertebrates have four CPEB like proteins, namely CPEB, CPEB2, CPEB3 and CPEB4 (Theis et al., 2003). *Drosophila melanogaster* Orb1 is similar to CPEB while *Drosophila melanogaster* Orb2 has higher similarity to CPEB 2-4 (Mendez and Richter, 2001). CPEB (also sometimes called CPEB1), is the founding member of the family. It was originally discovered in *Xenopus laevis,* but has now been shown to be present in many organisms including *Homo sapiens* (human), *Rattus norvegicus* (rat), *Mus musculus* (mouse), *Pan troglodytes* (chimpanzee), *Macaca mulatta* (rhesus monkey) and *Bos taurus* (cow). CPEB2 was originally discovered in mouse round spermatids, whereas CPEB3 and 4 were described in mouse brain and other tissues. It is now known that in mouse, CPEB2 is present in brain and testis. CPEB3 is present in brain and heart with weaker expression in liver, lung, kidney, embryo and ovary (Kurihara et al., 2003; Theis et al., 2003). CPEB4 mRNA expression is highest in

brain followed by heart, kidney, embryo, lung with weaker expression in liver, spleen and ovary.

There is high conservation in the RNA-binding domains of these various CPEB family members (45% homology) but CPEB2, 3 and 4 have higher homology to each other than to CPEB (98 to 99% homology). The full length proteins have lesser conservation compared to the RNA-binding domains; CPEB 2-4 show higher conservation with each other than to CPEB1 (Figure 1.2). CPEB3 and 4 bind to a U rich stem loop structure that is distinct from CPE (Huang et al., 2006). In transfected neurons, CPEB3 represses translation of reporter RNAs containing the stem loop structure; an endogenous mRNA target of CPEB3 is GluR2 whose translation is upregulated upon RNAi knockdown of CPEB3. The mechanism of action of CPEB3 is likely distinct from CPEB mediated translation regulation because CPEB3 neither binds AAUAAA nor interacts with cleavage and polyadenylation specificity factor (CPSF) (Huang et al., 2006). CPEB2-4 can be co- regulated by miRNAs 92 and 26 and the miRNA binding sites are located in the paralog positions suggesting conservation of this regulation throughout evolution (Morgan et al., 2010).

Figure 1.2 CPEB family proteins

Mouse CPEB family proteins (mCPEB1-4) have an N-terminal regulatory domain and a C terminal RNA binding domain containing the RNA Recognition Motifs (RRM) and Zinc Fingers (ZnF). Homology percentages of the full length CPEB1-4 proteins (in black) and the RNA binding domains (in red) are also shown.

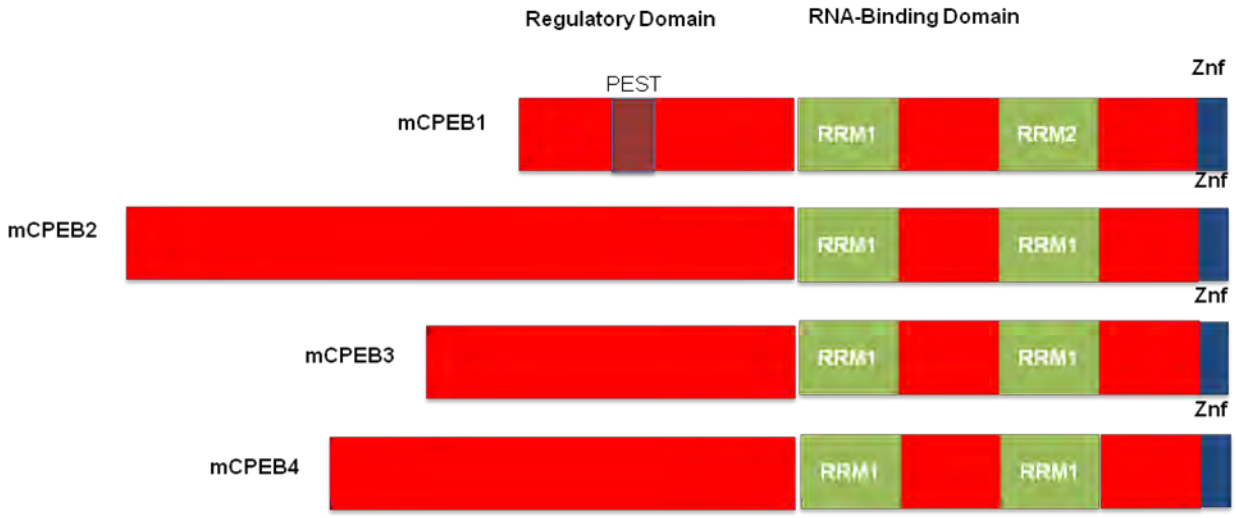

	CPEB1	CPEB2	CPEB3	CPEB4
CPEB1		23.8	24.8	24.6
CPEB2	44.9		69.9	67.7
CPEB3	44.9	99		56.8
CPEB4	44.9	98.5	97.5	

Figure 1.2

CPEB2 has been shown to bind to hypoxia inducible factor 1 alpha (HIF1 α) mRNA and influence its expression by slowing down polypeptide elongation; CPEB2 also binds to eEF2 and inhibits eEF2/ribosome triggered GTP hydrolysis, thus slowing down translation elongation of CPEB2 bound mRNAs (Chen and Huang, 2012; Hagele et al., 2009).

CPEB3 and 4 mRNA levels are elevated in hippocampus following kainite-induced seizures, suggesting their importance in synaptic activity (Theis et al., 2003). *Drosophila* Orb2, which has high homology to CPEB2-4 has a role in long term male courtship memory (Keleman et al., 2007). CPEB3 has a highly conserved self cleaving human delta virus (HDV) like ribozyme in one of its introns; a single nucleotide polymorphism in this ribozyme affects its cleaving properties and is associated with human episodic memory (Salehi-Ashtiani et al., 2006). In mouse, CPEB3 has been shown to affect synaptic plasticity by influencing the translation of GluA1 and GluA2 subunits of AMPA receptors and growth of new dendritic spines. The ubiquitin ligase neuralized monoubiquitinates CPEB3 and increases its activity, which in turn leads to increased AMPA receptors (Pavlopoulos et al., 2011). Apart from its role in translation, CPEB3 also partners with signal transducer-activated transcription (Stat) 5b and acts as a transcriptional inhibitor of the tyrosine kinase epidermal growth factor receptor (EGFR) upon shuttling to the nucleus. EGFR is known to regulate LTP, learning and memory (Peng et al., 2010).

CPEB4 mRNA possesses CPEs in its 3'UTR and is regulated by CPEB generating a positive loop to sustain cytoplasmic polyadenylation throughout the various stages of meiosis (Igea and Mendez, 2010). Even during mitosis, CPEB 4 and CPEB1 coordinately regulate polyadenylation of hundreds of mRNAs to achieve successful entry into M phase and promote cell proliferation (Novoa et al., 2010). Recently it has been revealed that CPEB4 has some pro-oncogenic properties. It is upregulated in pancreatic ductal adenocarcinomas and glioblastomas and knockdown of CPEB4 reduces tumor growth, vascularization and invasion. Translational control of tissue plasminogen activator (tPA) is one of the major causes for the tumor progression (Ortiz-Zapater et al., 2012).

CPEB family proteins have been shown to influence various aspects of cell physiology suggesting that these proteins play a crucial role.

Mitochondrial physiology

Mitochondria are the energy producing organelles of the body and also are required for calcium homeostasis, apoptosis, and amino acid and lipid metabolism. They are double membrane organelles enclosing a matrix in the centre and an intermembrane space in between the two membranes. The inner membrane is folded into cristae and houses the components of the Electron transport chain (ETC). The ETC is a series of protein complexes (I-V) through which electrons flow and protons are pumped out to the intermembrane space and thus, generate a proton gradient across the inner membrane. ATP synthase

transports protons from the intermembrane space to the matrix down their gradient and uses this energy to couple a phosphate group to ADP to generate ATP (Figure 1.3).

Figure 1.3 Schematic of mitochondrial structure and function.

The mitochondrion is a double membrane structure with an Outer and Inner membrane enclosing a matrix. Electron transport chain complexes I-IV transport electrons and generate a proton gradient across the inner membrane which is utilized by the complex V to produce ATP. Transport of newly synthesized proteins into mitochondria occurs through the TOM and TIM complexes; upon entry into mitochondria the mitochondrial targeting sequence is cleaved. Mitochondrial DNA (mtDNA) and the TCA cycle are also shown. Role of mitochondria in calcium buffering and Reactive Oxygen species (H_2O_2, O_2^-) is also shown.

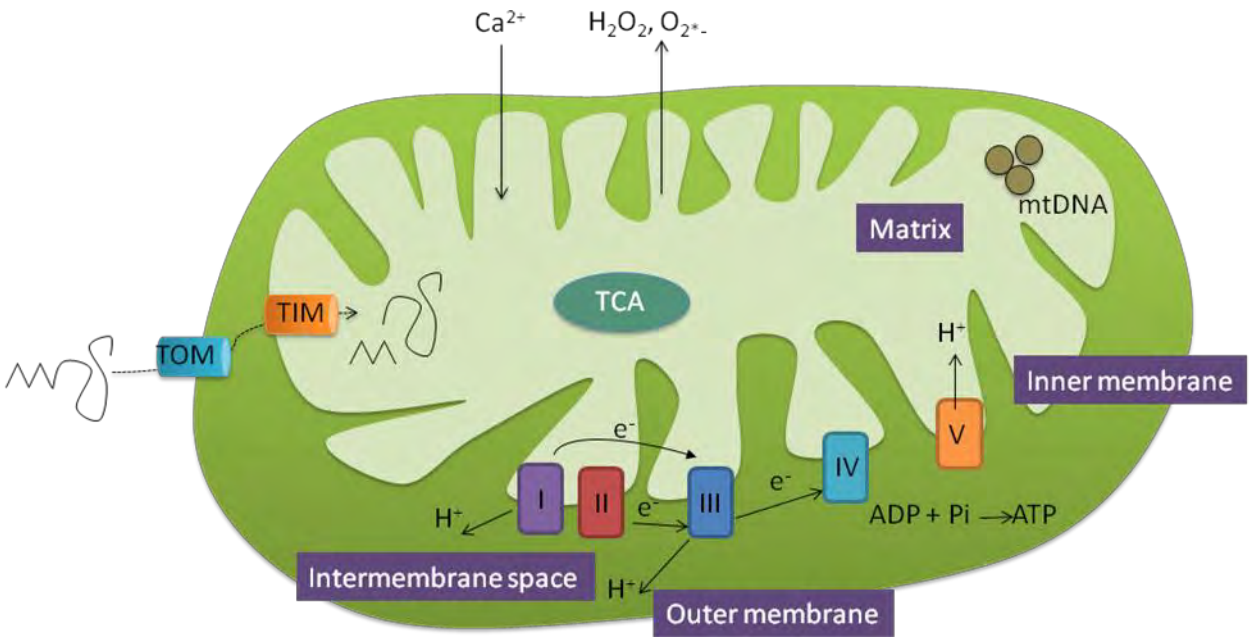
Ca2+
H2O2, O2•-
mtDNA
Matrix
TCA
TIM
TOM
H+
Inner membrane
V
e-
IV
I
II
III
e-
e-
H+
ADP + Pi →ATP
Intermembrane space
H+
Outer membrane

Figure 1.3

Different tissues possess varying amounts of mitochondria. Some tissue specificity arises due to different requirements and functions of the particular tissue. For instance, only liver tissue performs urea synthesis. One of the enzymes involved in this process ornithine transcarbomylase is present only in liver mitochondria. Other tissue specific metabolic pathways involving mitochondria are gluconeogenesis and ketone body production in liver, steroid hormone production in adrenal cortex, deamination of glutamine in kidney, utilization of lactic acid by sperm, uncoupling and generation of heat by brown adipose tissue (reviewed in (Johnson et al., 2007; Kunz, 2003). Tissue specificity also arises due to different subunit composition of the electron transport chain complexes. Cytochrome c oxidase (also called Complex IV) components display the most diverse tissue specific expression of isoforms. The enzyme is composed of 13 subunits, of which isoforms are known for 4 of the subunits namely IV, VIa, VIIa and VIII. The γ subunit of ATP synthase also has two isoforms- H type in muscle and heart and L type in brain, liver and kidney (Kunz, 2003). These two isoforms are produced as a result of alternate splicing. The differential composition of mitochondria is probably a consequence of different requirements of tissues. Brain for instance is a high energy requiring organelle and thus possesses higher amounts of mitochondria. As a consequence of different composition of mitochondria different tissues have variable sensitivities to defects in mitochondria (Kuznetsov et al., 2009).

The mitochondrial proteome is made up of approximately 1100 proteins (Pagliarini et al., 2008). Of these, 13 are encoded by the mitochondrial genome. Mitochondrial DNA in vertebrates is a covalently closed molecule of 16.5 kilobases. It encodes 13 protein components of Complexes I, III, IV and V, 22 tRNAs and 2 rRNAs (reviewed in (Chen and Butow, 2005). The remainder of the mitochondrial proteome is encoded by nuclear DNA. These nuclear encoded mitochondrial proteins possess a mitochondria targeting signal (MTS) in the amino terminal or internally in the protein, which is recognized by the translocation complex of outer mitochondrial membrane (TOM) and then by the translocation complex of inner mitochondrial membrane (TIM) (Chacinska et al., 2009). The nuclear encoded mitochondrial proteins are very tightly regulated. They are transcriptionally regulated by various transcription factors such as PGC1 alpha, EEG-1 etc (Hock and Kralli, 2009; Scarpulla, 2008).

Mitochondrial dysfunction can prove disastrous for the cell and consequentially to the organism. Many human diseases such as schizophrenia, bipolar disease, dementia, Alzheimer's disease, epilepsy, migraine headaches, strokes, neuropathic pain, Parkinson's disease, ataxia, transient ischemic attack, cardiomyopathy, coronary artery disease, chronic fatigue syndrome, fibromyalgia, retinitis pigmentosa, diabetes, hepatitis C, and primary biliary cirrhosis are caused or exacerbated by mitochondrial dysfunction (Pieczenik and Neustadt, 2007). Apart from disease, the normal progression of aging also has

mitochondrial links. ROS produced by mitochondria has been shown to lead to faster aging (Van Remmen and Richardson, 2001).

Electron Transport Chain Complex I

Mitochondrial electron transport chain complex I, also known as NADH dehydrogenase, whose function is to couple oxidation of NADH to the reduction of ubiquinone, is the first and largest complex in ETC. *Homo sapiens* (Human) and *Bos tauras* (bovine) CI is made up of about 45 subunits, 14 of which are part of the core complex. Electron microscopy studies have revealed that mammalian CI assumes an L shaped conformation consisting of a peripheral matrix protruding arm and mitochondrial inner membrane (MIM) imbedded membrane arm. The assembly of complex I is very intricate and involves at least 7 identified assembly factors and proceeds through formation of 6 identified intermediate complexes. It is an important source of reactive oxygen species (ROS) (Distelmaier et al., 2009; Koopman et al., 2010; Lazarou et al., 2009).

Mitochondrial Fusion and fission

Mitochondria form a dynamic network; their shape ranges from cell-wide extended tubular networks to single isolated tubules. Such dynamic structure is a result of various fission and fusion events occurring throughout the neurons. In vertebrates, the GTPases mitofusins (Mfn1 and Mfn2) of the outer mitochondria and OPA1 in the intermembrane space are important for fusion. Another dynamin related protein (Drp1) which is present in cytoplasm along with the mitochondria

outer membrane protein Fis1 is involved in fission (Chan, 2006). Aberrant mitochondrial fusion and fission events are associated with many disorders. Mfn1 and 2 are important for embryonic development, protection against cerebellar neurodegeneration and are the cause for Charcot Marie tooth disease as well as optic atrophy I (Delettre et al., 2000; Zuchner et al., 2004). Mitochondrial fission has been observed to be important for apoptosis and neuronal function in mammalian culture (Ishihara et al., 2009).

Mitochondria in brain

The brain is highly dependent on mitochondrial oxidative phosphorylation for its energy requirements. In fact, the brain constitutes only 2% of body weight, but consumes 20% of total body oxygen and 25% of glucose (Raichle and Gusnard, 2002). Maintenance of ion gradients, synaptic potentials, action potentials and uptake and recycling of neurotransmitters are some of the major energy consuming processes of brain. Even when neuronal firing decreases to the minimum and electroencephalogram (EEG) becomes silent showing negligent neuronal activity, oxidative ATP production only halves, suggesting that half of the ATP expenditure in the brain is utilized in housekeeping functions (Mironov, 2009). It is hypothesized that most mitochondria are synthesized in the cell body of neurons and dysfunctional mitochondria also are transported back to cell bodies. They are transported over great distances in the various long processes of neurons; this transport occurs via microtubules which are attached

to the mitochondria through motor adaptor proteins (Sheng and Cai, 2012). More than half of all mitochondria in brain are in dendrites and cell body (soma), 30% are in axons and rest in the glia (Mironov, 2009) . Synapses are particularly rich in mitochondria. In fact, in earliest electron microscopy explorations, synapses were indeed located based on their high density of mitochondria (Hollenbeck, 2005).

Brain activity dependent mitochondrial dynamics

Mitochondrial distribution and dynamics are adaptable to the cell physiological status. Mitochondria are found in increased numbers in presynaptic terminals and also in postsynaptic dendritic spines during synaptic activity (Kann and Kovacs, 2007). In fixed preparations, mitochondrial position can be correlated to the previous neuronal activity, with increased numbers of mitochondria found in areas of increased activity (Mironov, 2009). Mitochondria are transported to activated zones through two signals - one is the ATP levels and the other is the calcium concentration (Sheng and Cai, 2012). During development, mitochondria have been shown to move toward active growth cones in developing neurons (Morris and Hollenbeck, 1993).

Mitochondria and synaptic plasticity

Dendritic mitochondria have been shown to be important for the plasticity of dendritic spines. In *Drosophila*, Milton protein is important for mitochondrial distribution to nerve terminals. Mutant flies lacking Milton have defective synaptic

transmission, suggesting the importance of pre-synaptic mitochondria in synaptic function (Stowers et al., 2002). In mammalian neurons, it was shown that mitochondria are dynamically distributed to dendritic regions in response to synaptic stimulation (Li et al., 2004). Rat hippocampal neurons mutant for the mitochondrial fission proteins Drp1 and Opa1 have defective synaptic transmission (Li et al., 2004). Synaptic activity leads to changes in calcium currents in the neuron and mitochondria are important for calcium buffering, thus emphasizing the importance of mitochondria in synaptic plasticity. The mitochondrial permeability transition pore is a complex consisting of the voltage dependent anion channel (VDAC) in the outer membrane, adenine nucleotide transporter in the inner membrane and cyclophilin D in the matrix and is found in all mitochondria. This complex was shown to be important for synaptic plasticity and learning in mice (Weeber et al., 2002).

Mitochondrial function is regulated by various mechanisms as described above. CPEB-deficient human fibroblasts also have reduced mitochondrial mass and function (Burns and Richter, 2008). Because CPEB controls both energy production in human fibroblasts and synapse function in the brain (Alarcon et al., 2004; Zearfoss et al., 2008), we surmised that there might be a link between the two, and that there might be reduced mitochondrial activity in neurons that lack CPEB. In light of these observations, I studied the role of CPEB in mitochondrial

function in mouse. I specifically focused on brain tissue because neurons have higher energy demand and are rich in mitochondria.

CPEB family proteins also play important roles in neuronal function as detailed earlier. In this thesis, I have explored the role of CPEB4 in neuronal survival and its dynamics in response to neuronal stimulation, ischemia and calcium concentration changes.

Preface to Chapter II

Work presented in this chapter was largely performed by Aparna Oruganty (AO) with the following exceptions. Tsuyoshi Udagawa provided the shRNA constructs to knockdown CPEB and the constructs to over-express CPEB. *in vivo* dendritic branching analysis was performed by Teclise Ng in Dr. Eyleen Goh's lab.

CHAPTER II

Translational Control of Mitochondrial Energy Production Mediates Neuron Morphogenesis

Aparna Oruganty-Das[1], Teclise Ng[2], Tsuyoshi Udagawa[1,3], Eyleen L. K. Goh[2] & Joel D. Richter[1]

[1]Program in Molecular Medicine

University of Massachusetts Medical School

Worcester, MA 01605 USA.

[2]Program in Neuroscience and Behavioral Disorders

Duke-NUS Graduate Medical School, Singapore 169857

[3]present address

Department of Neurology

Nagoya University

Nagoya-shi, Aichi 466-8550

Abstract

Mitochondrial energy production is a tightly regulated process involving the coordinated transcription of several genes, catalysis of a plethora of posttranslational modifications, and the formation of very large molecular supercomplexes. The regulation of mitochondrial activity is particularly important for the brain, which is a high energy-consuming organ that depends on oxidative phosphorylation to generate ATP. Here we show that brain mitochondrial ATP production is controlled by the cytoplasmic polyadenylation-induced translation of an mRNA encoding NDUFV2, a key mitochondrial protein. Knockout mice lacking the Cytoplasmic Polyadenylation Element Binding protein (CPEB) have brain-specific dysfunctional mitochondria and reduced ATP levels, which is due to defective polyadenylation-induced translation of electron transport chain complex-I protein NDUFV2 mRNA. This reduced ATP results in defective dendrite morphogenesis of hippocampal neurons both *in vitro* and *in vivo*. These and other results demonstrate that CPEB control of mitochondrial activity is essential for normal brain development.

Introduction

Mitochondrial ATP production accounts for ~90% of the energy produced in mammalian cells and thus the regulation of mitochondrial function is critically important for cell growth and viability. Nuclear-encoded mitochondrial proteins are regulated transcriptionally by various factors such as Nuclear Respiratory factors NRF1 and NRF2, stimulatory protein 1 (Sp1), estrogen related receptor α (ERRα), and yin yang 1 transcription factor (YY1) (Scarpulla, 2008). PGC1α plays a role in coordinating the expression of mitochondrial subunits commensurate with changes in the environment (Lin et al., 2005). Mitochondrial activity is also regulated by the formation of supercomplexes that allow for substrate channeling (Shoubridge, 2012). Post-translational modifications affect mitochondrial function (Koc and Koc, 2012), as does tissue-specific expression of different mitochondrial proteins that generate unique mitochondrial dynamics to accommodate different requirements for a given tissue (Pagliarini et al., 2008).

The Cytoplasmic Polyadenylation Element Binding Proteins (CPEBs) are a family of four RNA binding proteins that are widely expressed in vertebrates (reviewed in (Mendez and Richter, 2001). CPEB1 is the founding member of this family; it associates with the cytoplasmic polyadenylation element (CPE), a U-rich (UUUUUAU) structure generally residing within 100 bases of the AAUAAA pre-mRNA cleavage and polyadenylation signal in the 3' UTRs of specific

mRNAs. CPEB proteins 2-4 probably also associate with U-rich structures (Novoa et al., 2010), but they do not appear to recognize the CPE with the same high affinity as CPEB1 (Huang et al., 2006). Although all CPEB proteins regulate mRNA expression (Chen and Huang, 2012; Huang et al., 2006; Novoa et al., 2010; Wang and Huang, 2012), CPEB is centrally important for promoting translation by stimulating cytoplasmic polyadenylation. CPEB is the key component of the cytoplasmic polyadenylation complex, which also includes cleavage and polyadenylation specificity factor (CPSF), the non-canonical poly(A) polymerase Gld2, the deadenylating enzyme PARN, the scaffold protein symplekin, poly(A) binding protein (PABP), and Maskin or Neuroguidin (Ngd), which also bind the cap-binding factor eIF4E (Barnard et al., 2004; Kim and Richter, 2006, 2007; Richter, 2007; Udagawa et al., 2012). When associated with these factors in a large ribonucleoprotein (RNP) complex, CPE-containing mRNAs have short poly(A) tails and are translationally repressed. In response to an environmental cue, the kinase Aurora A phosphorylates CPEB, which causes the dissociation of PARN from the RNP complex resulting in default Gld2-catalyzed polyadenylation (Kim and Richter, 2006; Mendez et al., 2000). The newly elongated poly(A) tail then is bound by PABP, which also binds the initiation factor eIF4G. eIF4G subsequently displaces Maskin from eIF4E and thereby recruits other initiation factors and the 40S ribosomal subunit to the 5' end of the mRNA (Cao et al., 2006; Kim and Richter, 2007).

CPEB-mediated translation is required for several biological phenomena including oocyte development (Tay and Richter, 2001), neuronal synaptic plasticity and learning and memory (Alarcon et al., 2004; Berger-Sweeney et al., 2006; Udagawa et al., 2012; Zearfoss et al., 2008), cell growth (Burns and Richter, 2008; Groisman et al., 2006), and hepatic insulin resistance (Alexandrov et al.). Fibroblasts derived from CPEB knockout (KO) mice bypass senescence as do human skin fibroblasts depleted of CPEB (Burns and Richter, 2008; Groisman et al., 2006); in both cell types, reduced p53 mRNA translation is a key event causing the immortalization (Burns and Richter, 2008; Groppo and Richter). CPEB-depletion, at least in human fibroblasts, results in the Warburg Effect, a cancer-related phenomenon in which ATP production by mitochondrial oxidative phosphorylation is impaired but compensated for by increased glycolysis (Burns and Richter, 2008; Levine and Puzio-Kuter, 2010; Vander Heiden et al., 2009). The reduced p53 levels in CPEB-depleted cells lowers synthesis of cytochrome c oxidase (SCO2), which in turn impairs electron transport chain complex IV activity.

In this study, we sought to investigate whether CPEB deficiency results in impaired mitochondrial function in animal tissue. Surprisingly, we observed that in CPEB knockout (KO) animals, mitochondrial energy production was reduced in the brain and neurons but not muscle or liver and was unaccompanied by elevated glycolysis as occurs in the Warburg Effect. Further analysis showed that the polyadenylation of electron transport chain complex I protein NDUFV2

mRNA was compromised in neurons, which caused reduced levels of the protein and hence inefficient oxygen consumption and ATP production. As a consequence of depressed ATP levels, dendrite morphogenesis was also reduced in CPEB-deficient hippocampal neurons both *in vitro* and *in vivo.* Impaired dendrite branching and growth in CPEB-deficient neurons was rescued when normal levels of ATP were restored. These and other observations reveal an essential and unexpected role for translational control in energy production in the brain.

Results

CPEB deficiency leads to reduced mitochondrial function

To assess whether CPEB KO mice have altered bioenergetics similar to CPEB-depleted fibroblasts, ATP levels were measured in extracts from brain, liver, and muscle. Although the latter two tissues had no change in ATP concentration compared to wild type (WT), the brain displayed a ~56% reduction while cultured hippocampal neurons derived from CPEB KO mice showed a 32% reduction (Figure 2.1A). We measured the recovery of ATP from brain lysates by titrating in known amounts of this nucleoside triphosphate. Using our extraction procedure, there was a 41% recovery of ATP from WT and a 50% recovery from CPEB KO brain lysates; consequently, the values shown in the figure reflect corrected values for the recovery of ATP. The reduced ATP in CPEB KO brain may be contrasted to the effect observed in human foreskin fibroblasts in which CPEB depletion, while reducing mitochondrial ATP production, had no effect on overall ATP levels because of a compensatory up-regulation of glycolysis. This phenomenon of reduced mitochondrial ATP production and elevated glycolysis is known as the Warburg Effect and is a characteristic of cancer cells that may contribute to malignant transformation (Dang, 2012; Vander Heiden et al., 2009). In the brain, normal levels of ATP were restored in the CPEB1 KO neurons when they were infected with lentivirus expressing CPEB-HA (Figure 2.1B), indicating

that the depletion of ATP is reversible. Next, we determined whether shRNA-depletion of CPEB in WT neurons had a similar effect on ATP generation. As shown in Figure 2.2A , a ~65% depletion of CPEB was accompanied by a ~65% reduction in ATP only upon shRNA depletion of this protein but not when a control non-silencing (NS) shRNA was used (Figure 2.1B). These results show that CPEB controls energy balance specifically in neurons.

To investigate how CPEB regulates ATP levels, oxygen consumption was measured and shown to be reduced by ~50% in CPEB KO brain as well as cultured CPEB KO hippocampal (Figure 2.1C) and cortical neurons (Figure 2.2B); oxygen consumption in CPEB KO glia, however, was unchanged (Figure 2.2C). Oxygen consumption in brain lysates and hippocampal neurons was also determined in the presence of mitochondrial inhibitors rotenone plus antimycin and shown to be completely inhibited, indicating that the oxygen consumption we measured was entirely mitochondrial (Figure 2.1C). We also found that oxygen consumption in brain lysates increased for 54 min after which time it diminished. This non-linear measurement could be due to clumps of cells in the brain lysates that might have incomplete access to nutrients and oxygen, thus leading to the death of some of the neurons. Lactate production, which indicates efficiency of glycolysis, was unaltered in CPEB KO brain or neurons (Figure 2.2D), demonstrating that the reduction in ATP was not compensated by enhanced glycolysis. Mitochondrial levels as determined by mitochondrial DNA (Figure 2.1D) and cytochrome C content (Figure 2.1E) were unchanged in neurons,

indicating that an alteration in the mass of mitochondria was not responsible for reduced ATP production in CPEB-depleted neurons. Mitochondrial morphology in WT and CPEB KO neurons as determined by confocal microscopic examination of mitotracker-stained cells showed no significant differences (Figure 2.2E), indicating that the gross morphology of mitochondria was unaffected by the loss of CPEB. However, mitochondrial membrane potential as measured by the fluorescent dye tetramethylrhodamine methyl ester (TMRM) was reduced by 40-60% in DIV 2-20 cultured CPEB KO neurons (Figure 2.1F). Mitochondria have a negative resting membrane potential and TMRM is a cationic dye which preferentially accumulates in the mitochondria and to alesser extent in Endoplasmic reticulum. These data demonstrate that mitochondrial function, but not mitochondrial mass, is reduced in CPEB KO brain and neurons.

Figure 2.1. CPEB controls mitochondrial ATP production.

(A) ATP levels in brain, liver, muscle, and hippocampal neurons from 5 WT and 5 CPEB KO mice. (B) ATP in WT and CPEB KO hippocampal neurons isolated from 3 different embryos infected with lentiviruses expressing shRNA against CPEB (CPEB KD), non-silencing shRNA (NS), or HA-tagged CPEB (CPEB). (C) Oxygen consumption in 4 WT and 4 CPEB KO brain and cultured hippocampal neurons with or without the inhibitors (inhi) rotenone plus antimycin. (D) Quasi-quantitative PCR of mitochondrial (mt) and tubulin DNAs in WT and CPEB KO brain. (E) Western blots of the mitochondrial protein cytochrome C and actin in WT and CPEB KO brain. (F) Mitochondrial membrane potential as measured by TMRM in 7 hippocampal neurons each from 8 WT and 8 CPEB KO embryos cultured for 2-20 days *in vitro* (DIV). (*$p<0.05$; **$p<0.01$ Student's t test, all experiments were done in 3 replicates, the bars indicate SEM).

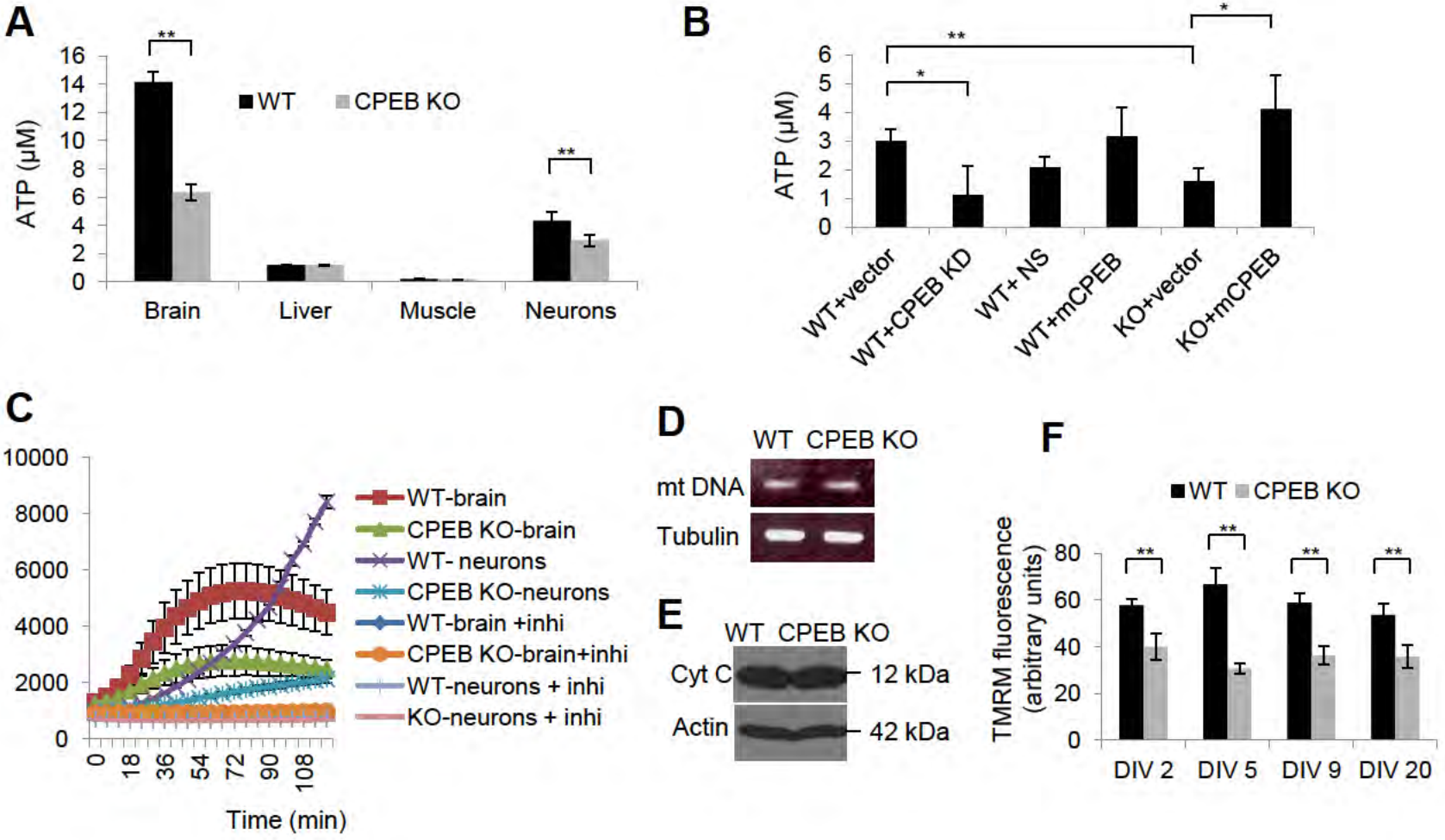
A
ATP (μM)
WT
CPEB KO
Brain
Liver
Muscle
Neurons
B
ATP (μM)
WT+vector
WT+CPEB KD
WT+ NS
WT+mCPEB
KO+vector
KO+mCPEB
C
A630
Time (min)
WT-brain
CPEB KO-brain
WT- neurons
CPEB KO-neurons
WT-brain +inhi
CPEB KO-brain+inhi
WT-neurons + inhi
KO-neurons + inhi
D
WT CPEB KO
mt DNA
Tubulin
E
WT CPEB KO
Cyt C
12 kDa
Actin
42 kDa
F
WT CPEB KO
TMRM fluorescence (arbitrary units)
DIV 2
DIV 5
DIV 9
DIV 20

Figure 2.1

Figure 2.2 Bioenergetics defect caused by CPEB deficiency is specific to neurons and is not compensated by glycolysis.

(A) Western blot showing knock down of CPEB using shRNA against CPEB (CPEB KD). Tubulin served as a loading control. (B) Oxygen consumption in WT and CPEB KO cortical neurons. (C) Oxygen consumption in glia cultured from WT and CPEB KO mouse brains. (D) Lactate levels in WT and CPEB KO brain and cultured hippocampal neurons. (E) Mitochondrial morphology imaged using mitotracker green FM in WT and CPEB KO neurons. (The bars refer to SEM).

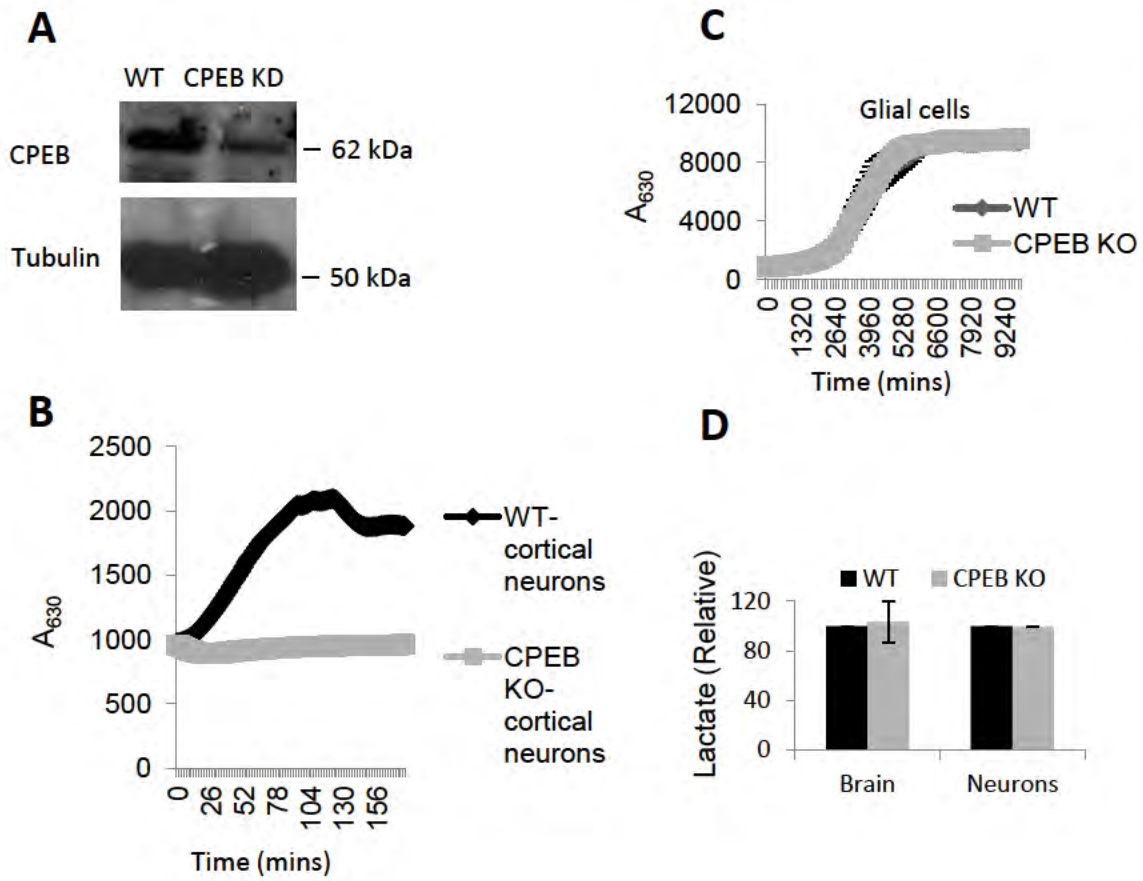
A
WT CPEB KD
CPEB
62 kDa
Tubulin
50 kDa
B
2500
2000
1500
1000
500
0
A630
0 26 52 78 104 130 156
Time (mins)
WT-cortical neurons
CPEB KO-cortical neurons
C
Glial cells
12000
8000
4000
0
A630
0 1320 2640 3960 5280 6600 7920 9240
Time (mins)
WT
CPEB KO
D
Lactate (Relative)
120
80
40
0
WT
CPEB KO
Brain
Neurons
E
WT
CPEB KO

Figure 2.2

Mitochondrial insufficiency is due to an impairment of electron transport chain complex I

The electron transport chain consists of four multi-protein complexes that sequentially transfer electrons to generate a proton gradient across the inner mitochondrial membrane, which is utilized by ATP synthase to phosphorylate ADP to produce ATP (Figure 2.3A). The actions of each of the complexes were measured in mitochondria isolated from WT and CPEB KO mouse brains. Because exogenous substrates were used for the assays, each complex was not influenced by the activity of any other. The activities of complexes I and II showed a statistically significant decline in the CPEB KO mitochondria; complex I activity in particular was strongly reduced by ~60% (Figures 2.3B-E). Citrate synthase, which indicates mitochondrial function unrelated to electron transport was similar in WT and CPEB KO brain (Figure 2.4A). Complex I and II activities were also determined by measuring oxygen consumption of isolated respiring mitochondria using an oxygen electrode. Oxygen consumption was measured in the presence of complex I substrates malate plus glutamate or succinate, a complex II substrate. As shown in Figure 2.3F and Table 2.1, oxygen consumption in both WT and CPEB KO mitochondria increased significantly upon addition of mitochondria to the reaction mix. The rate of oxygen consumption further increased upon addition of ADP (state 3 respiration). However, the rate of oxygen consumption was lower in CPEB KO mitochondria in the presence of complex I substrates but was unaffected in the presence of the

complex II substrate, again demonstrating that CPEB KO mitochondria are defective for complex I activity.

Figure 2.3 CPEB regulates the activity of electron transport chain complex I

(A) Schematic of mitochondrial electron transport chain complexes I-V. (B-E) Activities of electron transport chain (ETC) complexes I-IV in mitochondria from 3 WT and 3 CPEB KO mouse brain. (F) Oxygen consumption of mitochondria isolated from WT or CPEB KO brains. Mitochondria were incubated in a chamber containing an oxygen sensor; oxygen consumption was measured in the presence of complex I (malate plus glutamate) or complex II substrates (succinate). ADP was added to stimulate state 3 respiration. (*$p<0.05$; **$p<0.01$ Student's t test, 3 replicates, the bars indicate SEM).

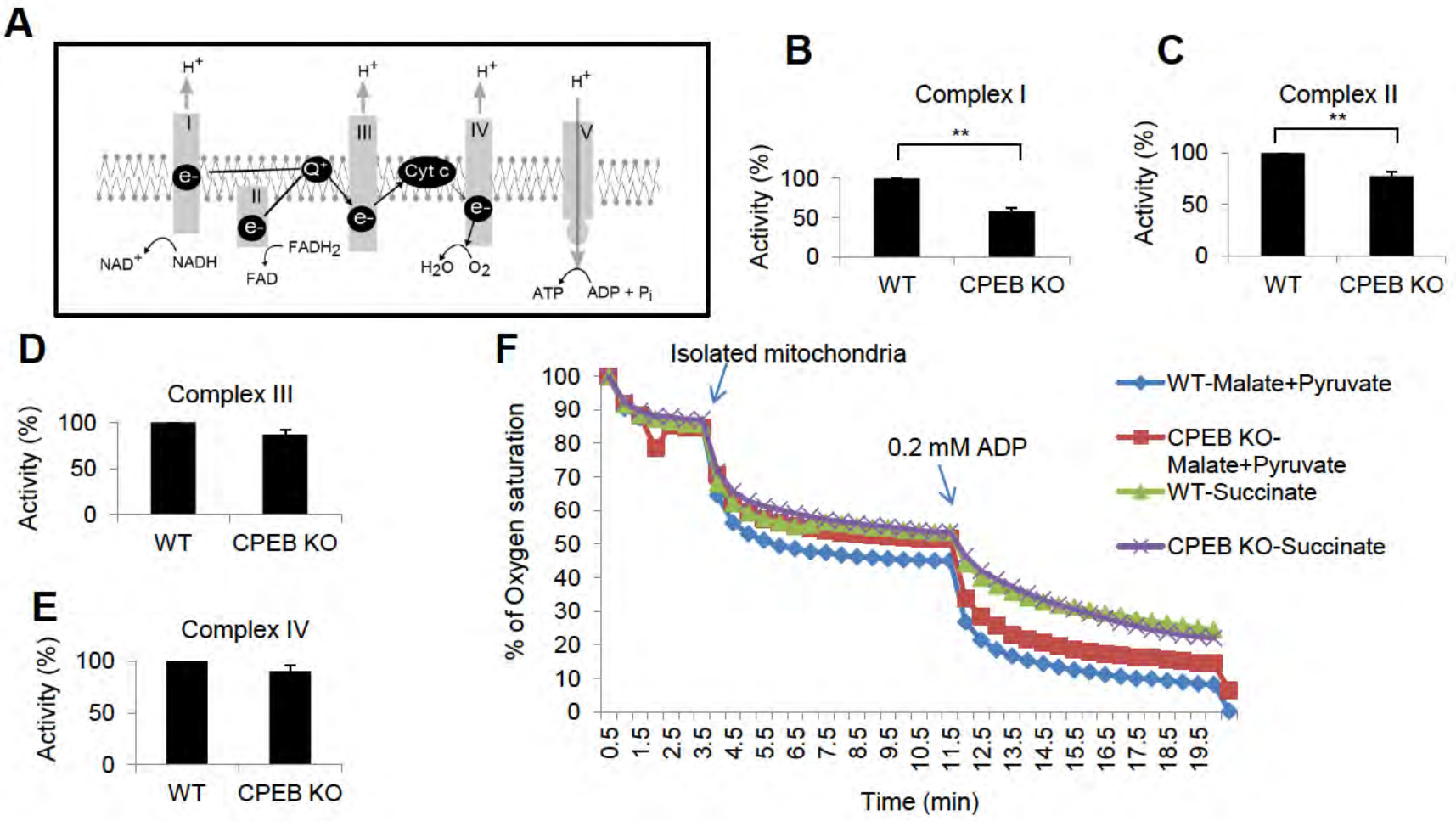
A
H+
I
III
IV
V
II
e-
Q
Cyt c
NAD+
NADH
FADH2
FAD
H2O
O2
ATP
ADP + Pi
B
Complex I
Activity (%)
100
50
0
**
WT
CPEB KO
C
Complex II
Activity (%)
100
50
0
**
WT
CPEB KO
D
Complex III
Activity (%)
100
50
0
WT
CPEB KO
E
Complex IV
Activity (%)
100
50
0
WT
CPEB KO
F
Isolated mitochondria
0.2 mM ADP
% of Oxygen saturation
100
90
80
70
60
50
40
30
20
10
0
0.5
1.5
2.5
3.5
4.5
5.5
6.5
7.5
8.5
9.5
10.5
11.5
12.5
13.5
14.5
15.5
16.5
17.5
18.5
19.5
Time (min)
WT-Malate+Pyruvate
CPEB KO-Malate+Pyruvate
WT-Succinate
CPEB KO-Succinate

Figure 2.3

Table 2.1 State 3 respiration rates in WT and CPEB KO mitochondria

	WT 0.2 mM ADP	CPEB KO 0.2 mM ADP
Complex I, III, IV 5 mM Glutamate+ 5 mM Malate	229 ± 25*	180 ± 43*
Complex II, III, IV 5 mM Succinate	178 ± 46	168 ± 11

Mitochondria isolated from WT and CPEB KO brains were analyzed for Complex I activity using glutamate and malate as substrates and for complex II using succinate as the substrate. Both measurements took place in presence of 0.2 mM ADP. The values represent mean ± SEM from 3 replicates. *P value= 1.22 (Not significant).

Reactive oxygen species (ROS) were increased by ~ 60 and 80% in the CPEB KO brain and neurons, respectively (Figure 2.4B). Complex I is a significant generator of ROS in mitochondria, which could explain why CPEB KO mitochondria have increased ROS. To determine whether the increased ROS leads to increased oxidative damage, the levels of protein carbonyl groups were measured as an indicator of oxidative damage. Carbonyl groups are produced on amino side chains (especially of proline, arginine, lysine, threonine) when they are oxidized. As shown in Figure 2.4C, CPEB KO brain had only very slightly elevated protein oxidative damage.

Figure 2.4 Citrate synthase and ROS levels in WT and CPEB KO brain lysates and neurons

(A) Citrate synthase activity measured in WT and CPEB KO brain mitochondria after normalizing to total protein. (B) Reactive oxygen species (ROS) measured in WT and CPEB KO brain lysates and neurons. (C) Oxidative damage assessed by measuring amount of protein carbonyl groups in WT and CPEB KO brain lysates. (The bars refer to SEM).

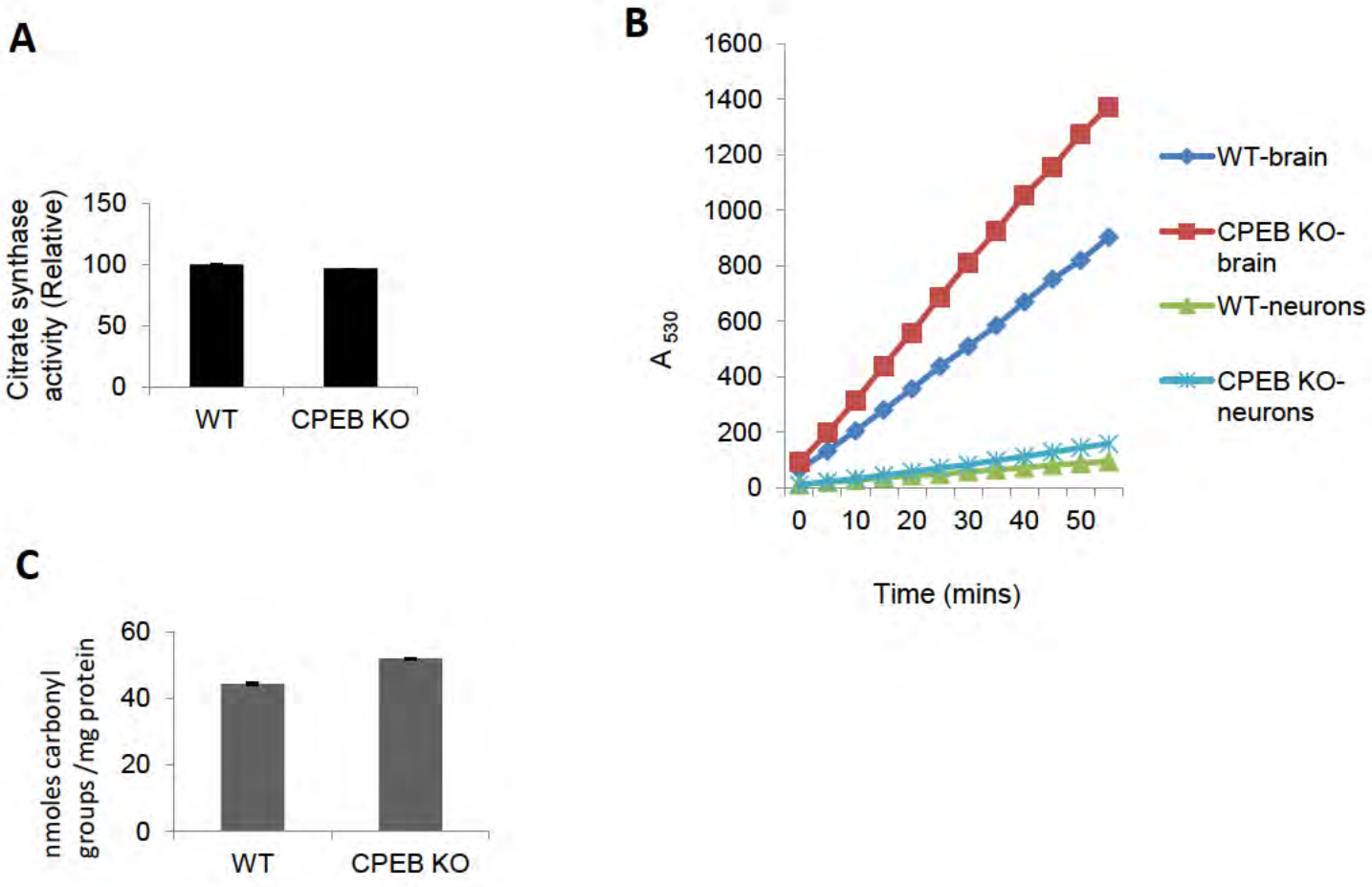
A
Citrate synthase activity (Relative)
150
100
50
0
WT
CPEB KO
B
1600
1400
1200
1000
800
600
400
200
0
A 530
0
10
20
30
40
50
Time (mins)
WT-brain
CPEB KO-brain
WT-neurons
CPEB KO-neurons
C
nmoles carbonyl groups /mg protein
60
40
20
0
WT
CPEB KO

Figure 2.4

We next used blue native PAGE and western blotting to examine specific proteins in each intact complex isolated from WT and CPEB KO mitochondria. Because the blue native PAGE is non-denaturing, the electron transport chain complexes remain intact and are not dissociated into their constituent subunits. Figure 2.5A shows that in contrast to proteins in complexes II, III, IV, and V, complex I was reduced by ~40% (as shown by blotting for its proteins NDUFV2 and NDUFA9) in the CPEB KO mitochondria. Complex II was not affected in the blue native PAGE analysis but its activity was reduced by about 20% in CPEB KO mitochondria (Figure 2.3C), suggesting that the dysfunction in complex II is not due to the loss of its constituent proteins. Examination of complex I proteins in total brain extracts demonstrates a reduction, by ~35%, only of NDUFV2 in the CPEB KO samples (Figure 2.5B). NDUFV2 mRNA levels, however, were comparable in WT and CPEB KO brain, pehaps the untranslated mRNA gets turned over (Figure 2.5C). These data suggest not only that reduced NDUFV2 in CPEB KO mitochondria is responsible for impaired ATP production, but that the levels of this protein might also be regulated at the posttranscriptional level.

Figure 2.5 CPEB regulates the expression of complex I protein NDUFV2

(A) Blue Native PAGE-resolved intact ETC complexes from mitochondria isolated from 3 WT and 3 CPEB KO brains and selected proteins in complexes I-V were analyzed by western blotting. Quantification is shown on the histogram. (B) Western blots were probed for mitochondrial proteins from total lysates from 3 WT and 3 CPEB KO brains. Quantification is shown on the histogram. (C) Quantitative RT-PCR analysis of NDUFV2, NDUFS4, and tubulin mRNAs in 3 WT and 3 CPEB KO brains. (*$p<0.05$; **$p<0.01$ Student's t test, 3 replicates, the bars indicate SEM).

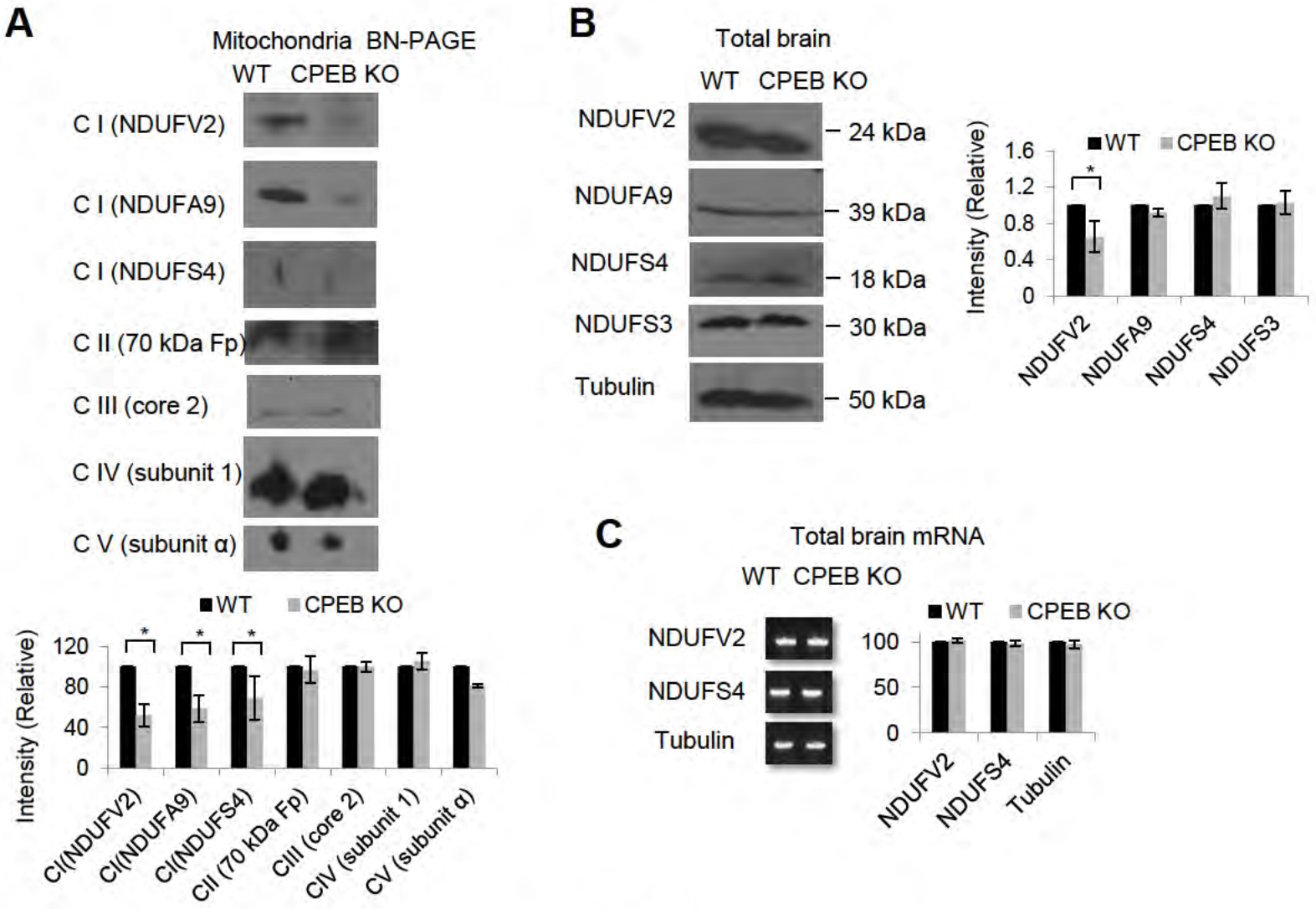
A
Mitochondria BN-PAGE
WT CPEB KO
C I (NDUFV2)
C I (NDUFA9)
C I (NDUFS4)
C II (70 kDa Fp)
C III (core 2)
C IV (subunit 1)
C V (subunit α)
WT
CPEB KO
Intensity (Relative)
120
80
40
0
*
CI(NDUFV2)
CI(NDUFA9)
CI(NDUFS4)
CII (70 kDa Fp)
CIII (core 2)
CIV (subunit 1)
CV (subunit α)
B
Total brain
WT CPEB KO
NDUFV2
NDUFA9
NDUFS4
NDUFS3
Tubulin
24 kDa
39 kDa
18 kDa
30 kDa
50 kDa
Intensity (Relative)
1.6
1.2
0.8
0.4
0
C
Total brain mRNA
WT CPEB KO
100
50
0
Tubulin

Figure 2.5

Complex I protein NDUFV2 expression is reduced in CPEB KO mice

NDUFV2 is one of 14 core catalytic subunits of complex I; it is synthesized in the cytoplasm and imported into mitochondria via an amino terminal mitochondrial targeting sequence (MTS) (Figure 2.6A). To test whether reduced NDUFV2 in CPEB KO mitochondria is responsible for impaired ATP production, CPEB KO neurons were infected with lentiviruses expressing NDUFV2 or as controls, NDUFV2 that lacks either its MTS or NDUFS4. Figure 2.6B shows that ATP levels were restored to nearly WT levels by ectopic MTS-containing, but not MTS-lacking NDUFV2. ATP levels were unaffected by ectopic expression of NDUFS4 (a complex I constituent whose levels were unchanged in CPEB KO) suggesting that the effect on ATP in CPEB KO neurons is specifically due to reduced NDUFV2 (Figure 2.6B). Complex I activity in CPEB KO neurons was also restored to nearly wild-type levels by ectopic expression of NDUFV2 (Figure 2.6C). These results demonstrate that reduced NDUFV2 in CPEB KO neurons leads to deficient mitochondrial ATP production.

NDUFV2 mRNA contains 3' UTR CPEs, which although downstream of the AAUAAA, could still support cytoplasmic polyadenylation (Fox et al., 1989). Based on this observation, we thought this mRNA might be directly regulated by CPEB. To assess this possibility, WT neurons were infected with a lentivirus expressing CPEB-HA, followed by HA immunoprecipitation and RT-PCR analysis for co-precipitating RNAs. As shown in Figure 2.6D, NDUFV2 mRNA was

immunoprecipitated with CPEB-HA but not when the cells were not transduced with CPEB-HA (mock IP). GAPDH and NDUFS4 mRNAs were not co-precipitated with CPEB-HA, indicating its specificity for NDUFV2.

The decrease in amount of NDUFV2 in CPEB KO brains (Figure 2.5B) could be due to decreased translation or increased degradation. To determine whether the synthesis of NDUFV2 is altered in CPEB KO neurons, cells were pulse labeled with ^{35}S-methionine for 1 hour followed by immunoprecipitation with NDUFV2 antibody. Because of the short incubation time, the radiolabeled NDUFV2 reflects new synthesis but very little degradation because protein destruction usually occurs over several hours. Figure 2.6E shows that NDUFV2 was synthesized ~40% less efficiently in CPEB KO compared to WT neurons, suggesting that CPEB mediates the translation of NDUFV2 mRNA. To investigate this possibility further, neurons were transfected with plasmids encoding firefly luciferase mRNA (transfection control) and Renilla luciferase mRNA appended with the NDUFV2 3' UTR containing or lacking the CPEs (see Figure 2.6A). When determined 3 days after transfection, the Renilla luciferase activity was 25% higher when the reporter RNA contained the 3' UTR CPEs (Figure 2.6F). These data indicate that the cytoplasmic polyadenylation elements promote the translation of NDUFV2 mRNA.

Finally, an examination of NDUFV2 mRNA shows that the length of its poly(A) tail was reduced by ~ 30 nts in CPEB KO versus WT brain; the poly(A)

tail of tubulin mRNA was similar in each genotype (Figure 2.6G). Equal amounts of NDUFV2 and tubulin mRNAs from WT and CPEB KO were used for the assay. Taken together, the data in Figure 2.6 indicate that the control of ATP levels in neurons by CPEB is mediated by polyadenylation and translation of NDUFV2 mRNA.

Figure 2.6 CPEB regulates NDUFV2 mRNA translation

(A) Schematic of NDUFV2 mRNA showing the mitochondrial targeting signal, polyadenylation hexanucleotide AAUAAA, and CPEs. (B) ATP was measured in WT and CPEB KO hippocampal neurons infected with lentiviruses expressing NDUFV2, or a mutant NDUFV2 lacking the MTS or NDUFS4. (C) Complex I activity was measured in WT and CPEB KO hippocampal neurons infected with lentivirus expressing NDUFV2. (D) WT hippocampal neurons were infected with lentivirus expressing HA-CPEB. HA antibody was used to co-immunoprecipitate CPEB followed by RT-PCR for NDUFV2, NDUFS4, and GAPDH mRNAs. (E) WT and CPEB KO hippocampal neurons were incubated with ^{35}S-methionine followed by immunoprecipitation of NDUFV2 and analysis by SDS-PAGE. WCE refers to whole cell extract. The histogram shows the quantification of immunoprecipitation. (F) The coding region of Renilla luciferase was appended with the WT NDUFV2 3' UTR or one that lacked the CPEs (3'UTR mut) (see panel A). Plasmids encoding these constructs as well as firefly luciferase to serve as a control were transfected into neurons and analyzed for luciferase activity 3 days later. The data are plotted as the ratio of Renilla luciferase activity to firefly luciferase activity. (G) A PCR-based polyadenylation assay was used to determine the poly(A) tails of NDUFV2 and tubulin mRNAs in WT and CPEB KO brain (primers a/dT anchor). The internal primers (a/b) indicate the relative amount of RNA in each sample. (*$p<0.05$; **$p<0.01$ Student's t test, 3 replicates, the bars indicate SEM).

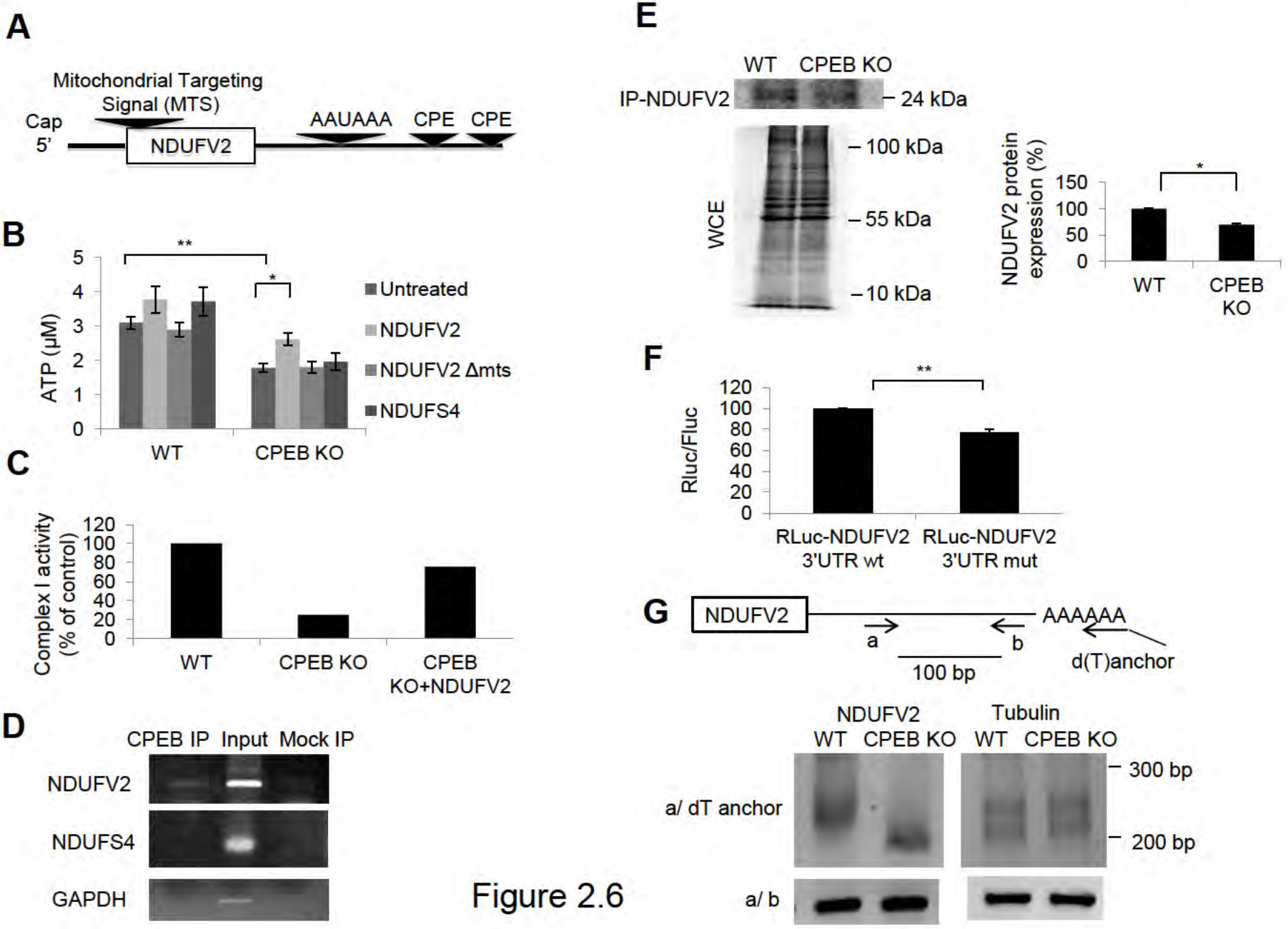
A
Mitochondrial Targeting Signal (MTS)
Cap 5'
NDUFV2
AAUAAA
CPE
CPE
B
ATP (μM)
**
*
Untreated
NDUFV2
NDUFV2 Δmts
NDUFS4
WT
CPEB KO
C
Complex I activity (% of control)
WT
CPEB KO
CPEB KO+NDUFV2
D
CPEB IP
Input
Mock IP
NDUFV2
NDUFS4
GAPDH
E
WT
CPEB KO
IP-NDUFV2
24 kDa
WCE
100 kDa
55 kDa
10 kDa
NDUFV2 protein expression (%)
F
Rluc/Fluc
RLuc-NDUFV2 3'UTR wt
RLuc-NDUFV2 3'UTR mut
G
NDUFV2
AAAAAA
a
b
100 bp
d(T)anchor
NDUFV2
Tubulin
a/ dT anchor
a/ b
300 bp
200 bp

Figure 2.6

Dendritic branching is impaired in CPEB KO mice

We surmised that reduced brain ATP in CPEB KO mice might impair neuron growth and/or morphogenesis. To assess this possibility, neurons from WT and CPEB KO mice were immunostained for tubulin and subjected to a Sholl analysis where concentric rings surrounding a neuron with the cell body in the center are used to measure dendrite branching. Although neurons from both genotypes appeared similar during the initial days of culture, by day 5 (Figure 2.7A) the CPEB KO neurons showed 16% fewer dendrite branches (Figure 2.7B); dendrite length was also reduced by ~19% (Figure 2.7C). This result is similar to that observed by Bestman and Cline (Bestman and Cline, 2008), who examined the role of CPEB in dendrite morphogenesis using *Xenopus laevis* optic tectal neurons. Dendrite branching was restored when CPEB was ectopically expressed in the DIV5 CPEB KO neurons following lentivirus infection (Figures 2.8A-B). Moreover, reduced branching was observed in DIV5 WT neurons following shRNA-mediated CPEB depletion (Figure 2.8A-B). These data demonstrate that CPEB controls dendrite morphology.

To investigate whether reduced ATP production is causative for diminished dendrite arborization, CPEB KO neurons were cultured in medium containing phosphocreatine for 4 days *in vitro*, which increased ATP levels to nearly WT levels (Figure 2.7D) and dendrite branching to near WT levels (Figures 2.7E, F). Treatment of WT neurons with phosphocreatine, which

donates a high-energy phosphate to ADP to produce ATP, enhanced dendrite branching (Figures 2.7E, F). These results indicate that inhibited dendrite development in CPEB KO neurons is most likely due to impaired ATP generation.

Figure. 2.7 CPEB and ATP promote dendritic development.

(A) Morphology of WT and CPEB KO hippocampal neurons immunostained for tubulin at different days of culture. Scale bar= 50 μm. (B) Sholl analysis was performed on WT and CPEB KO neurons cultured for 5 days (n= 60 neurons from 3 mice). (C) Dendrite length was determined for cultured WT and CPEB KO neurons (n= 50 dendrites of 14 neurons from 3 mice). (D) WT and CPEB KO neurons were continuously supplemented with phosphocreatine followed by determination of ATP at DIV6. (E) Morphology of DIV6 WT and CPEB KO neurons following treatment with phosphocreatine; they were immunostained for tubulin (scale bar= 50 μm). (F) Sholl analysis was performed on WT and CPEB KO neurons cultured in phosphocreatine (n=55 neurons from 3 mice) (* $p<0.05$, ** $p<0.01$ Student's t test, 3 replicates; the bars indicate SEM).

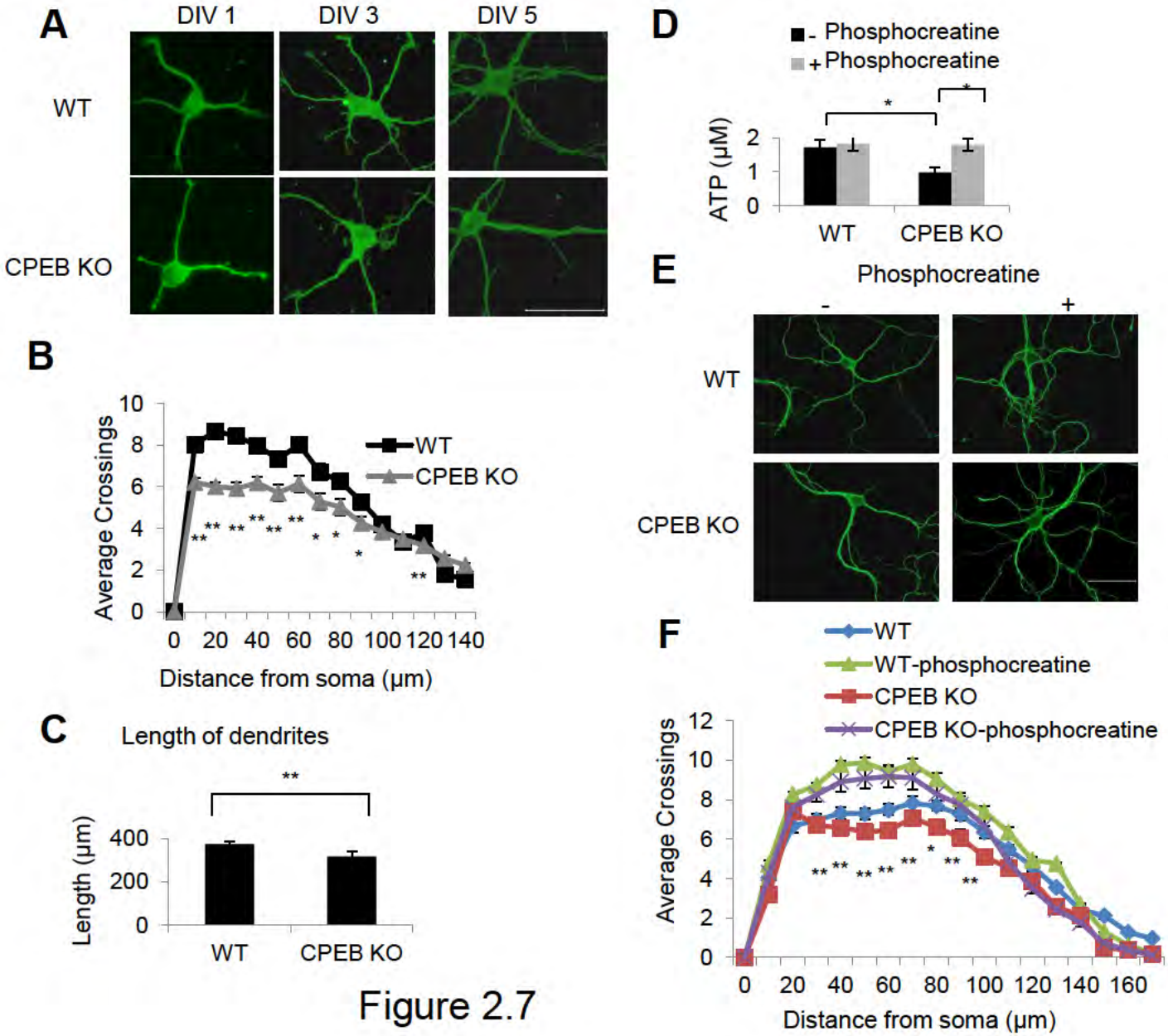
A
DIV 1
DIV 3
DIV 5
WT
CPEB KO
B
Average Crossings
WT
CPEB KO
Distance from soma (μm)
C
Length of dendrites
Length (μm)
WT
CPEB KO
D
- Phosphocreatine
+ Phosphocreatine
ATP (μM)
WT
CPEB KO
E
Phosphocreatine
-
+
WT
CPEB KO
F
WT
WT-phosphocreatine
CPEB KO
CPEB KO-phosphocreatine
Average Crossings
Distance from soma (μm)

Figure 2.7

Figure 2.8. CPEB knockdown and ectopic expression control dendrite branching

(A)WT and CPEB KO hippocampal neurons were treated with lentiviruses expressing shRNA against CPEB (CPEB KD) or HA-tagged CPEB (mCPEB) and dendrite branching was imaged by immunostaining for tubulin. Scale bar= 50 μm. (B) Neurons treated as above were subjected to Sholl analysis. (The bars refer to SEM).

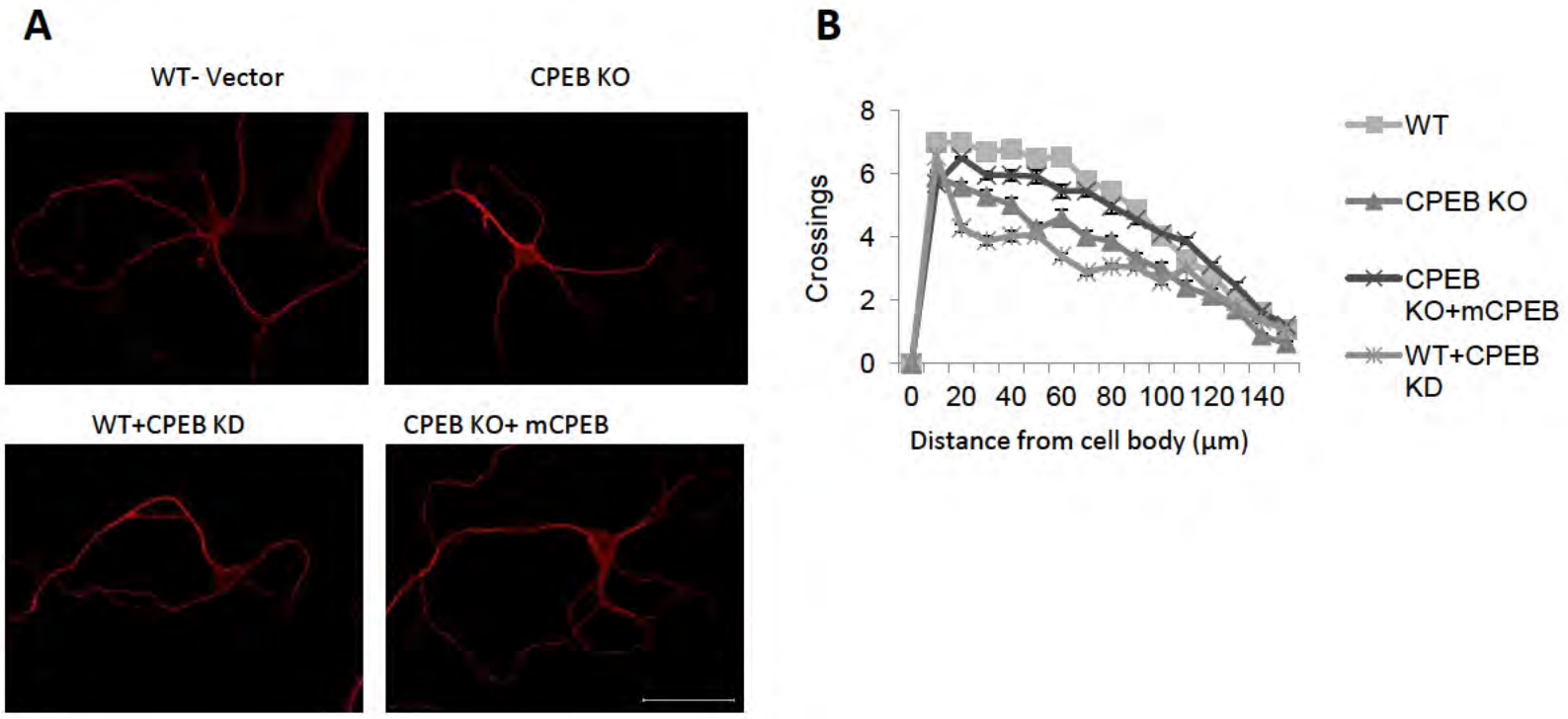
A
WT- Vector
CPEB KO
WT+CPEB KD
CPEB KO+ mCPEB
B
Crossings
0
2
4
6
8
0 20 40 60 80 100 120 140
Distance from cell body (µm)
WT
CPEB KO
CPEB KO+mCPEB
WT+CPEB KD

Figure 2.8

To examine whether CPEB regulates dendrite extension *in vivo*, retroviruses expressing GFP and a scrambled or CPEB-directed shRNA were injected into the dentate gyrus (DG) of 6- to7- week- old mice (Ge et al., 2006). Two weeks post-injection, the dividing DG neurons were analyzed by serial sectioning and 3 dimensional reconstruction of confocal images of GFP-immunostained cells. Total dendrite length and branching were reduced by more than 50% in the knockdown (KD) compared to WT neurons (Figure 2.9A-C). CPEB depletion also reduced dendritic branching complexity of the neurons (Figure 2.9D). Injection of a second shRNA against CPEB resulted in similar deficits in dendrite length and branching (not shown). Taken together, these data demonstrate that CPEB mediates neuronal maturation *in vitro* and *in vivo*.

To assess whether ectopic expression of NDUFV2 in neurons rescues the reduction in dendrite morphology by CPEB depletion *in vivo*, retroviruses expressing CPEB shRNA and NDUFV2 containing or lacking its mitochondrial targeting sequence (MTS) were injected into the DG as was performed previously followed by serial sectioning and 3D reconstruction of GFP-stained images. Figures 2.9 E and F show that dendrite branch number as well as dendritic length were increased upon expression of NDUFV2 containing but not lacking its MTS (mitochondrial targeting sequence). The dendrite branching defect was also rescued by ectopic expression of NDUFV2, but not NDUFS4 in CPEB KO neurons in culture (Figure 2.9G), thus reaffirming the importance of NDUFV2 and mitochondrial energy production in dendrite branching.

Figure 2.9 CPEB and NDUFV2 control dendrite morphology *in vivo*.

(A) Three-dimensional (3D) confocal image reconstruction of dendrites from hippocampal dentate gyrus (DG) neurons that were stereotactically injected with retroviruses expressing GFP (control) or GFP and CPEB shRNA (14 dpi) (scale bar= 20 μm). (B,C) Quantification of total dendritic length and branch number of dividing DG neurons. (D) Sholl analysis of dendrite complexity of dividing DG neurons (14 dpi) (n=4-6 animals) (* $p<0.05$, Student's t test, 3 replicates; ## $p<0.01$, 3 replicates); the bars indicate SEM). (E,F), Quantification of dendritic branch length and number following stereotactic DG injection of retroviruses expressing GFP and shRNA for CPEB plus either WT NDUFV2 or NDUFV2 that lacks its mitochondrial targeting sequence (MTS). (n=12 animals) (G) Sholl analysis of tubulin immunostained WT, CPEB KO and CPEB KO hippocampal neurons infected *in vitro* with lentiviruses expressing NDUFV2 or as control NDUFS4. (the bars indicate SEM).

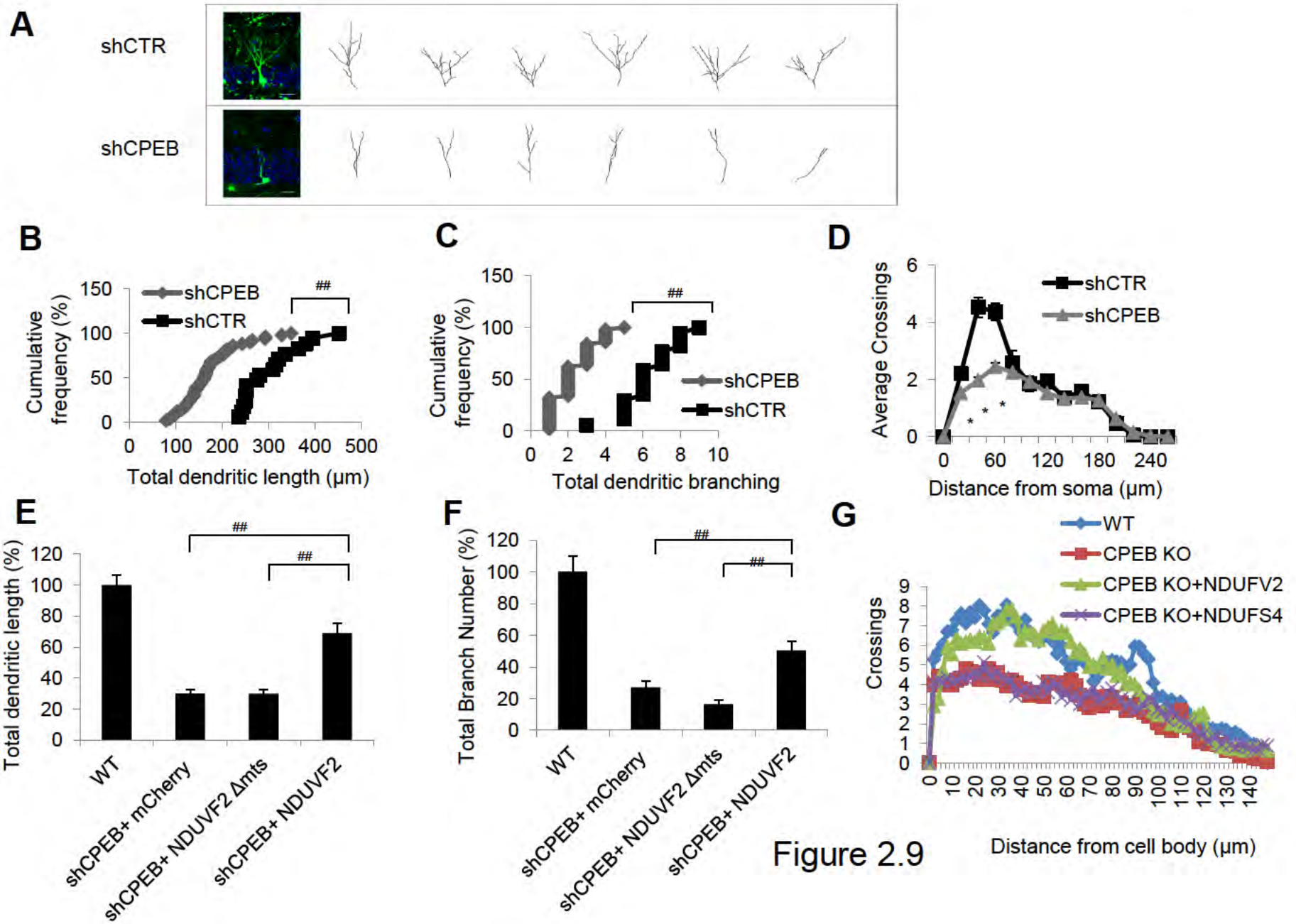
A
shCTR
shCPEB
B
Cumulative frequency (%)
shCPEB
shCTR
##
Total dendritic length (μm)
C
Cumulative frequency (%)
##
shCPEB
shCTR
Total dendritic branching
D
Average Crossings
shCTR
shCPEB
Distance from soma (μm)
E
Total dendritic length (%)
##
##
WT
shCPEB+ mCherry
shCPEB+ NDUVF2 Δmts
shCPEB+ NDUVF2
F
Total Branch Number (%)
##
##
WT
shCPEB+ mCherry
shCPEB+ NDUVF2 Δmts
shCPEB+ NDUVF2
G
WT
CPEB KO
CPEB KO+NDUFV2
CPEB KO+NDUFS4
Crossings
Distance from cell body (μm)

Figure 2.9

Figure 2.10 shows a model that summarizes the data described above. In wild-type neurons, CPEB is associated with the 3' UTR CPEs of NDUFV2 mRNA. At steady state or perhaps in response to an environmental cue, CPEB promotes poly(A) tail growth and translation of the mRNA, resulting in NDUFV2 protein import into the inner mitochondrial membrane where it is incorporated into complex I, thereby increasing flow of electrons through the electron transport chain and finally ATP is generated. When neurons are CPEB deficient, reduced NDUFV2 mRNA translation and ATP production lead to neurite stunting and perhaps loss of synaptic connections and inhibited synapse efficacy (Alarcon et al., 2004; Zearfoss et al., 2008).

Figure 2.10 Model for CPEB control of energy production in neurons.

CPEB associates with the 3'UTR CPEs of NDUFV2 mRNA in the cytoplasm of neurons. This interaction promotes poly(A) tail growth and translation of NDUFV2 mRNA resulting in mitochondrial import of NDUFV2 protein, its incorporation into complex I, and elevated ATP production. ATP in turn is necessary for promoting neurite morphogenesis. In CPEB knockout (KO) neurons, a short poly(A) tail of NDUFV2 mRNA results in inefficient translation, which impedes complex I assembly and the generation of ATP. As a consequence, neurite outgrown is curtailed.

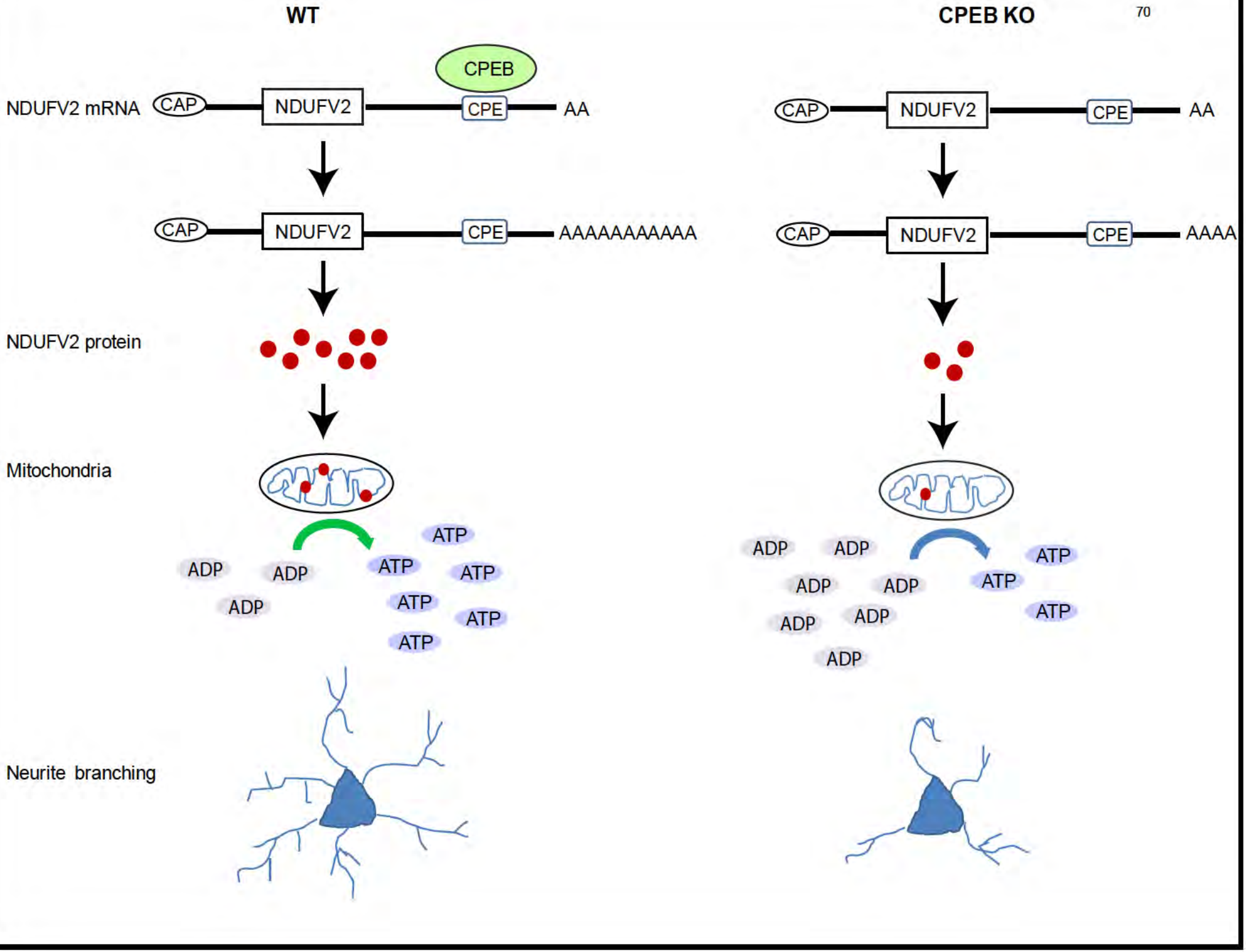
WT
CPEB KO
CPEB
NDUFV2 mRNA
CAP
NDUFV2
CPE
AA
AAAAAAAAAA
AAAA
NDUFV2 protein
Mitochondria
ATP
ADP
Neurite branching

Discussion

Our studies show that in CPEB KO brain and neurons, deficient polyadenylation-induced translation of the complex I component NDUFV2 mRNA impairs mitochondrial ATP production, thus demonstrating a role for translational control in mouse neuronal bioenergetics. Why CPEB deficiency should inhibit ATP production only in the brain is unclear, but neurons as well as germ cells contain the greatest abundance of this protein, and thus NDUFV2 mRNA may not be regulated in other tissues because of a relative paucity of CPEB. Complex I levels also differ among tissues, which have different energy requirements and sensitivities to defects in oxidative phosphorylation (Distelmaier et al., 2009; Koopman et al., 2010; Kunz, 2003). Perhaps the brain, which is the largest consumer of energy, may require CPEB to stimulate ATP generation in response to stress or synapse stimulation (Kann and Kovacs, 2007; Nicholls and Budd, 2000). It is important to note that steady state levels of ATP are the result of both generation and consumption by cells. Although our report demonstrates that CPEB controls ATP production by enhancing the translation of complex I protein NDUFV2 mRNA, we cannot rule out a possible effect of CPEB on ATP consumption as well. The control of ATP production by CPEB reported here contrasts to that which occurs during the Warburg Effect. In transformed cells, aerobic glycolysis is due in part to aberrant splicing of pyruvate kinase; a

predominant embryonic isoform, PKM2, is produced instead of the adult PKM1 form (Christofk et al., 2008; David et al., 2010). As a consequence, conversion of phosphoenolpyruvate (PEP) to pyruvate is reduced, limiting the amount of substrate for the tricarboxylic acid cycle (TCA) but stimulating the amount available for glycolysis (Chen et al., 2010).

Experiments using Xenopus oocytes demonstrated that Aurora A-catalyzed CPEB phosphoryation is necessary to stimulate very robust polyadenylation and translation (Barnard et al., 2004; Groisman et al., 2002; Kim and Richter, 2006; Mendez et al., 2000). In neurons, CPEB phosphorylation is also important for polyadenylation in response to synaptic activity (Udagawa et al., 2012). In these cases, CPEB responds to external signaling cues (hormones, synaptic stimulation) to promote the expression of generally quiescent or at least inefficiently translated mRNAs. This CPEB-mediated on-off switch for translation may not function in quite the same way for the polyadenylation of NDUFV2 mRNA observed here. That is, NDUFV2 would always be synthesized at some basal rate, but its expression might be turned up at times when ATP generation is particularly important such as when neurites respond to guidance cues as they navigate to their final destinations. Thus, CPEB may act more like a rheostat to turn translation up or down rather than a switch to turn translation on or off. The rheostat analogy may be similar to the case in MEFs or primary human fibroblasts where CPEB controls the expression of p53 in a relatively modest manner, although even a 50% change in p53 mRNA

translation results in large alterations in cell physiology such as senescence bypass (Burns and Richter, 2008; Groisman et al., 2006; Groppo and Richter).

The importance of CPEB phosphorylation for neurite outgrowth was suggested by experiments of Bestman and Cline (Bestman and Cline, 2008, 2009), who electroporated a phosphorylation-defective “dominant negative” CPEB into Xenopus tadpole optic tectal neurons and observed reduced dendrite branching as well as glutamatergic synaptic strength. These authors also showed that antisense morpholinos directed to CPEB mRNA, which would inhibit its translation, produced a similar effect. In this same vein, Lin et al (Lin et al., 2009) demonstrated that a “dominant negative” CPEB introduced into Xenopus retinal ganglion neurons inhibited axon growth cones from properly extending axons. Although neither study identified the mRNA substrate(s) whose presumed reduced translation was responsible for the morphological defects in the neurons transduced with the dominant negative CPEB, our observations suggest that reduced ATP production caused by impaired NDUFV2 mRNA translation could be involved.

Because CPEB is transported to dendrites (Huang et al., 2003) where it mediates polyadenylation (Udagawa et al., 2012), we surmise that NDUFV2 mRNA polyadenylation and translation also occurs in dendrites and probably cell bodies as well. Mitochondria are present at the base of dendritic spines where their ATP production is important for synapse function (Li et al., 2004). We

envision that dendritic ATP is also important for neurite outgrowth and morphogenesis and that when neurons are CPEB-deficient, reduced NDUFV2 mRNA translation and ATP production lead to neurite stunting and perhaps loss of synaptic connections and inhibited synapse efficacy (Alarcon et al., 2004; Zearfoss et al., 2008). Moreover, synapse stimulation not only induces CPEB-dependent polyadenylation (Udagawa et al., 2012), but alterations in mitochondrial transport and localization as well (Chen and Chan, 2006). Thus, the CPEB-mediated increase in mitochondrial activity could be an additional layer of stimulation-dependent regulation of ATP production.

Mitochondrial dysfunction is linked to several neurologic diseases including Parkinson's, Alzheimer's, and Huntington's diseases as well as amyotrophic lateral sclerosis (Lin and Beal, 2006). Aberrant complex I in particular may be causative for Leigh disease, a neurodegenerative disorder (Loeffen et al., 1998), and a number of encephalopathies such as seizures, brainstem lesions, and dystonia (Distelmaier et al., 2009). These observations suggest that CPEB KO mice might also show signs of neurodegeneration elicited by impaired complex I activity. Gross examination of the CPEB KO mice shows no obvious signs of this malady, however, neurodegenerative diseases are progressive and may become obvious only in older mice. Consequently, further investigations are required to determine whether there is a neurodegenerative consequence to CPEB deficiency. In any case, CPEB KO mice display reduced complex I activity by only ~50%, which might be insufficient to cause obvious

phenotypes such as those noted above. On the other hand, CPEB depletion reduces dendrite branching and development in the brain and alters synaptic efficacy. Moreover, impaired mitochondrial function inhibits dendrite spine density and synaptic plasticity (Li et al., 2004), suggesting that in the case of CPEB KO mouse, defective complex I could be responsible, at least in part, for a deficit in hippocampal long-term potentiation and hippocampus-dependent learning and memory which could be tested by generating a transgenic CPEB KO mouse which over-expresses NDUFV2 and testing the LTP, learning and memory phenotypes (Alarcon et al., 2004; Berger-Sweeney et al., 2006).

Materials and Methods

Animals, neuron culture, and isolation of mitochondria

WT and CPEB C57BL/6 KO mice (Tay and Richter, 2001) were maintained in accordance with Institutional Animal Care and Use Committee (IACUC) of the University of Massachusetts Medical School.

The culture of primary hippocampal and cortical neurons was performed as described (Huang and Richter, 2007) in Neurobasal media (Invitrogen) containing B27 supplement (B27 media) and glutamine (1 µg/ml). Liver, muscle, and brain were dissected from 1 month old female mice, washed and homogenized in Krebs-Ringers bicarbonate buffer (125 mM NaCl, 1.4 mM KCl, 20 mM HEPES, pH 7.4, 5 mM $NaHCO_3$, 1.2 mM $MgSO_4$, 1.2 mM KH_2,PO_4, 1 mM $CaCl_2$) containing 1% BSA. Protein concentrations were determined using the BCA assay (Pierce). Mitochondria were isolated using a MITO-ISO1 kit (Sigma) and following the manufacturer's instructions.

ATP determination

Fifty to 100 µg of brain lysate was used to measure ATP concentration using the CellTiter-Glo Luminescent Cell Viability kit (Promega) in a 96 well format. To measure ATP concentration in neurons, 60,000 cells were trypsinized from the dish, washed, and resuspended in 100 µl Krebs-Ringers bicarbonate buffer plus

HEPES. The brain lysates and the cultured neuron lysates were aliquoted into 96 well plates and assayed according to manufacturer's instructions. To measure the recovery of ATP from brain lysates, known amounts of ATP (0.1, 1, 10, and 100 μM) were used to measure ATP bioluminescene using the CellTiter-Glo method as above in presence or absence of WT or CPEB KO brain lysate. The recovery of ATP was calculated from these values.

Oxygen consumption

To measure oxygen consumption in brain lysates, WT and CPEB KO mouse brains were washed and homogenized in 1 ml Krebs-Ringers bicarbonate buffer plus HEPES (125 mM NaCl, 1.4 mM KCl, 20 mM HEPES, pH 7.4, 5 mM $NaHCO_3$, 1.2 mM $MgSO_4$, 1.2 mM KH_2,PO_4, 1 mM $CaCl_2$) containing 1% BSA. Fifty to 100 μg of protein from each lysate was aliquoted into a BD Oxygen biosensor systems plate (BD Biosciences) in triplicate and assayed on a SAFIRE multimode microplate spectrophotometer at 1 min intervals for 120 min at an excitation wavelength of 485 nm and emission wavelength of 630 nm. To measure oxygen consumption in neurons and glia, 80,000 cells were washed, suspended in 200 μl Krebs-Ringers bicarbonate buffer, and aliquoted onto a BD Oxygen Biosensor systems plate in triplicate and assayed as described above. To measure non-mitochondrial oxygen consumption, the brain lysates and neurons were treated with 1 μM rotenone plus 10 μM antimycin.

Lentivirus production

Lentiviruses expressing CPEB, NDUFV2, NDUFV2 Δmts or NDUFS4 were constructed by inserting mCPEB-HA, NDUFV2-HA, NDUFV2 Δmts-HA or NDUFS4 into the BamHI and XhoI sites of pFugw vector (Addgene). For virus production, 10 µg of virus transfer vector that expressed the various constructs, 5 µg gag-pol expressing vector, psPAX2 (from Addgene), and 5 µg VSV-G expressing vector, pMD2.G (from Addgene) were co-transfected into $1X10^7$ 293T cells plated in 10 cm culture dishes using the calcium chloride method. Twenty-four hours after transfection, the medium was replaced with Neurobasal medium containing B27 supplement (B27 media). Forty-eight hours after transfection, the medium containing lentivirus was collected and passed through a 0.45 µm filter. To deplete CPEB, a pll 3.7 vector harboring shRNA against CPEB or a non-silencing control was used to generate the lentivirus as described above.

Mitochondrial DNA measurement

Total genomic DNA was isolated from WT and CPEB KO brains using a Gentra Puregene Tissue kit (Qiagen). Mitochondrial DNA was PCR amplified using the primers 5' ACCATTTGCAGACGCCATAA 3' and 5'TGAAATTGTTTGGGCTACGG3' to amplify the region between 2891 and 3173. PCR amplification was carried out in a 20 µl volume containing 10 µl Gotaq Green master mix (Promega), 1 µM each primer, and 20 ng of DNA. The PCR cycling conditions were: initial denaturation 94 °C for 3 mins, then 18 cycles of denaturation at 94 for °C for 1 min 30 secs, annealing at 53 °C for 2 min and

elongation at 72 °C for 2 min 30 secs followed by final denaturation at 72 °C for 13 mins.

TMRM staining

Cultured hippocampal neurons from WT and CPEB KO mice grown on coverslips for various days *in vitro* (DIV) were treated with 200 nm TMRM for 30 mins after which time they were washed with PBS and imaged using a Nikon ECLIPSE E600 fluorescence microscope. The fluorescent signal was then quantified using ImageJ software.

Lactate measurement

The concentration of lactate in 40,000 neurons was measured as described (Chang et al., 1992). The NADH produced by conversion of lactate to pyruvate by lactate dehydrogenase was measured at 340 nm using a SAFIRE spectrophotometer. Fifty to 100 µg of brain lysate or 40,000 neurons were suspended in 250 µl PBS before addition of HCl to a final concentration of 0.03 N. The cells were then suspended in 50µl of 400 mM 2-amino-2-methylpropanol (Sigma), pH 9.9. A 4 ml assay cocktail containing 1 ml 15mM β-nicotinamide adenine dinucleotide (Sigma), 1 ml 400mM glutamate, pH 9 in 10mM PBS, and 2 ml 10mM PBS, pH6.5. A typical assay included 40µl assay cocktail, 100µl sample or lactate standards (to generate a standard curve). Using a Tecan plate reader, absorbance of 340nm light prior to incubation with enzymes was performed. Twenty microliters of enzyme cocktail (200 U/ml L-lactate

dehydrogenase and 80 U/ml glutamic-pyruvic transaminase in 10mM phosphate buffer, pH 6.5) was then added and the mixture was incubated 20 min at room temperature; absorbance at 340nm was then measured.

Mitochondrial morphology determination

To label mitochondria, neurons grown on coverslips were incubated with 100 nM mitotracker green FM for 20 min. Images were obtained using Zeiss AxioVert Confocal with a PerkinElmer UltraView Spinning Disc.

Electron transport chain enzyme activities

Purified mitochondrial samples were freeze-thawed three times before use in enzyme analysis to enable access of the substrate to the inner mitochondrial membrane. Enzyme activities were determined by adding exogenous substrates of the respective complexes and measuring the rate of conversion to product in isolated mitochondria. All analyses were performed on an Ultraspec 2000 UV/visible spectrophotometer (Pharmacia Biotech) in triplicate. Specific enzyme activities were calculated by subtracting the background activities using inhibitors to the complexes.

Complex I

Complex I activity was determined by measuring the decrease in absorbance of NADH at 340 nm (Birch-Machin and Turnbull, 2001). The assay was performed in buffer containing 50 mM KH_2PO_4, pH 7.4, 2 mM KCN, 5 mM $MgCl_2$, 2.5 mg/mL

BSA, 2 µM antimycin, 100 µM decylubiquinone, and 0.3 mM K_2NADH.The reaction was started by adding purified mitochondria (20 µg) and the absorbance was measured every 30 secs for 5 min. Specific activity was measured by calculating slope of the reaction in the presence or absence of 1 µM of the complex I inhibitor rotenone.

Complex II

Complex II activity was determined by measuring reduction of DCIP at 600 nm (Ellis et al., 2005). The assay was performed in buffer containing 25 mM potassium phosphate, pH 7.4, 20 mM succinate, 2 mM KCN, 50 µM 2,6-Dichlorophenolindophenol (DCIP), 2 µg/mL rotenone, 2 µg/mL antimycin and 10 µg purified mitochondria. The reaction was initiated by adding 56 µM decylubiquinone. Specific activities were measured by calculating the slope of the reaction in the presence or absence of 0.5 mM thenolytrifluoroacetone, a complex II inhibitor.

Complex III

Complex III activity was determined by measuring the reduction of cytochrome C at 550 nm. The assay was performed in buffer containing 25 mM potassium phosphate, pH 7.2, 5 mM succinate, 5 µM rotenone, 1 mM KCN, 50 µM cytochome C and 20 µg purified mitochondria. The absorbance was measured every 30 secs for 5 min and specific activity determined by calculating slope of

the reaction in presence or absence of 10 µg/ml antimycin A, a complex III inhibitor.

Complex IV

Complex IV activity was determined by measuring oxidation of ferrocytochrome C at 550 nm. Five µg of purified mitochondria was used to perform the assay using a COX activity kit (Sigma) following the manufacturer's instructions. The specific activity was determined by calculating slope of the reaction in the presence or absence of 2.2 mM KCN, a complex IV inhibitor.

Citrate synthase

Citrate synthase activity was measured using 100 µl purified mitochondria in a total of 1 ml reaction solution containing 0.1 mM DTNB (Sigma), 0.15 mM acetyl-CoA (Roche), 0.5 mM oxaloacetate (Sigma), and 65 mM Tris pH 8.1 (USB). Oxaloacetate was added just prior to the measurement. The absorbance was measured at 412 nm every 20 sec for 3 mins using the Ultraspec 2000 UV/visible spectrophotometer. The slope was calculated using Microsoft EXCEL. The citrate synthase activities were normalized to the total protein content.

Measurement of mitochondrial respiration

Mitochondria were isolated from WT and CPEB KO mouse brain using differential centrifugation as described earlier. Oxygen consumption in the intact

mitochondria was measured using Clark type oxygen-sensitive electrode (YSI Incorporated). The assays were performed as described (Li and Graham, 2012).

Blue Native PAGE electrophoresis

Mitochondria isolated from WT and CPEB KO mouse brain were resolved by Blue Native (BN)-PAGE as described (Wittig et al., 2006) and immunoblotted for mitochondrial proteins. 100 µg mitochondria was solubilized in 10 µl solubilization buffer (50 mM sodium chloride, 100 mM Bis-tris, 2 mM 6-aminohexanoic acid, 1 mM EDTA, pH 7) and permeabilized at room temperature for 10 min using 2 µl of 20% sodium dodecylmaltoside. The permeabilized mitochondrial fraction was collected by centrifugation at 20,000 xg for 25 min at 4 °C; to the supernatant, 2 µl of 50% glycerol and 1 µl of 5% Coomassie Blue G-250 dye was added and loaded on 4-15 % Blue Native Bis-tris gel (NuPAGE, Invitrogen). The cathode buffer was 50 mM Tricine, 15 mM Bis-tris, and 0.02 % Coomassie Blue G-250 and the anode buffer was 50 mM Bis-tris, pH 7. The gel was run at 4 °C with the current limited to 15 mA and voltage limited to 500 V. After the dye front had moved about one-third of the distance, the cathode buffer was removed and replaced with cathode buffer containing 0.002% Coomassie Blue. After completion of the run, the proteins were immunoblotted onto PVDF membrane using electroblotting buffer (50 mM Tricine, 7.5 mM Bis-tris, pH 7) at 4°C for 3 hr with voltage set to 30 V. The membrane was destained with methanol and immunoblotting was performed using antibodies against the ETC complex

proteins NDUFV2 (Genetex 1:1000), NDUFS4 (Mitosciences 1:1000), NDUFA9 (Mitosciences 1:1000), NDUFS3 (Mitosciences 1:1000), CII subunit 70 kDa Fp (Mitosciences 1:1000), CIII subunit core 2 (Mitosciences 1:1000), CIV subunit 1 (Mitosciences 1:1000), and ATP synthase subunit alpha (Mitosciences 1:1000).

Reactive oxygen species measurement

ROS levels in 50 to 100 µg of brain lysate or 160,000 hippocampal neurons were determined using 10 µm CM-H_2DCFDA (5-(and-6)-chloromethyl-2',7'-dichlorodihydrofluorescein diacetate, acetyl ester, (Invitrogen) in Krebs ringer bicarbonate buffer. CM-H_2DCFDA was excited at 504 nm and the emission at 529 nm was recorded every 5 mins for 1 hr in a Tecan plate reader.

Oxidative damage measurement

Proetin carbonyl content was measured in lysates prepared from WT and CPEB KO mice brains using the 2,4-dinitrophenylhydrazine (DNPH) method as described (Forster et al., 1996). Brain lysate was made in 5 mM phosphate buffer (pH 7.5) containing 0.1 % Triton X-100 and protease inhibitors. The homogenate was centrifuged at 700 g and 300 µl aliquots of the supernatant were treated with 300 µl of 10 mM DNPH or with 2 M HCl as control. Samples were incubated at room temperature for 1 hr, precipitated with 10% TCA and centrifuged for 3 min at 16000g. The pellet was washed 3 times with Ethanol/ Ethyl acetate (1:1 vol/vol) and redissolved in 1 ml 6 M guanidine. Difference in absorbance between

DNPH treated and HCl treated samples was determined at 366 nm and the results expressed as nmol carbonyl groups/mg protein.

RNA analysis

Total RNA was extracted from WT and CPEB KO mouse brain (100 mg) using 1 ml Trizol (Invitrogen) according to the manufacturer's instructions.

Co-immunoprecipitation and RT-PCR

Immunoprecipitation of mRNA-protein complexes was carried out on DIV 6 cortical neurons infected with pFugw-CPEB-HA as described (Peritz et al., 2006). Immunoprecipitation was carried out using anti-HA antibody (Covance). The following gene specific primers were used for the 18 cycle PCR reaction carried out in a 20 µl reaction volume. The primers used for PCR were:

NDUFV2 forward primer- 5' CGAAAGCCAGTTGGGAAGTA,

NDUFV2 reverse primer- 5' CATCGGTGCATTTACACAGG,

NDUFS4 forward primer- 5' AATGGCTACAGCTGCCGTTT,

NDUFS4 reverse primer- 5' AAGCTGTGTGTCCCGAGTCT,

GAPDH forward primer- 5' CCTCAACTACATGGTCTAC,

GAPDH reverse primer- 5' CCTTCCCACATGCCAAAGT

Translational efficiency

DIV10 WT hippocampal neurons were co-transfected with 2 µg of pGL-3 and 2 µg of pRLTK-NDUFV2 3'UTR WT or 2 µg pRLTK-NDUFV2 3'UTR mutant. The transfected neurons were analyzed for Renilla luciferase and firefly luciferase using the dual luciferase assay system (Promega). The Renilla luciferase values were normalized to the firefly luciferase activity levels, which accounts for transfection efficiencies.

Metabolic labeling

DIV 6 cortical neurons were cultured in 100 mm plate for 30 min in methionine and cysteine free media (Invitrogen); 60 µCi ^{35}S-methionine (ProMix, Amersham) was then added and the cells were cultured for 1 hr. The radioactive media was removed, the cells were washed with 2 ml ice-cold PBS and scraped off the plate and pelleted. The cells were suspended in 1 ml of 50 mM Tris-HCl, pH 8, 150 mM sodium chloride, 1% NP-40, 0.5 % sodium deoxycholate, 0.1% SDS and protease inhibitors (Complete ULTRA tablets, Roche Applied Science) and incubated on ice for 30 min. The lysate was cleared by centrifugation at 16,000 g for 15 min at 4 °C. The supernatant was used for immunoprecipitation. To 40 µl slurry of protein A Sepharose beads, 5 µl NDUFV2 antibody (Genetex) was added and the mixture rotated for 1 hr. in a cold room. Lysates from WT and CPEB KO cells containing equivalent counts of radioactivity were then added to the antibody-protein A bead mixture, which was rotated overnight at 4 °C. The

beads were washed 3 times with ice cold wash buffer (50 mM Tris, pH 7.4, 300 mM sodium chloride, 5 mM EDTA, 0.1 % triton-100) and resuspended in 100 µl SDS gel loading buffer for analysis by electrophoresis and phosphorimaging.

PAT assay

For analysis of the poly(A) tail of the NDUFV2 mRNA, 10 µg of total RNA was extracted from brain using Trizol reagent (Invitrogen) and following the manufacturer's instructions. The RNA was annealed to oligo d(T) anchor (200 ng/µl; 5' GCGAGCTCCGCGGCCGCGTTTTTTTTTTTT 3') at 65 °C for 5 min and then extended in a cDNA synthesis reaction using Superscript III (Invitrogen) at 50 °C for 60 min according to manufacturer's instructions. 1 µl of cDNA template along with NDUFV2-specific primer and oligo d(T)anchor were used in a 25 µl PCR reaction with GoTaq (Invitrogen). PCR products were analyzed on 2.5 % agarose gels.

Quantification of dendritic growth

Hippocampal neurons grown on coverslips were fixed in 4% paraformaldehyde in PBS containing 4% sucrose for 20 mins at room temperature at various days *in vitro* (DIV). Coverslips were washed in PBS, permeabilized in 0.2 % Triton X-100 for 7 min, blocked in 10% BSA solution and immunostained with anti-alpha tubulin (Sigma, 1:1000 dilution). The neurons were then imaged using Nikon ECLIPSE E600 fluorescence microscope. The length of branches was calculated by tracing the dendrites in NeuronJ (plugin in ImageJ) software. The

amount of branching was determined using the Sholl analysis plugin in ImageJ (NIH) software. Other neurons were supplemented daily with 1 mM phosphocreatine on DIV 2,3,4,5 before performing Sholl analysis on DIV 6.

Construction, production and stereotactic injection of engineered retroviruses

Engineered self-inactivating murine retroviruses were used to express GFP specifically in proliferating cells and their progeny. GFP expression was under the control of the eEF1α promoter and the shRNA was co-expressed under the control of the human U6 promoter in the same vector. shRNA against mouse CPEB (position 1466: gtcgtgtgactttcaataa) was cloned into a retroviral vector using a PCR SHAGing strategy. Adult (7-8 weeks old) female C57Bl/6 mice (Charles River) housed under standard conditions were anaesthetized (100 µg ketamine, 10 µg xylazine in 10 µl saline per gram) and retroviruses were stereotactically injected into the dentate gyrus as previously described (Ge et al., 2006). Mice were sacrificed at 14 days post infection (dpi) for morphological analysis. Images were acquired on a Carl Zeiss LSM 710 confocal system and analyzed using Carl Zeiss Zen software. For analysis of the dendritic structure of neurons, the images were semi-automatically traced with NIH ImageJ using the NeuronJ plugin. Only granule cells with complete dendritic trees that were not overlapping with the other infected neurons were used for morphological characterization (neurons from 4 to 6 animals per condition were examined. The

Sholl analysis for dendritic complexity was carried out by counting the number of dendrites that cross a series of concentric circles at 20 μm intervals from the soma. For ectopic expression of NDUVF2, a retroviral construct encoding for NDUVF2 fused to mCherry via a T2A linker was used (Szymczak et al., 2004). To determine whether NDUFV2 expression can rescue the dendritic branching dysfunction in the CPEB-deficient neurons *in vivo*, mouse DG were stereotactically injected with either of three groups of retroviruses: group 1 contained viruses expressing shRNA for CPEB and mcherry; group 2 contained viruses expressing shRNA for CPEB and wild type NDUFV2; group 3 contained viruses expressing shRNA for CPEB and NDUFV2 that lacked its mitochondrial targeting sequence (MTS). The neurons were then analyzed as described above. Statistical significance ($p < 0.001$) was determined by 1-way ANOVA with Newman-Keuls' post hoc test. All animal procedures and applicable regulations of animal welfare were in accordance with the Institutional Animal Care and Use committee (IACUC) guidelines and were approved by Singhealth IACUC in Singapore.

Statistical analysis

Data were interpreted using Students t-test and the error bars indicate Standard Error of Mean (SEM). Statistical significance was determined by 1-way ANOVA with Newman-Keuls' post hoc test.

Acknowledgements

We thank Nemisha Dawra and Maria Ivshina for mouse genotyping, Silvia Corvera for use of her clark type oxygen electrode, plate reader and cytochrome c antibody, and members of the Richter lab for helpful discussions. TU was supported by fellowship from the FRAXA Foundation. This work was supported by grants from the NIH (AG30323, GM46779, and HD37267). Additional core support from the Diabetes Endocrinology Research Center (DK32520) is gratefully acknowledged.

Preface to Chapter III

A large part of the work presented in this Chapter was a collaborative effort between Ming Chung Kan (MCK), a former graduate student, and I (AO). Nuclear localization of CPEB4 upon NMDA stimulation was discovered by MCK but the immunostaining for the same as presented in this chapter was performed by AO. CPEB4 localization in dendrites was jointly performed by MCK and AO. MCK discovered the various effectors for CPEB4 nuclear localization and identified the nuclear localization and export signals. Identification of CPEB family members as nucleo-cytoplasmic shuttling proteins was done by MCK. Ischemia and Oxygen glucose deprivation studies were also performed by MCK in collaboration with Guang Jin in Dr. Klaus van Leyen's lab. The role of nuclear CPEB4 in neuronal survival was revealed by AO. Immunoelectron microscopic visualization of CPEB4 on endoplasmic reticulum was performed by Amalene Cooper-Morgan, a postdoctoral associate. The importance of endoplasmic reticulum calcium reduction as opposed to cytoplasmic calcium increase as the main reason for CPEB4 nuclear localization was elucidated by AO.

CHAPTER III

CPEB4 is a Cell Survival Protein Retained in the Nucleus Upon Ischemia or Endoplasmic Reticulum Calcium Depletion

Ming-Chung Kan[1*], Aparna Oruganty-Das[1*], Amalene Cooper- Morgan[1], Guang Jin[2], Sharon Swanger[3], Gary Bassell[3], Harvey Florman[4], Klaus van Leyen[2], and Joel D. Richter[1]

[1]Program in Molecular Medicine

[4]Department of Cell Biology

University of Massachusetts Medical School, Worcester, MA 01605

[2]Neuroprotection Research Laboratory

Massachusetts General Hospital, Charlestown, MA 02129

[3]Departments of Cell Biology and Neurology

Emory University School of Medicine, Atlanta, GA 30322

*equal contributors

Abstract

The RNA binding protein CPEB regulates cytoplasmic polyadenylation and translation in germ cells and the brain. In neurons, CPEB is detected at postsynaptic sites as well as in the cell body. The related CPEB3 protein also regulates translation in neurons albeit probably not through polyadenylation; it as well as CPEB4 is present in dendrites and the cell body. Here, we show that treatment of neurons with ionotropic glutamate receptor agonists causes CPEB4 to accumulate in the nucleus. All CPEB proteins are nucleus-cytoplasm shuttling proteins that are retained in the nucleus in response to calcium-mediated signaling and αCaMKII activity. CPEB2, 3, and 4 have conserved nuclear export signals that are not present in CPEB. CPEB4 is necessary for cell survival, and becomes nuclear in response to focal ischemia *in vivo* and when cultured neurons are deprived of oxygen and glucose. Further analysis indicates that CPEB4 nuclear accumulation is controlled by the depletion of calcium from the ER, specifically through the IP3 receptor indicating a communication between these organelles in redistributing proteins between subcellular compartments.

Introduction

The Cytoplasmic Polyadenylation Element Binding (CPEB) protein, a sequence-specific RNA binding protein, is found in the cell body and at synapses of hippocampal and other neurons; in response to synaptic experience, CPEB promotes polyadenylation and translation (Richter, 2007; Wells et al., 2001; Wu et al., 1998). CPEB knockout mice (Tay and Richter, 2001) have deficiencies in synaptic plasticity, particularly theta-burst induced long-term potentiation (LTP) (Alarcon et al., 2004; Zearfoss et al., 2008), as well as in particular forms of hippocampus-dependent memories (Berger-Sweeney et al., 2006). Some of these CPEB-related functions may be related at least in part to its ability to direct CPE-containing RNA transport in dendrites (Huang et al., 2003) in addition to its regulation of translation (Zearfoss et al., 2008).

In neurons, most of the CPEB-related proteins CPEB3 and CPEB4 are found in the cell soma. However, a relatively small amount of these proteins is localized to synaptic regions and co-fractionate with postsynaptic density proteins, suggesting possible roles in RNA translation and/or localization (Huang et al., 2006). While investigating the possible translocation of CPEB3 and 4 to dendritic spines in response to N-methyl-D-aspartate (NMDA) receptor activation, as is the case with Fragile X mental retardation protein (FMRP) (Ferrari et al., 2007), we noticed a surprising re-localization of CPEB4 from the cell soma to the

nucleus. Although the treatment of neurons with ionotropic glutamate receptor activating agents such as glutamate and AMPA, as well as NMDA, induced nuclear localization of CPEB4, an agonist of the metabotropic glutamate receptors, dihydroxyphenylglycine (DHPG), did not. CPEB4 remained cytoplasmic when CaMKII activity was inhibited, suggesting a link between calcium levels and nuclear import and/or retention. When fused to epitope tags and expressed in neurons, CPEB, CPEB3, and CPEB4 also became concentrated in the nucleus in response to NMDAR activation. All three proteins, however, were also nuclear when neurons were treated with leptomycin B (LMB), an agent that inactivates the nuclear export factor, chromosome region maintenance 1 (Crm1), indicating that CPEB family proteins are continuously shuttling between the nucleus and cytoplasm. Moreover, these data suggest that NMDAR activation does not necessarily induce nuclear translocation, but nuclear retention of the CPEB proteins.

One physiological event that causes widespread glutamate overload is ischemia, which occurs when the brain's supply of glucose and oxygen is disrupted by stroke or cardiac arrest (Plum, 1983). ATP production is reduced when the blood supply is insufficient, causing neuron polarization and accumulation of glutamate in the extracellular space due to reversed uptake(Rossi et al., 2000). This excess glutamate is responsible for neuron death in transient ischemia (Choi and Rothman, 1990), and its stimulation of massive calcium influx through the NMDA receptors plays a major role in

excitotoxicity (Tymianski et al., 1993a; Tymianski et al., 1993b). A mouse model for transient focal ischemia caused CPEB4 nuclear accumulation, as did an in *vitro* model for oxygen glucose deprivation. Lentivirus-mediated shRNA knockdown of CPEB4 demonstrates that this protein is essential for neuron survival, and might suggest that its nuclear accumulation is a physiological response to high levels of intracellular calcium. However, additional experiments with cultured neurons show that the depletion of calcium from the endoplasmic reticulum (ER), rather than elevated levels of cytosolic calcium per se, is responsible for CPEB4 nuclear accumulation. We have also demonstrated the involvement of IP3 receptors in this ER calcium depletion-mediated nuclear accumulation of CPEB4. We propose that dispatch of a signal, dependent upon the expulsion of ER calcium, signals to CPEB4 to accumulate in the nucleus where it may offer some protection against cell death.

Results

NMDA induces nuclear localization of CPEB4

In cultured hippocampal neurons, CPEB4 is detected mainly in the cytoplasm and in dendrites; it is also enriched in post-synaptic density (PSD) fractions from adult rat brain and hippocampal neurons. To assess if CPEB4 changes in response to synaptic activity, neurons were treated with 0.1 mM NMDA for 40 minutes in the presence of tetrodotoxin (TTX). Compared to a control, NMDA treatment unexpectedly caused strong and permanent nuclear CPEB4 immunostaining, which was prevented when APV, an NMDA antagonist, was added to the cells (Figure 3.1A and B; see also Figure 3.2 for specificity of CPEB4 antibody). Although TTX was used here to silence spontaneous neural activity, we have observed similar nuclear localization of CPEB4 even in the absence of TTX (data not shown).The number of neurons in which CPEB4 was predominantly nuclear or cytoplasmic, or distributed in both compartments (see Figure 3.3 for representative images) as a function of activity shows that NMDA caused a dramatic nuclear localization of CPEB4 that was nearly completely prevented by APV (Figure 3.1, right panel; comparing TTX vs. TTX+NMDA treatment, $p<0.01$, Student's t test). Also, upon treatment with lower concentrations of NMDA (0.01 mM and 0.001 mM), fewer number of neurons

show nuclear accumulation of CPEB4 (data not shown), thus exhibiting a dose response to NMDA.

Figure 3.1 Stimulation of NMDA receptor causes CPEB4 nuclear localization.

A. DIV16 hippocampal neurons incubated in TTX for 24 hours were treated with buffer alone (TTX) or NMDA (TTX+NMDA), and then fixed and immunostained with affinity-purified CPEB4 antibody. DAPI shows nuclear DNA staining. The cells were examined by confocal microscopy. To quantify the localization of CPEB4 in the nucleus or cytoplasm, other cells were stained for CPEB4 where the protein was predominantly cytoplasmic, nuclear, or evenly distributed in cytoplasm and nucleus (see Figure 3.3 for representative images). Using this protein distribution as a standard, the percent of cells in which CPEB4 was in these compartments following TTX, NMDA, treatment was determined (histogram). The asterisks refer to statistical significance ($p<0.01$, Student's t test) between neurons samples treated TTX versus TTX+NMDA. B. DIV16 hippocampal neurons incubated in TTX for 24 hours were treated with APV (TTX+NMDA+APV) for 5 minutes prior to application of NMDA for 40 minutes and then fixed and immunostained with affinity-purified CPEB4 antibody. DAPI shows nuclear DNA staining. The cells were examined by fluorescence microscopy. The asterisks refer to statistical significance ($p<0.01$, Student's t test). Size bar= 10 μm.

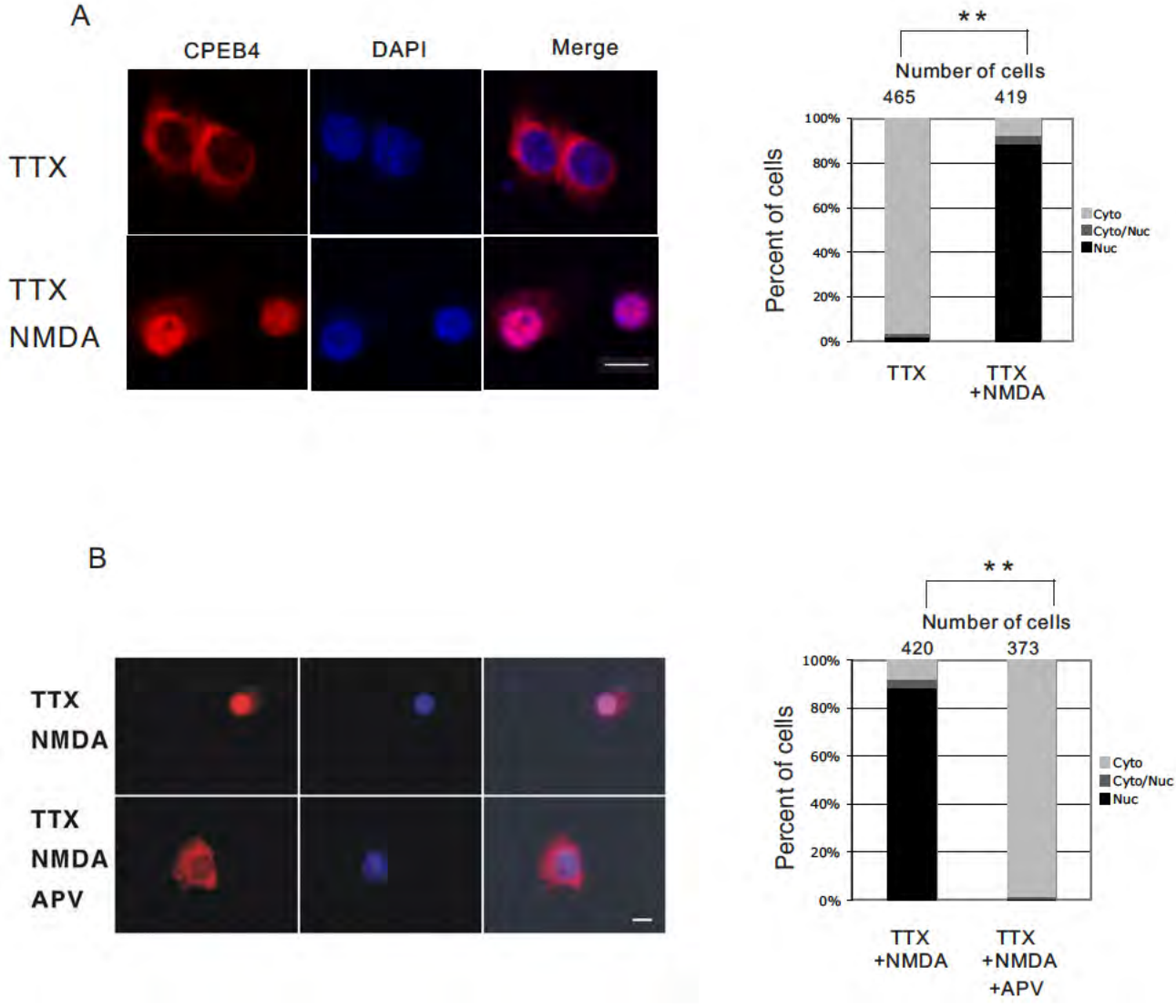
A
CPEB4
DAPI
Merge
TTX
TTX
NMDA
**
Number of cells
465
419
100%
80%
60%
40%
20%
0%
Percent of cells
Cyto
Cyto/Nuc
Nuc
TTX
TTX
+NMDA
B
TTX
NMDA
TTX
NMDA
APV
**
Number of cells
420
373
100%
80%
60%
40%
20%
0%
Percent of cells
Cyto
Cyto/Nuc
Nuc
TTX
+NMDA
TTX
+NMDA
+APV

Figure 3.2 Specificity of CPEB4 antibody.

A. Protein from total brain or testis were separated by SDS-PAGE and blotted on PVDF membrane before probing with affinity purified CPEB4 antibody. B. DIV2 hippocampal neurons were transfected by pLL3.7-syn-C4KD2 or pLL3.7-syn-C4G5 that expresses shRNA against CPEB4 coding region or 3'UTR respectively. Three days after transfection, neurons were fixed and immunostained with affinity purified CPEB4 antibody.

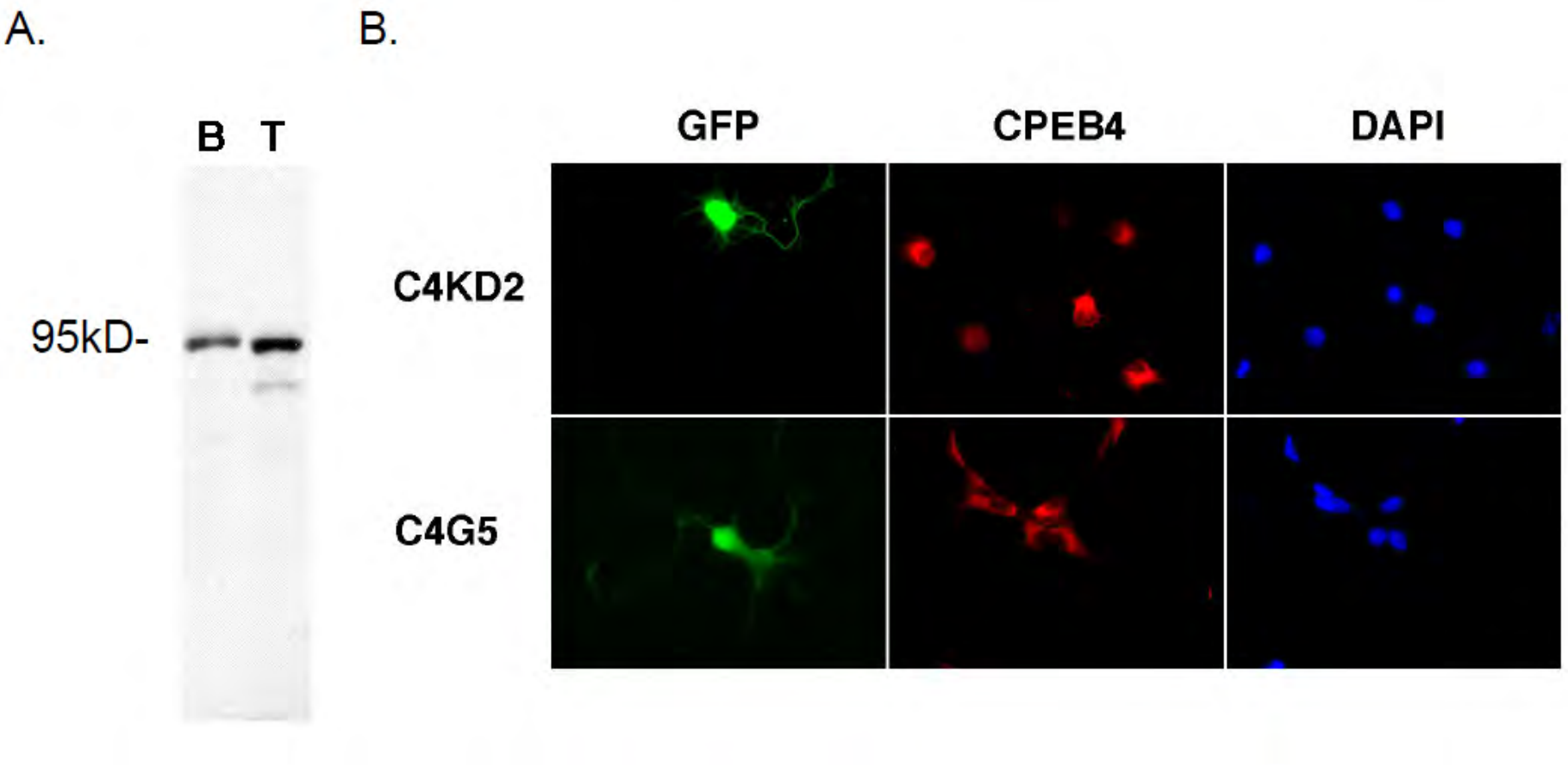
A.
B T
95kD-
B.
GFP
CPEB4
DAPI
C4KD2
C4G5

Figure 3.3 Examples of subcellular protein distribution patterns.

Top panel shows the distribution of protein mainly in cytoplasm. Middle panel shows equal distribution of protein between nucleus and cytoplasm. Lower panel shows the distribution of protein mainly in nucleus. DAPI staining is used to indicate the location of nucleus.

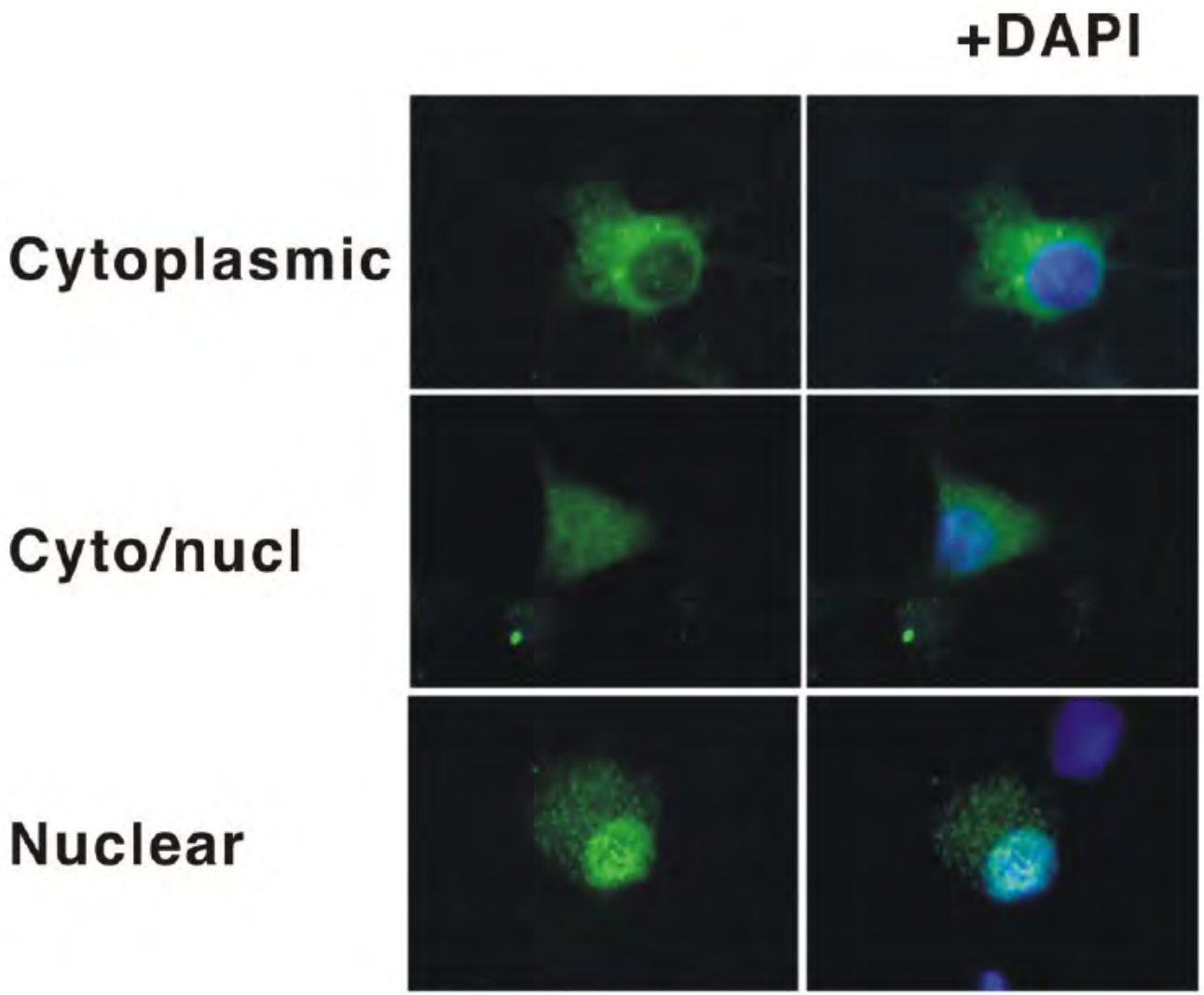
+DAPI
Cytoplasmic
Cyto/nucl
Nuclear

NMDA also caused a substantial loss of CPEB4 from dendrites. Although NMDA did not significantly alter the overall amount of CPEB4 in neurons, it did lead to an increase in the fluorescence intensity of CPEB4 in the nucleus relative to that in the cell body without stimulation (Figure 3.4). These data suggest that dendritic (and cell body) CPEB4 was not destroyed in an activity-dependent manner, but instead was probably transported retrogradely to the nucleus.

Figure 3.4 CPEB4 in dendrites.

A. CPEB4 levels in dendrites from control (TTX only) or NMDA (plus TTX) treated DIV16 neurons; the histogram shows a quantification of the fluorescent dendritic signal. B. Quantification of the CPEB4 fluorescent signal in the cell body or nucleus of DIV16 neurons following TTX or TTX + NMDA treatment. The panel also shows a western blot for CPEB4 and actin, as a loading control, from neurons treated with TTX or TTX+NMDA as before.

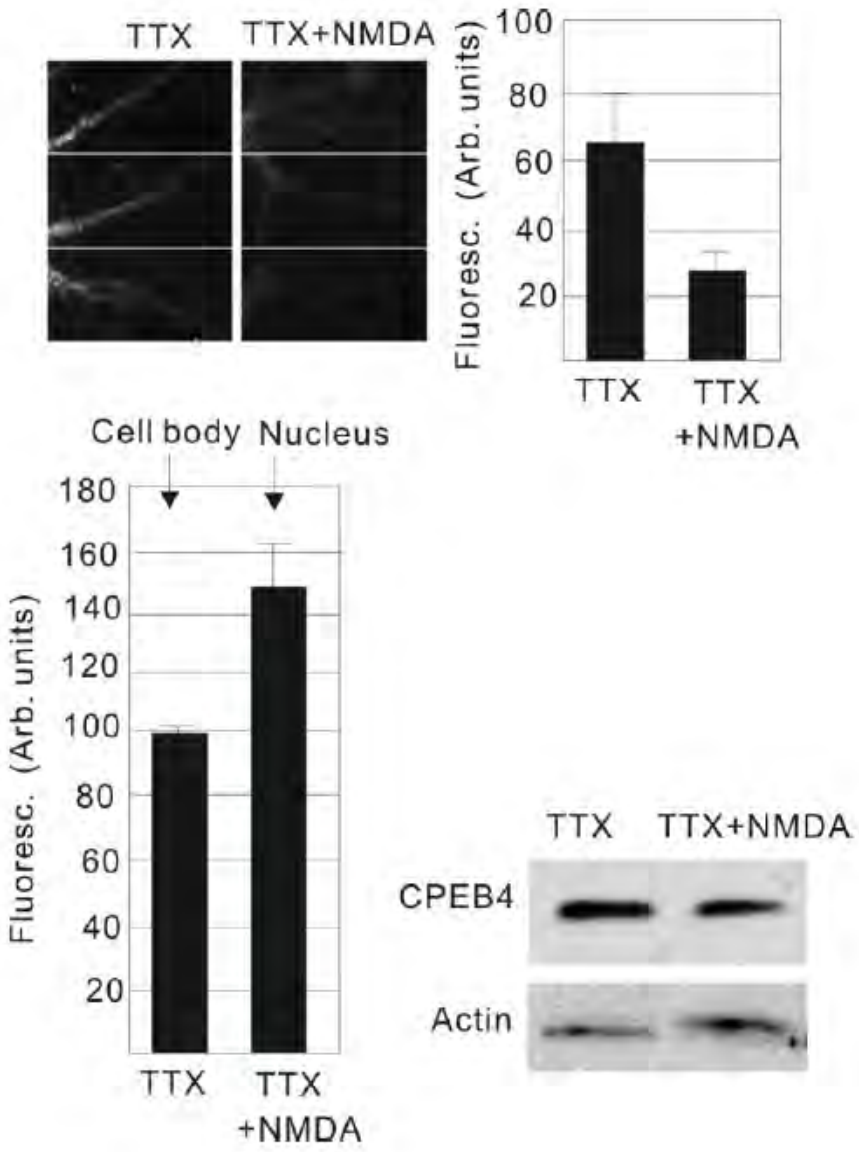
TTX
TTX+NMDA
Fluoresc. (Arb. units)
100
80
60
40
20
TTX
TTX +NMDA
Cell body
Nucleus
180
160
140
120
100
80
60
40
20
Fluoresc. (Arb. units)
TTX
TTX +NMDA
TTX
TTX+NMDA
CPEB4
Actin

Ligand binding to ionotropic glutamate receptors causes calcium influx and induces downstream signaling events through CaMKII (calcium/calmodulin-dependent protein kinase II) (Hudmon and Schulman, 2002). To examine whether extracellular calcium is important for CPEB4 nuclear accumulation, EGTA was applied to neurons before NMDA; this caused CPEB4 to remain predominantly cytoplasmic (Figure 3.5A). To assess whether NMDA/calcium induced CPEB4 nuclear accumulation occurs via CaMKII, a membrane-permeable CaMKII inhibitory peptide, AIPII (Ishida et al., 1998; Watterson et al., 2001) was applied to neurons 20 minutes before NMDA treatment. This peptide reduced NMDA-induced CPEB4 nuclear translocation (Figure 3.5B), indicating that extracellular calcium and CaMKII are part of an NMDA-induced signaling pathway that causes CPEB4 nuclear accumulation. In addition, treatment of neurons with glutamate, AMPA or NMDA induced CPEB4 nuclear staining; DHPG, a metabotropic glutamate receptor agonist, however, had no effect (Figure 3.5B). These data, together with the determination of the number of cells that respond to these treatments (Figure 3.5C), show that ionotropic glutamate receptor activation induces CPEB4 nuclear accumulation.

Figure 3.5 Effectors of CPEB4 nuclear localization.

A. DIV16 neurons were incubated with EGTA for 20 minutes prior to application of NMDA for 40 minutes; the cells were then fixed and stained for CPEB4. B. TTX treated DIV16 hippocampal neurons were treated with DHPG, AMPA, glutamate, or NMDA for 40 min before being immunostained with CPEB4 antibody. Other cells were treated with AIPII for 20 minutes and then subjected to NMDA for 40 minutes before fixation. C. Quantification of CPEB4 in the cytoplasm, nucleus, or both nucleus and cytoplasm was determined as in Figure 1. The asterisks refer to statistical significance ($p<0.01$, Student's t test) between the indicated samples.

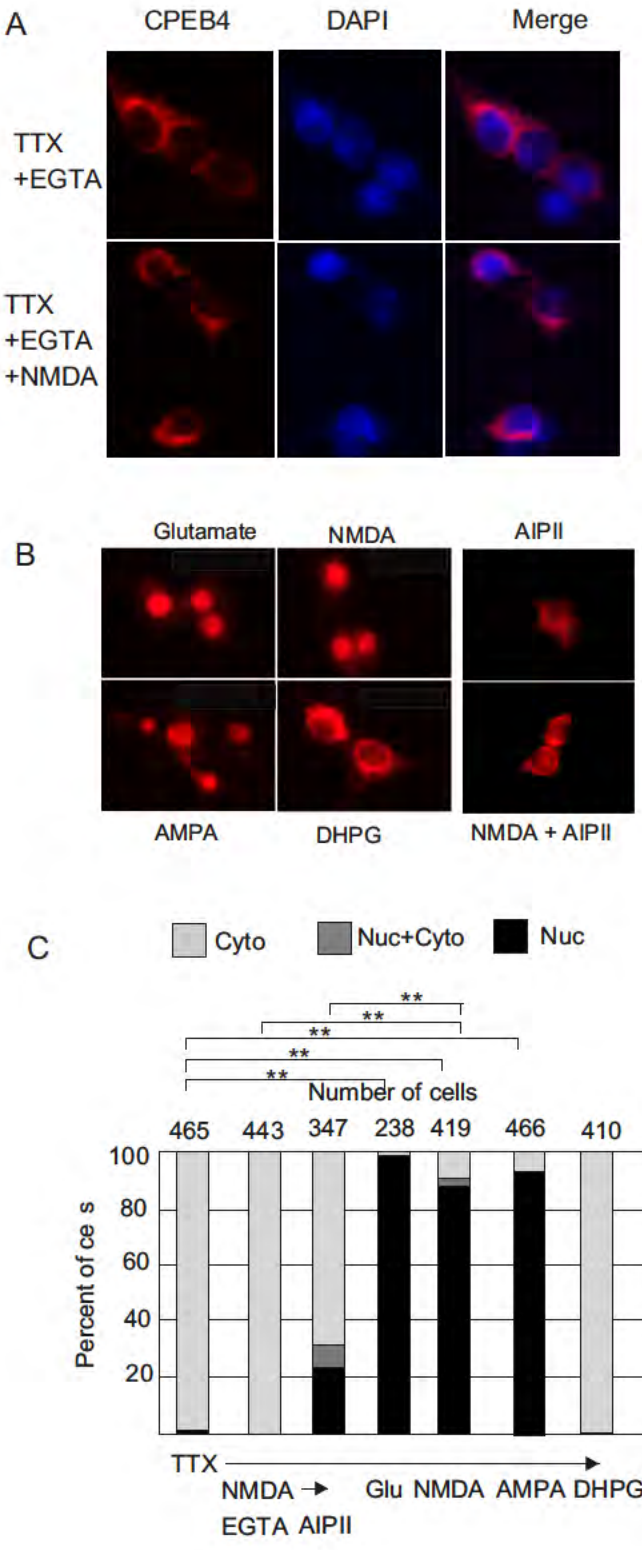
A
CPEB4
DAPI
Merge
TTX
+EGTA
TTX
+EGTA
+NMDA
B
Glutamate
NMDA
AIPII
AMPA
DHPG
NMDA + AIPII
C
Cyto
Nuc+Cyto
Nuc
**
**
**
**
**
Number of cells
465
443
347
238
419
466
410
100
80
60
40
20
Percent of ce s
TTX
NMDA
EGTA AIPII
Glu NMDA AMPA DHPG

CPEB family proteins are nucleus-cytoplasm shuttling proteins

CPEB4 nuclear accumulation could be due to active cytoplasm-to-nucleus import or inhibited nuclear export if this protein continuously shuttles between the two compartments. To distinguish between these possibilities, neurons were treated with leptomycin B (LMB), an inhibitor of the nuclear export factor Crm1 (Kudo et al., 1999; Nishi et al., 1994; Petosa et al., 2004). Application of LMB to cultured neurons resulted in nuclear accumulation of CPEB4, suggesting that CPEB4 is a nucleus/cytoplasm shuttling protein (Figure 3.6A).

To investigate whether other CPEB family proteins are nucleus/cytoplasm shuttling proteins and accumulate in the nucleus in response to NMDA, DIV14 hippocampal neurons were infected with lentiviruses expressing epitope-tagged CPEB1, CPEB3, and CPEB4, which were then subjected to either LMB or NMDA treatment. These proteins all accumulated in the nucleus when nuclear export was blocked by LMB, suggesting they are all shuttling proteins (Figure 3.6B). NMDA treatment also caused these proteins to accumulate in nuclei (Figure 3.6B; quantification of responsive cells in Figure 3.6C), supporting the notion that nuclear accumulation is a common feature among CPEB proteins in neurons following synaptic stimulation. To determine whether CPEB4 nuclear accumulation is neuron-specific, we treated HeLa cells and 293T cells with LMB; in both cases CPEB4 was retained in the nucleus (unpublished data). We also treated HeLa cells with digitonin, which causes cytoplasmic leakage through

pores in the plasma membrane. When a fusion of the CPEB4 RNA binding domain (RBD, i.e., both RNA cognition motifs – RRMs and both zinc fingers) to GST was added to the treated cells after they were washed to remove the leaked cytoplasm, there was no evidence of nuclear accumulation. However, when the permeabilized cells were supplemented with fresh HeLa cytosol, nuclear CPEB4-GST was readily apparent (Figure 3.6D). These data show that CPEB4 nuclear transport is not neuron-specific and that the RBD contains the nuclear localization signal (NLS) of CPEB4.

Figure 3.6 CPEB family proteins are nucleus/cytoplasm shuttling proteins.

A. DIV 16 hippocampal neurons are treated with 0.1% ethanol alone or with 10nM LMB for 40 minutes before fixation and immunostained for endogenous CPEB4. B. DIV16 neurons infected with lentivirus expressing HA-CPEB, myc-CPEB3, or myc-CPEB4 for 2 days were treated with 10 nM LMB for 1 hr and then immunostained with HA or myc antibodies. Other infected cells were stimulated with NMDA for 1 hour prior to immunostaining. C. Quantification of CPEB, CPEB3, or CPEB4 in the nucleus or cytoplasm following the treatments noted in panel B. The asterisks refer to statistical significance ($p<0.01$, Student's t test) between the indicated samples. D. Hela cells were treated with digitonin and the permeabilized cells were incubated with an ATP regenerating system, purified recombinant GST-CPEB4RBD fusion protein and with or without HeLa cell cytosol. After 40 min, the cells were fixed and stained with GST antibody. Size bar=10 μm.

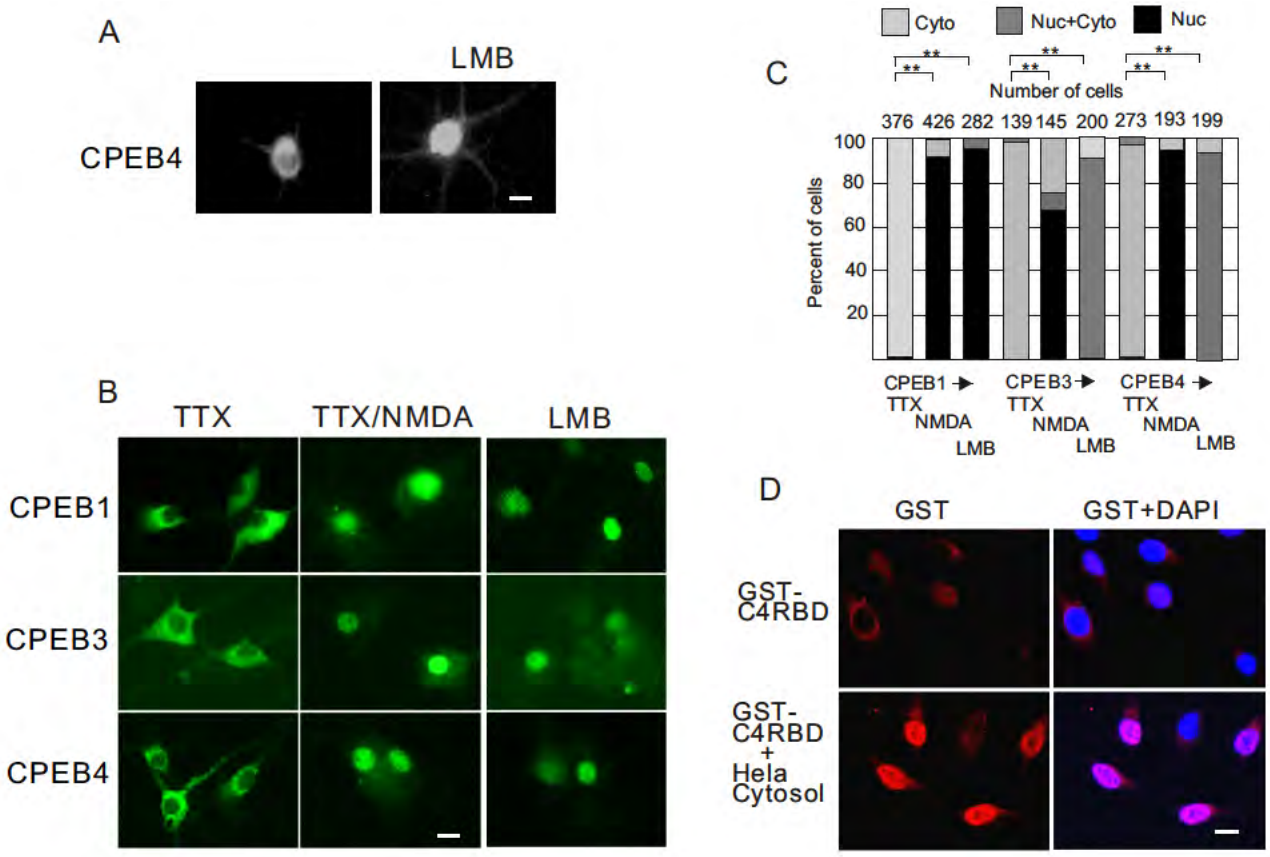
A
LMB
CPEB4
B
TTX
TTX/NMDA
LMB
CPEB1
CPEB3
CPEB4
C
Cyto
Nuc+Cyto
Nuc
Number of cells
376 426 282 139 145 200 273 193 199
Percent of cells
100
80
60
40
20
CPEB1
CPEB3
CPEB4
TTX
NMDA
LMB
D
GST
GST+DAPI
GST-C4RBD
GST-C4RBD + Hela Cytosol

Identification of CPEB4 nuclear import/export cis-elements

To identify the CPEB4 NLS and nuclear export signal (NES), plasmids encoding serial deletions of CPEB4 (D1-D7) were generated (Figure 3.7A) and transfected into NIH3T3 cells, which because of their flattened morphology, are particularly amenable for use in immunocytochemistry to distinguish between cytoplasmic and nuclear proteins. A CPEB4 truncation mutant that lacks the NLS would be expected to be constitutively cytoplasmic irrespective of LMB treatment; protein with an NES deletion should reside in the nucleus irrespective of LMB treatment.

Although the entire CPEB4 protein was sequentially deleted (Figure 3.7A), none of the mutants remained cytoplasmic when cells were treated with LMB. Thus, CPEB4 probably has two or more independently acting NLSs. However, CPEB4 truncation mutant D4, lacking residues 351-463, was nuclear in the absence or presence of LMB, indicating this truncated region contains the NES (Figure 3.7B; quantification of responsive cells presented in Figure 3.7C). The expression levels of the CPEB4 mutant proteins are shown in the lower right panel of Figure 3.7B.

Figure 3.7 Identification of the CPEB4 shuttling elements.

A. The CPEB4 internal deletion constructs are depicted. The boxes indicate the parts of the protein that were deleted and the grey boxes indicate the known functional domains (RRM1, RRM2, ZF) of CPEB4. The bar in N-terminus is a myc epitope tag. RRM1 and RRM2 refer to RNA recognition motifs 1 and 2; ZF refers to two zinc fingers. B. NIH3T3 cells were transfected with plasmid DNA encoding the proteins shown in panel A; 12 hours later, the cells were treated with LMB for 1 hr prior to fixation. Antibody against the myc epitope was used for immunostaining. Exogenous proteins and alpha-tubulin were monitored by immunoblotting. Size bar=10 μm. C. Quantification of the CPEB4 proteins in the nucleus, cytoplasm as in Figure 3.1. The asterisks refer to statistical significance ($p<0.01$, Student's t test) between the indicated samples.

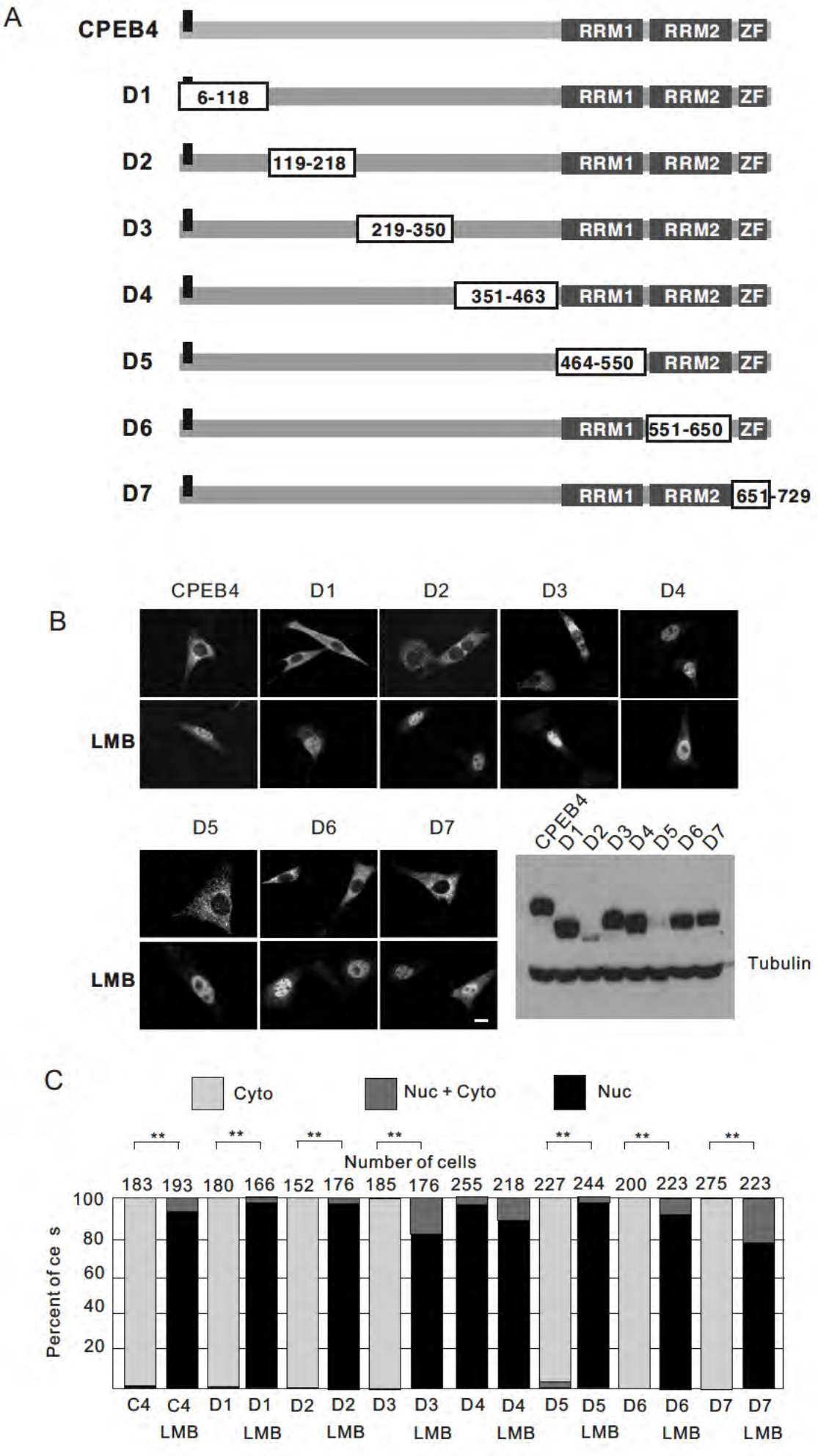
A
CPEB4
RRM1
RRM2
ZF
D1
6-118
D2
119-218
D3
219-350
D4
351-463
D5
464-550
D6
551-650
D7
651-729
B
CPEB4
D1
D2
D3
D4
LMB
D5
D6
D7
LMB
CPEB4
D1
D2
D3
D4
D5
D6
D7
Tubulin
C
Cyto
Nuc + Cyto
Nuc
**
Number of cells
183 193 180 166 152 176 185 176 255 218 227 244 200 223 275 223
100
80
60
40
20
Percent of ce s
C4
C4 LMB
D1
D1 LMB
D2
D2 LMB
D3
D3 LMB
D4
D4 LMB
D5
D5 LMB
D6
D6 LMB
D7
D7 LMB

Using the Multalin program (Corpet, 1988) that compares protein sequence similarity, a sequence from the peptide deleted in mutant D4 was aligned with corresponding regions from CPEB2, 3, and 4 from rat, human, *Xenopus*, zebrafish, and *Drosophila* (in this case, a single CPEB4-like protein is called Orb2). Figure 3.8A shows that CPEB4 residues 383-397 within the deleted peptide are highly conserved among all the protein sequences examined. Leucine residues are often found in NESs; mutation of two of them at positions 385 and 390 (arrows and denoted in bold) to alanine (CPEB4 LL/AA) caused the accumulation of CPEB4 in the nucleus of transfected 3T3 cells irrespective of whether they were treated with LMB (Figure 3.8A lower left; quantification of cells in 5A lower right). Thus, these leucine residues are essential for CPEB4 nuclear export. To assess sufficiency of nuclear export, various segments of CPEB4 containing the NES were fused to EGFP-MS2, which also contained a SV40 T NLS (N-EGFP, Figure 3.8B). As expected, the control N-EGFP lacking a CPEB4 NES was nuclear in transfected 3T3 cells (Figure 3.8B, middle left panel). Upon fusion with the CPEB4 NES-containing fragment, three of the fusion proteins, N-EGFP-268, N-EGFP-145, and N-EGFP-83, became localized to the cytoplasm in the absence but to the nucleus in the presence of LMB. However, two proteins lacking CPEB4 residues 341-376 (N-EGFP-110 and N-EGFP-48) were evenly distributed to both nuclear and cytoplasmic compartments, suggesting a lack of NES function (Figure 3.8B middle; quantification of cells in bottom panel). From

these results, we conclude that CPEB4 residues 341 to 424 constitute a minimal NES.

Figure 3.8 Identification of CPEB4 nuclear export signal.

A. Alignment of the human CPEB4 protein sequence from residues 383 to 397 with homologous regions from rat and zebrafish CPEB4 and human and *Xenopus* CPEB2 and CPEB3 as well as *Drosophila* Orb2. Two arrows point to conserved leucine residues that have been mutated to alanine in the LL-AA mutant. NIH3T3 cells were transfected with DNA encoding myc-tagged wild type or LL-AA mutant CPEB4 proteins for 12 hours, treated with LMB for 1 hour and then fixed and immunostained for the myc-tagged protein. Quantification of the CPEB4 proteins in the nucleus, cytoplasm as in Figure 3.1. The asterisks refer to statistical significance ($p<0.01$, Student's t test) between the indicated samples. B. Fusion proteins used to identify the minimal CPEB4 NES domain. Various regions of the CPEB4 coding region (the numbers refer to amino acid residue) that contain the NES were fused to the SV40 T NLS, the bacteriophage MS2 coat protein, and EGFP. The dark bar indicates the leucine residues indicated in panel A (top). NIH3T3 cells were transfected with DNA encoding the fusion proteins noted above. The left panel shows that the NLS-EGFP-MS2 protein, without any CPEB4 sequence, was nuclear. The other panels show the nuclear/cytoplasmic distribution of the fusion proteins in neurons, some of which were treated with LMB. Size bar=10 μm. The bottom portion shows the quantification of the GFP-CPEB4 fusion proteins in the nucleus or cytoplasm as in Figure 3.1. The asterisks refer to statistical significance ($p<0.01$, Student's t test) between the indicated samples.

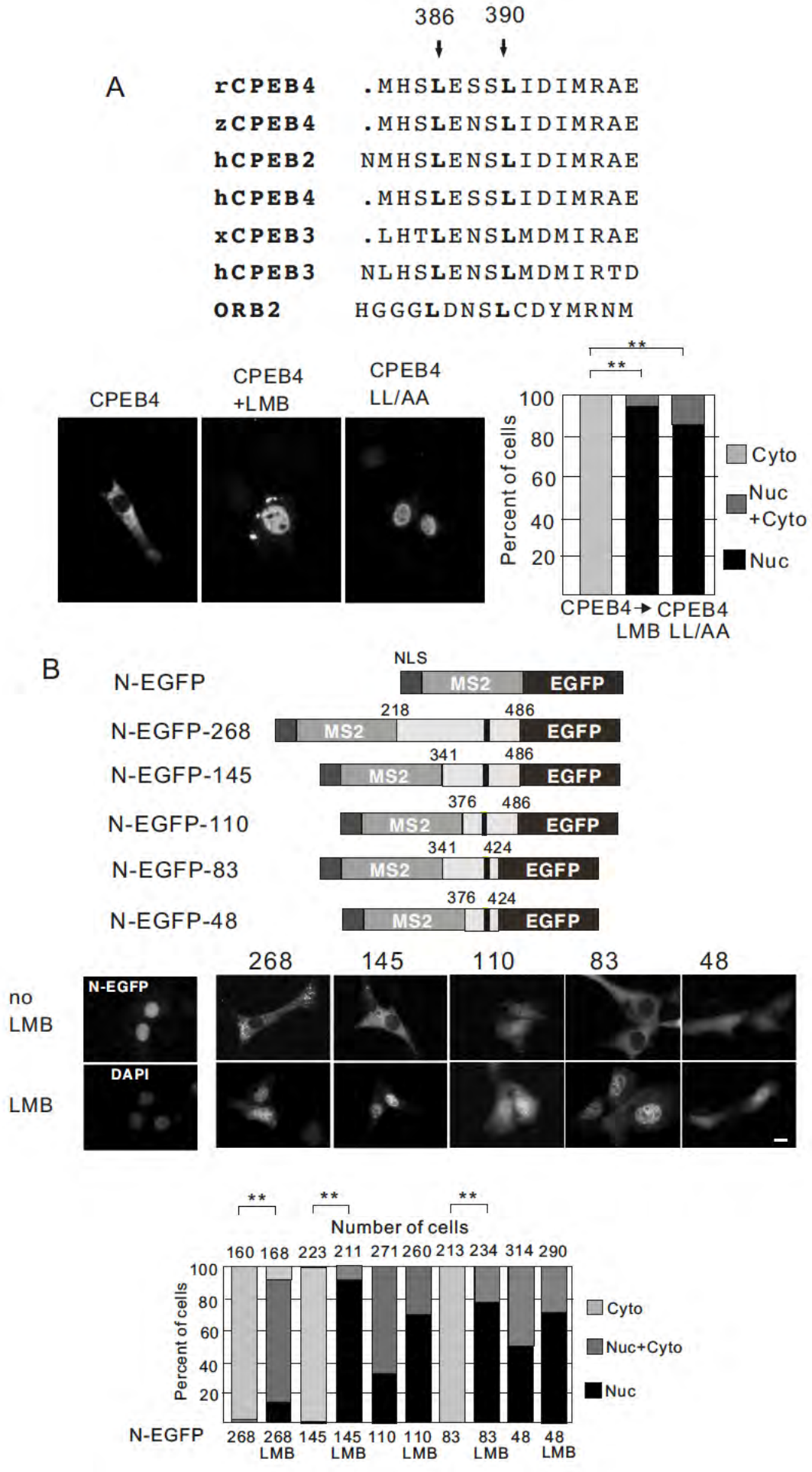
386
390
A
rCPEB4 .MHSLESSLIDIMRAE
zCPEB4 .MHSLENSLIDIMRAE
hCPEB2 NMHSLENSLIDIMRAE
hCPEB4 .MHSLESSLIDIMRAE
xCPEB3 .LHTLENSLMDMIRAE
hCPEB3 NLHSLENSLMDMIRTD
ORB2 HGGGLDNSLCDYMRNM
CPEB4
CPEB4 +LMB
CPEB4 LL/AA
**
**
Percent of cells
100
80
60
40
20
Cyto
Nuc +Cyto
Nuc
CPEB4 → CPEB4 LMB LL/AA
B
NLS
N-EGFP
MS2
EGFP
N-EGFP-268
218
486
N-EGFP-145
341
486
N-EGFP-110
376
486
N-EGFP-83
341
424
N-EGFP-48
376
424
268
145
110
83
48
no LMB
LMB
N-EGFP
DAPI
**
**
**
Number of cells
160 168 223 211 271 260 213 234 314 290
Percent of cells
100
80
60
40
20
Cyto
Nuc+Cyto
Nuc
N-EGFP
268 268 LMB 145 145 LMB 110 110 LMB 83 83 LMB 48 48 LMB

Brain ischemia causes CPEB4 nuclear accumulation

Glutamate plays dual roles in the brain: at physiological levels it induces excitatory synapse activation and plasticity; under pathological conditions such as ischemia and epilepsy, elevated levels of extracellular glutamate cause neuron degeneration through excitotoxicity. To determine whether CPEB4 nuclear accumulation is induced by glutamate release in vivo, brain sections from rats subjected to high frequency stimulation (HFS) for 90 min were probed with CPEB4 antibody. While this HFS paradigm induced the expression of the immediate early gene, activity regulated cytoskeleton-association protein (Arc), in granular cells of the dentate gyrus (Steward et al., 1998), it did not cause CPEB4 nuclear accumulation (unpublished data).

To investigate whether pathological levels of glutamate or the stress associated with it might cause CPEB4 nuclear accumulation, we turned to a mouse model for transient focal ischemia. In this paradigm, the middle cerebral artery is occluded (MCAO), which causes a focal deprivation of blood flow for 90 minutes, followed by a reperfusion of blood for 24 hours before sacrifice and histological preparation (van Leyen et al., 2006). A clear infarction was evident in the ipsilateral portion of the brain, which not only caused neuron death (as determined by TUNEL staining), but also dramatically reduced CPEB4 staining (Figure 3.9A). However, in the motor cortex (Ipsi-MC) and insular cortex (Ipsi-IC), which are in the penumbra of the severely affected area, CPEB4 staining was

enriched in the nucleus. In contrast, CPEB4 staining was cytoplasmic in the corresponding contralateral regions (Figure 3.9B).

Figure 3.9 Ischemia causes CPEB4 protein to become concentrated in the nucleus.

A. Frozen section of the brain taken from mouse that had a middle cerebral artery occlusion (MCAO) was fixed and stained for CPEB4. Consecutive section from same animal was labeled by TUNEL staining. The white boxes refer to regions of the motor cortex (MC) and insular cortex (IC) that were examined under higher magnification in panel B. Size bar=1mm. B. Section from ischemic brain was immunostained with anti-CPEB4 antibody. DAPI staining shows nuclei. The images were taken from the motor cortex (MC) or insular cortex (IC); ipsilateral (Ipsi) and contralateral sides (Con) of these regions are shown. Size bar=20 μm.

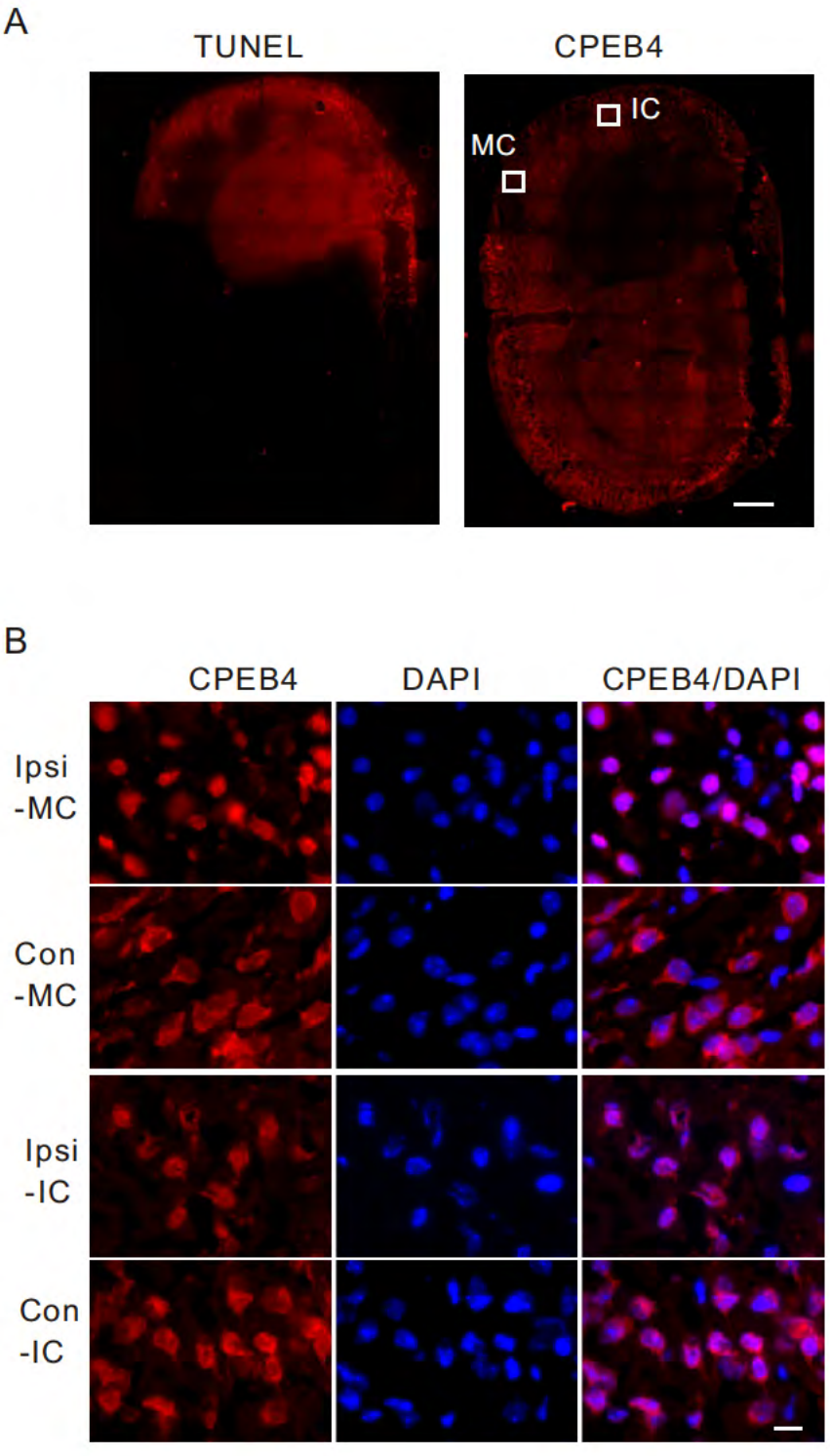
A
TUNEL
CPEB4
IC
MC
B
CPEB4
DAPI
CPEB4/DAPI
Ipsi
-MC
Con
-MC
Ipsi
-IC
Con
-IC

Ischemia not only causes hypoxia, but also hypoglycemia in the affected part of the brain. One cell culture model that mimics these two ischemia-induced deficits is oxygen glucose deprivation (OGD); here, neurons are cultured under conditions of reduced atmospheric oxygen and glucose. Hippocampal neurons (14 DIV) were subjected to OGD treatment for one hour and then returned to normal culture conditions for 3 hours before fixation and staining for CPEB4 and apoptosis. In control cells grown under normal conditions, CPEB4 was cytoplasmic and TUNEL staining was absent (Figure 3.10A). After one hour of OGD treatment and three hours of recovery, CPEB4 protein was undetectable in most neurons but in others, it was concentrated in the nucleus. Interestingly, CPEB4 nuclear staining was inversely correlated with TUNEL staining (Figure 3.10A right panel), suggesting that nuclear CPEB4 may offer some protection against apoptosis. The above mentioned MCAO and OGD experiments suggest that excessive glutamate causes CPEB4 nuclear accumulation. However, this nuclear accumulation could be due to stress caused by the excessive glutamate.

To investigate whether CPEB4 is important for neuron survival, cultured hippocampal neurons were infected with lentiviruses expressing GFP as well as two different shRNAs to knockdown (KD) CPEB4. Figure 3.10B shows that while the KD2 shRNA effectively reduced CPEB4 levels, KD3 did not. Neither shRNA affected CPEB3 or tubulin levels. Neurons were doubly infected with viruses expressing KD2 shRNA and CPEB4 (C4) or CPEB4 ΔNES (C4 ΔNES). C4 and C4 ΔNES were mutated to maintain proper amino acid sequence but not to

anneal with the shRNA. C4 ΔNES expresses a CPEB4 protein that resides solely in the nucleus. Most neurons died when CPEB4 was reduced (KD2 shRNA), but survived up to three days when CPEB4 levels were restored with either full length C4 or C4 ΔNES (Figure 3.10C). Thus, CPEB4 (specifically nuclear CPEB4) is necessary for neuron survival.

Figure 3.10 Oxygen glucose deprivation and CPEB4-mediated neuron survival.

A. CPEB4 nuclear localization in DIV14 hippocampal neurons after OGD treatment. Hippocampal neurons were incubated in medium without glucose in an atmosphere deprived of oxygen for 1 hour (OGD 1 hr), which was followed by recovery in normal culture media in atmosphere containing oxygen for 3hrs (OGD 1hr, recovery 3 hr). Control (Con) refers to cells without OGD treatment. The images show CPEB4 staining, TUNEL staining, CPEB4/TUNEL/DAPI staining to show the location of nuclei. The panel on right shows quantification of the CPEB4 proteins in the nucleus, cytoplasm as in Figure 1. The asterisks refer to statistical significance ($p<0.01$, Student's t test) between the indicated samples. B. Hippocampal neurons were cultured with lentivirus expressing GFP only (V), or GFP and two different CPEB4 shRNAS (KD2, KD3). Some neurons were also cultured with two lentiviruses expressing KD2 and CPEB4 or CPEB4 ΔNES (C4 or C4 ΔNES, containing mutations to prevent knockdown but still encoding the correct protein). Extracts from the cells were probed for CPEB4, CPEB3, tubulin, and GFP. C. Survival of the neurons infected with some of the viruses noted above was determined (n=200). Error bars represent standard error of mean.

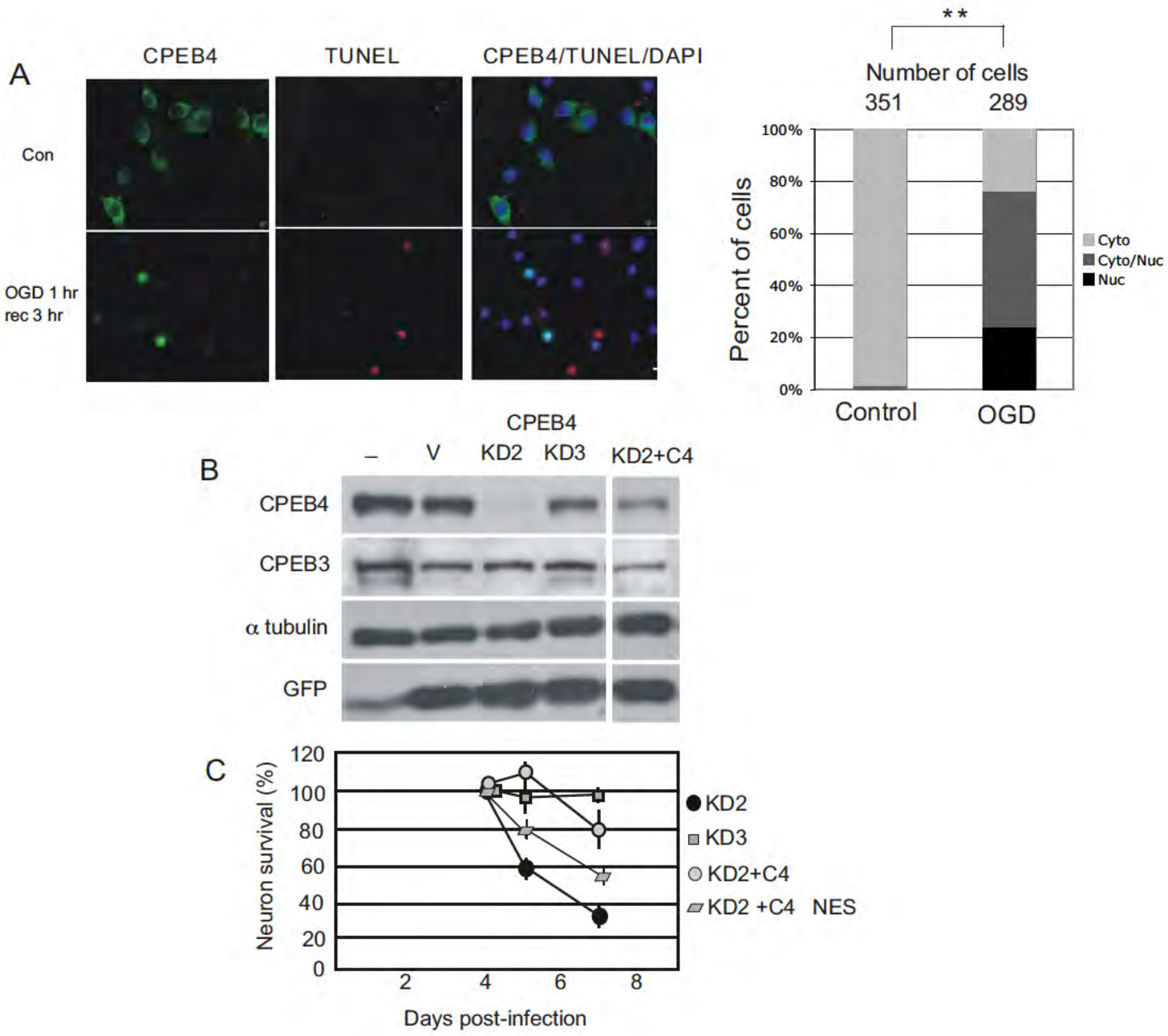
A
CPEB4
TUNEL
CPEB4/TUNEL/DAPI
Con
OGD 1 hr
rec 3 hr
**
Number of cells
351
289
Percent of cells
100%
80%
60%
40%
20%
0%
Control
OGD
Cyto
Cyto/Nuc
Nuc
B
CPEB4
–
V
KD2
KD3
KD2+C4
CPEB4
CPEB3
α tubulin
GFP
C
Neuron survival (%)
120
100
80
60
40
20
0
2
4
6
8
Days post-infection
KD2
KD3
KD2+C4
KD2 +C4 NES

CPEB4 is present on ER and its nuclear localization is induced by ER calcium depletion

Transient ischemia induces protein aggregation in the ER, possibly due to inhibited folding capacity when luminal calcium levels are reduced (Hu et al., 2000). This possibility suggests that CPEB4 nuclear accumulation might also be mediated by reduced ER calcium, consequently, a membrane permeable calcium chelator, BAPTA-AM, was used to immobilize free calcium inside the ER. Twenty minutes after BAPTA-AM addition, neurons were placed in fresh media for an additional 40 minutes. After the membrane permeable moiety of BAPTA-AM is cleaved by cytosolic esterases, the remaining BAPTA becomes trapped intracellularly. Because the dissociation constant of BAPTA for calcium is close to cytosolic calcium level, BAPTA does not substantially affect cytosolic calcium levels (Paschen et al., 2003). On the other hand, BAPTA targets free calcium in the ER because of its high calcium level (~700μM) (Demaurex and Frieden, 2003). This chelation of ER calcium induced the nuclear accumulation of CPEB4 (Figure 3.11A).

A reduction in ER calcium diminishes protein chaperone activity in the lumen, causing the accumulation of unfolded protein that will induce the ER stress response (Paschen et al., 2003). To determine whether CPEB4 nuclear accumulation is a response to ER calcium depletion or ER stress, cells were incubated with thapsigargin (TG) and tunicamycin (TM). Although both agents

activate the unfolded protein response (UPR), TG does so by causing ER calcium efflux while TM disrupts protein glycosylation. In neurons treated with 16 μM TG, CPEB4 protein began to accumulate in the nucleus 30 minutes after drug application (Figure 3.11B). However, CPEB4 remained cytoplasmic when cells were treated with TM although the UPR response did occur as determined by the expression of C/EBP homology protein (CHOP) (Figure 3.11C). These data suggest that CPEB4 nuclear accumulation is induced by ER calcium depletion. A dose-response experiment demonstrates that while a 1 hour treatment of 4 μM TG had no effect on CPEB4 localization, 8 μM caused an even distribution between nucleus and cytoplasm while 16 μM TG caused strong nuclear CPEB4 staining (Figure 3.11D). These data are consistent with the notion that the retention of CPEB4 in the nucleus is triggered by ER calcium depletion.

To investigate how ER calcium depletion might stimulate CPEB4 nuclear localization, mouse brain lysate was underlain on a discontinuous sucrose gradient and then centrifuged; molecules associated with membranes in such a flotation assay should band at a sucrose concentration with a similar density. Figure 3.11E shows that Protein Disulfide Isomerase (PDI), an ER specific marker banded in fractions 8-10; CPEB4 was most prevalent in fractions 8 and 9. The material in these fractions was then pelleted and analyzed by immuno-electron microscopy using CPEB4 antibody. Gold particles marking CPEB4 were found to co-localize with ER structures, thus confirming presence of CPEB4 on ER (Figure 3.11E). Although we do not know what other molecules might be

involved in tethering CPEB4 to the ER, we surmise that calcium depletion from this structure releases CPEB4 and facilitates its nuclear localization.

Figure 3.11 Relationship between ER calcium levels and CPEB4 nuclear localization in cultured hippocampal neurons.

A. DIV16 hippocampal neurons that had been treated with TTX for 24 hours were incubated with BAPTA-AM for 20 min. The neurons were then washed, cultured in fresh media, and then treated with either DMSO or NMDA for 40 min before fixation and immunostaining for CPEB4. B. DIV16 hippocampal neurons were treated with DMSO as control, or 16 μM thapsigargin (TG) for 30 min or 1 hour. At the end of treatment, neurons were fixed and stained with CPEB4 antibody and DAPI. C. DIV16 Hippocampal neurons were treated with tunicamycin for 1 hour, 4 hours or 6 hours before fixation and immunostained with CPEB4 or CHOP antibodies. D. DIV16 hippocampal neurons were treated with 4, 8 or 16 μM thapsigargin for 1 hour before fixation and immunostaining for CPEB4. DAPI staining shows location of the nucleus. Size bar=10 μm. E. Sucrose gradient fractionation was performed on post-nuclear supernatants of brain lysates; the fractions were immunoblotted for CPEB4 and ER marker PDI. The CPEB4 enriched fractions (fractions 8-10) were then analyzed by immunoelectron microscopy using CPEB4 antibody. Size bar = 200 nm.

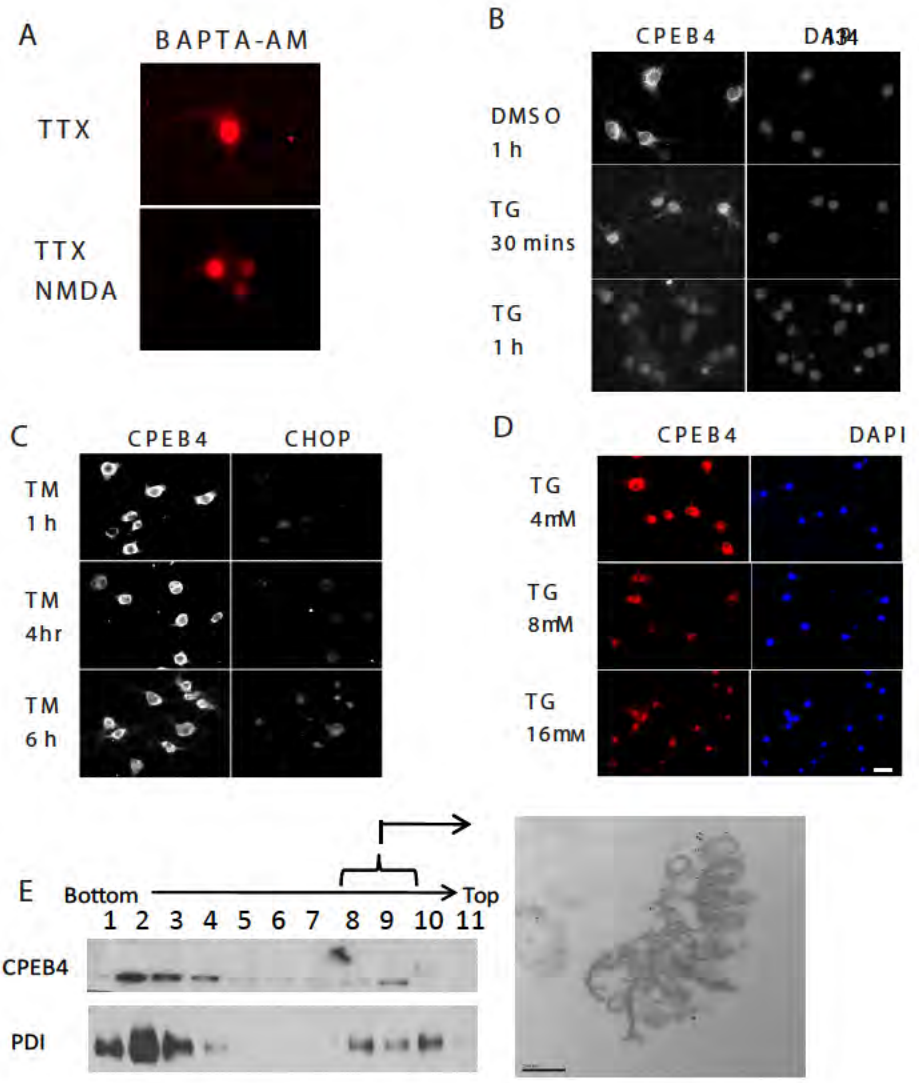

Figure 8. Relationship between ER calcium levels and CPEB4 nuclear localization in cultured hippocampal neurons. A. DIV16 hippocampal neurons that had been treated with TTX for 24 hours were incubated with BAPTA-AM for 20 min. The neurons were were then washed, cultured in fresh media, and then treated with either DMSO or NMDA for 40 min before fixation and immunostaining for CPEB4. B. DIV16 hippocampal neurons were treated with DMSO as control, or 16 µM thapsigargin (TG) for 30 min or 1 hour. At the end of treatment, neurons were fixed and stained with CPEB4 antibody and DAPI. C. DIV16 Hippocampal neurons were treated with tunicamycin for 1 hour, 4 hours or 6 hours before fixation and immunostained with CPEB4 or CHOP antibodies. D. DIV16 hippocampal neurons were treated with 4, 8 or 16 µM thapsigargin for 1 hour before fixation and immunostaining for CPEB4. DAPI staining shows location of the nucleus. Size bar=10 µm.

We have conducted several additional experiments to delve further into the notion that CPEB4 nuclear accumulation is driven substantially by ER calcium depletion as opposed to an increase in cytosolic calcium. Because the various agents used in this study to alter calcium levels would likely do so to varying extents, we measured relative intracellular calcium levels with Fluo-3, a calcium sensitive fluorescent indicator. DIV16 neurons were incubated with Fluo-3 followed by treatment with each agent (NMDA, Ionomycin, BAPTA-AM, thapsigargin); fluorescence intensity was then determined using a fluorescence plate reader. Figure 3.12A shows that a high intracellular calcium concentration per se did not induce CPEB4 to become predominantly nuclear, indeed, BAPTA-AM, which reduced cytosolic calcium, resulted in nuclear CPEB4. In this case, chelation of ER calcium was most likely responsible for CPEB4 nuclear accumulation. Taken together, these data indicate that the reduction of ER calcium stores, and probably not an increase in cytosolic calcium per se, is responsible for CPEB4 nuclear accumulation.

We next determined the extent to which some of the agents that cause CPEB4 nuclear accumulation induce ER calcium depletion. To address this, neurons were transfected with D1ER, a plasmid devised by (Palmer et al., 2004) that encodes an ER localization signal (derived from calreticulin), cyan fluorescent protein (CFP), calmodulin, M13 calmodulin-binding peptide, yellow fluorescent protein (YFP), and a KDEL ER retention sequence. In the ER lumen, calcium binding by calmodulin will cause it to also bind the M13. This interaction

will induce a conformational change in the fusion protein such that CFP and YFP will be juxtaposed. When transfected neurons are excited by 440 nm light, YFP (the acceptor) will emit a 535 nm FRET signal. The intensity of the 535 nm signal is therefore proportional to the amount of calcium that is bound to calmodulin ((Palmer et al., 2004); Figure 3.12B,). To first "calibrate" the FRET signal, the intensity of 535 nm light emission from untreated cells was set at zero (i.e., R_{max}, maximal ER calcium), and that from cells treated with ionomycin plus EGTA set at -100 (i.e., R_{min}, minimum ER calcium). The data collected from cells treated with various agents were then plotted as percent ER calcium change (Figure 3.12C). As expected, NMDA treatment indeed caused a loss of ER calcium, as did thapsigargin and BAPTA-AM, although to varying extents (Figure 3.12C). Thus, agents that cause CPEB4 to concentrate in the nucleus do indeed induce depletion of ER calcium (see also Figure 3.13).

Finally, we addressed whether the IP3 receptor, which resides predominantly in the ER, can mediate ER calcium depletion and transduce a signal to cause CPEB4 nuclear accumulation. Neurons were treated with 2-aminoethoxydiphenyl borate (2-APB), an inhibitor of IP3 receptor signaling, with or without NMDA. Figure 3.12D shows that 2-APB partially blocked NMDA-induced CPEB4 nuclear accumulation. Thus, implicating IP3 receptor in mediating the subcellular localization of CPEB4 in response to depletion of calcium from the endoplasmic reticulum.

Figure 3.12 ER Calcium depletion causes CPEB4 to be retained in the nucleus.

A. DIV16 neurons were loaded with 1 μM Fluo-3/AM for 30 minutes and then incubated for another 30 minutes to allow for de-esterification before being treated with the agents noted in the panel. The cells were then placed in a fluorescence plate reader to quantify Fluo-3 fluorescence, a relative measure of calcium concentration. B. Schematic structure of the D1ER cameleon construct showing an ER targeting sequence, CFP, calmodulin (CaM, the calcium binding domains are depicted as balls with a putative flexible coiled region in between), M13 calmodulin binding peptide, YFP, and a KDEL ER retention sequence. When the calmodulin moiety binds calcium in the ER it interacts with the M13 peptide, which in turn brings CFP and YFP into close proximity. An excitation at 440 nm elicits a 535 nm FRET emission from the YFP; this FRET signal is thus proportional to the amount of calcium the ER. C. DIV12 neurons were transfected with pD1ER cameleon construct, the FRET and CFP signals were determined. The maximum and minimum FRET/CFP signals were measured when the cells were untreated or treated with ionomycin and EGTA, and were set at 0 and -100, respectively. The percent of ER calcium change has been plotted (see also Palmer *et al*, 2004). ER calcium was determined when the cells were treated with NMDA, ionomycin, thapsigargin, or BAPTA-AM. Each experiments was performed 3 times (mean and SEM are shown). D. DIV 16 neurons were incubated with 2-APB for 45 mins prior to application of NMDA for 40 mins; the cells were then fixed and stained for CPEB4. Panel on the right shows

quantification for the same. The asterisks refer to statistical significance ($p<0.01$, Student's t test) between the indicated samples. Size bar= 10 μm.

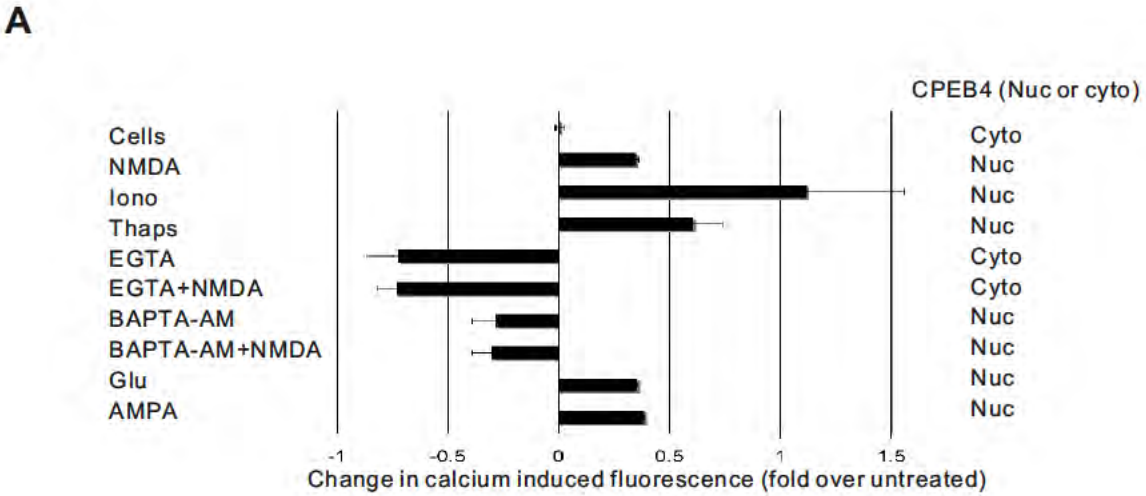
A
CPEB4 (Nuc or cyto)
Cells
NMDA
Iono
Thaps
EGTA
EGTA+NMDA
BAPTA-AM
BAPTA-AM+NMDA
Glu
AMPA
Cyto
Nuc
Nuc
Nuc
Cyto
Cyto
Nuc
Nuc
Nuc
Nuc
-1
-0.5
0
0.5
1
1.5
Change in calcium induced fluorescence (fold over untreated)

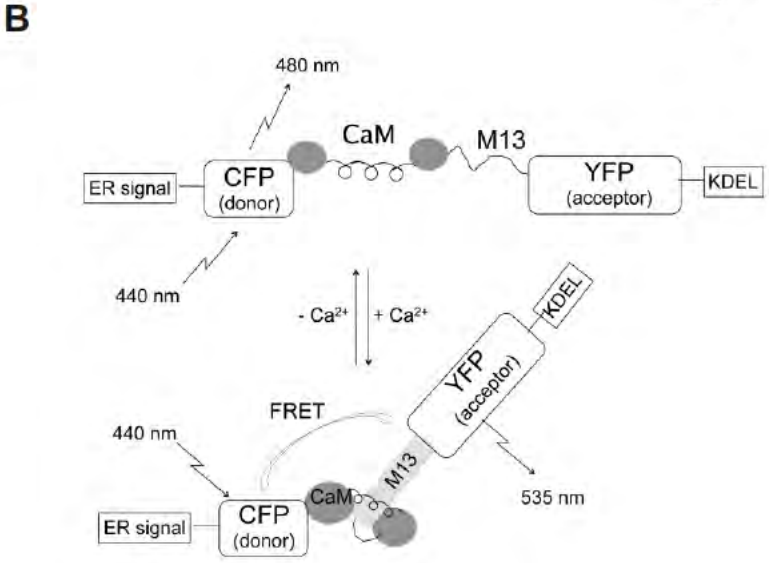
B
480 nm
CaM
M13
ER signal
CFP
(donor)
YFP
(acceptor)
KDEL
440 nm
- Ca2+
+ Ca2+
FRET
535 nm

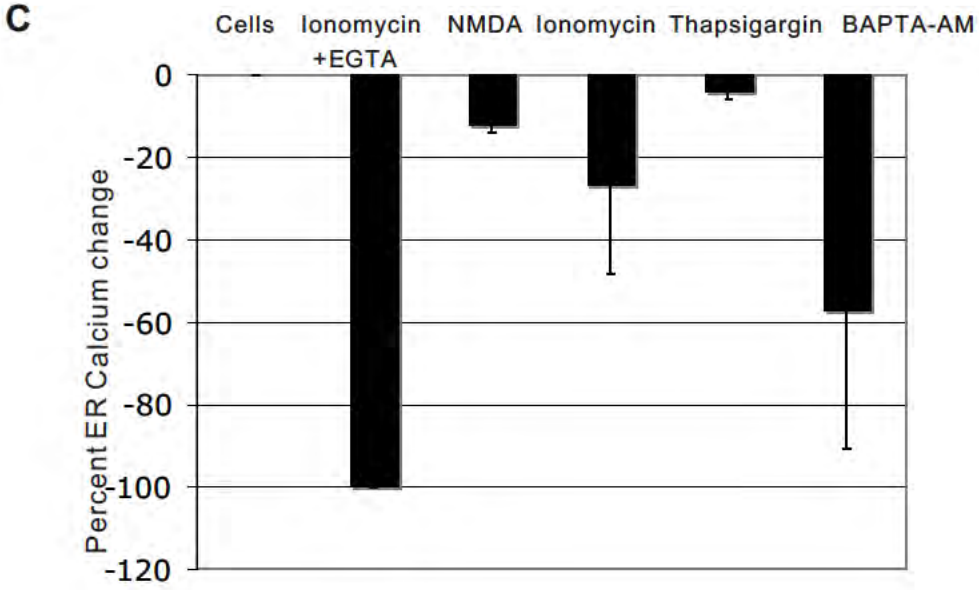
C
Cells
Ionomycin +EGTA
NMDA
Ionomycin
Thapsigargin
BAPTA-AM
Percent ER Calcium change
0
-20
-40
-60
-80
-100
-120

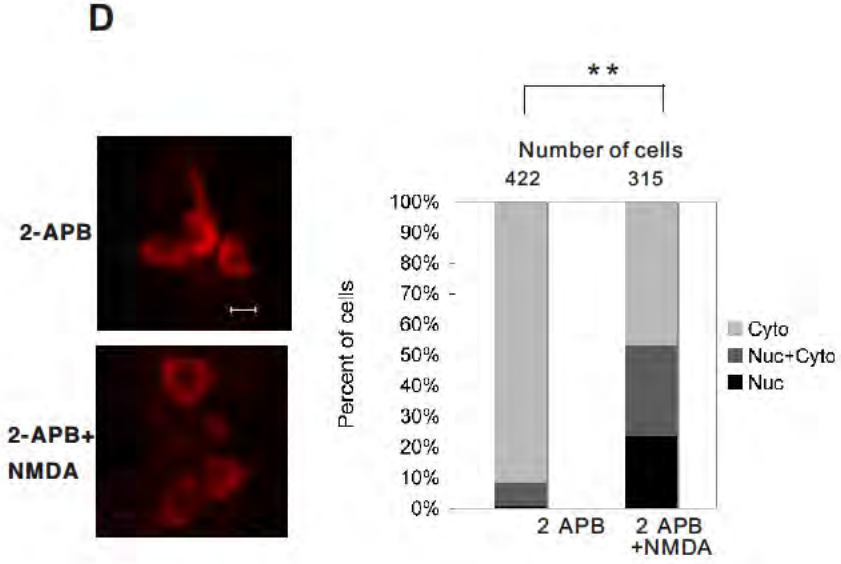
D
2-APB
2-APB+ NMDA
**
Number of cells
422
315
Percent of cells
100%
90%
80%
70%
60%
50%
40%
30%
20%
10%
0%
Cyto
Nuc+Cyto
Nuc
2 APB
2 APB +NMDA

Figure 3.13 Effect of Ionomycin on CPEB4 localization.

DIV16 neurons were treated with ionomycin (5 μM) for 1 hour before immunostaining for CPEB4.

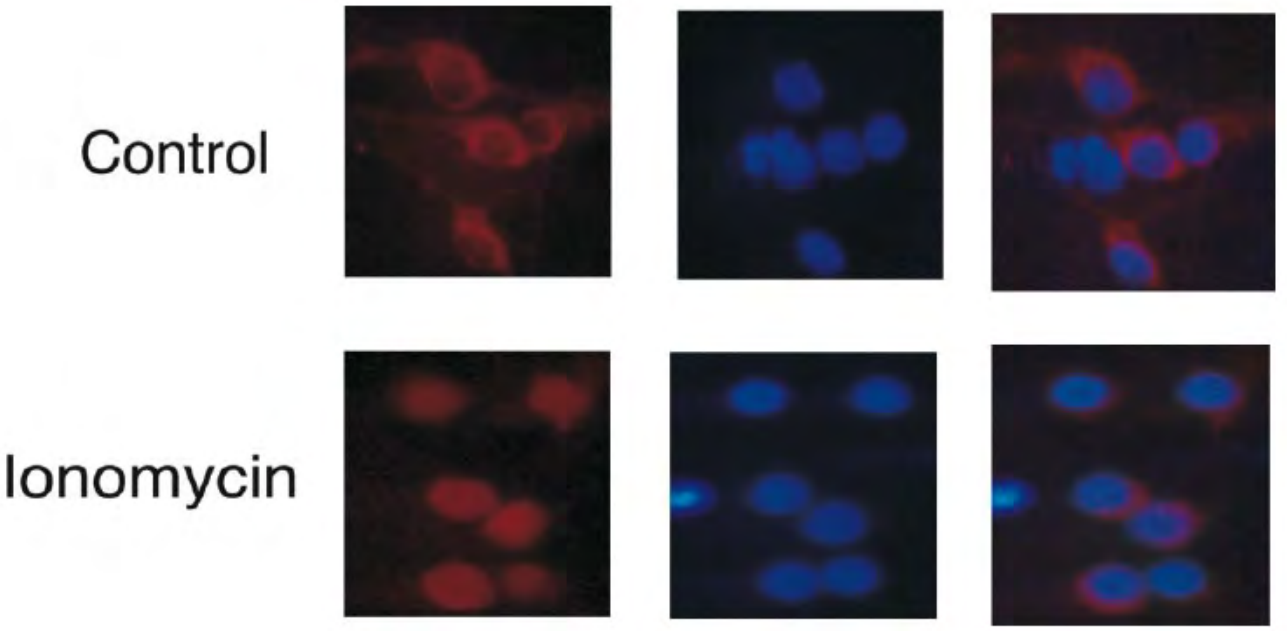
Control
Ionomycin

Discussion

Most investigations of the biological functions of CPEB, the most studied member of the CPEB family of proteins, have concentrated on cytoplasmic events such as cytoplasmic polyadenylation, translation, and RNA transport. The finding that the CPEB proteins are nucleus/cytoplasm shuttling proteins suggests new functions for these proteins involving nuclear RNA metabolism. For example, the CPEB interacting proteins CPSF and symplekin are involved in nuclear pre-mRNA polyadenylation as well as cytoplasmic polyadenylation (Hofmann et al., 2002; Mandel et al., 2006); thus, it is possible that CPEB may also modulate nuclear polyadenylation as well as alternative splicing (Lin et al., 2010). Another possible role for CPEB proteins is RNA nuclear export and subcellular localization. Unlike Staufen2 and She2, two nucleus/cytoplasm shuttling proteins that accumulate in nucleoli when RNA binding activity is disrupted (Du and Richter, 2005; Macchi et al., 2004), CPEB4 truncation mutants that have part of their RNA binding domains removed retain their shuttling activity, suggesting that it is actively transported across the nuclear membrane instead of passively exported by way of tethering to RNA.

The failure to identify a nuclear import signal (NLS) in CPEB4 using serial deletions suggests that there is more than one NLS. One putative NLS is probably located in an RNA binding domain because recombinant CPEB4 RNA

binding domain alone is sufficient to induce nuclear import in the presence of HeLa cell cytosol in an *in vitro* import assay. On the other hand, the CPEB4 NES clearly requires leucine residues 386 and 390. Because these residues are present in CPEB2 and 3, they probably mediate the export of these proteins as well. Moreover, because they are conserved in, for example, *Drosophila* Orb2, we infer that they have a similar function in invertebrates as well. The observation that the two leucine residues are not present in CPEB underscores the divergent nature of these two branches of the CPEB family of proteins. Nonetheless, the fact that CPEB, like CPEB2, 3, and 4 shuttles between nucleus and cytoplasm in an NMDA-stimulated manner indicates that they have retained, and perhaps even share, important nuclear functions.

CPEB4 is retained in the nucleus following ischemia

The nuclear staining of CPEB4 in the penumbra region of the mouse ischemic brain demonstrates that this pathological condition causes a subcellular re-distribution of this protein. The penumbra represents the area of brain that sustains secondary damage caused by the diffusion of glutamate and potassium ions from the immediate site of the infarct, as well as hypoperfusion; it is also a target of treatment that aims to reduce brain injury caused by stroke. In addition to CPEB4, other proteins have also been shown to translocate to the nucleus upon ischemia. One of them, apoptosis inducing factor (AIF), resides in mitochondria and functions as an oxido-reductase in cells but translocates to the

nucleus and induces chromatin condensation when apoptosis or necrosis is induced (Daugas et al., 2000; Susin et al., 1999). During ischemia and OGD, nuclear translocation of AIF is considered to be one of the mechanisms that cause neuron death (Cao et al., 2003; Plesnila et al., 2004; Zhao et al., 2004; Zhu et al., 2003). HGF (hepatocyte growth factor), which protects neurons from ischemia induced cell death when perfused into the brain, prevents the translocation of AIF to the nucleus (Niimura et al., 2006).

Excessive NMDAR activation and ER calcium depletion

To examine the relationship between CPEB4 nuclear accumulation and cellular calcium, we treated cells with a variety of agents and then measured intracellular calcium concentration with Fluo-3AM, a cytosolic calcium indicator. In general, agents that induce increased calcium correlated with CPEB4 nuclear accumulation. However, BAPTA-AM, which resulted in CPEB4 nuclear accumulation, did not lead to any detectable increase in cellular calcium. On the other hand, the BAPTA-AM results are consistent with a decrease in ER calcium. Moreover, because the relationship between excessive NMDAR stimulation and (possible) ER calcium depletion is not clear, we examined ER calcium levels in neurons directly by fluorescence resonance energy transfer (FRET). In this case, neurons were transfected with a plasmid (cameleon D1ER) encoding a fluorescent calcium sensor specifically targeted to the ER (Palmer et al., 2004). Upon treatment with NMDA, ionomycin, thapsigargin, and BAPTA-AM, agents

that cause CPEB4 to become concentrated in the nucleus, we observed clear decreases in ER calcium (Figure 3.12). While the amount of ER depletion varied depending on the agent, the correlation between nuclear CPEB4 immunostaining and ER calcium depletion was very consistent. Thus, based on these direct measurements, we infer that ER calcium depletion is responsible for CPEB4 nuclear accumulation.

It has been shown that ER stress is induced in ischemic tissue as demonstrated by the accumulation of misfolded proteins (Hu et al., 2000) and induction of the UPR pathway (Morimoto et al., 2007). The UPR is induced by decreased ER folding capacity or increased synthesis of proteins that transit through the ER. Although it has been suggested that calcium depletion may be responsible for ER stress after ischemia, no clear evidence has been provided. In our results, both ER calcium depletion and NMDA application caused CPEB4 nuclear accumulation; we further demonstrate that NMDAR activation causes ER calcium depletion, indicating a causal relationship. It has been reported that activation of NMDAR may induce the release of calcium from the ER through calcium induced calcium release (CICR) (Emptage et al., 1999; Rose and Konnerth, 2001). In neurons, the ER forms an extended structure that reaches synaptic spines (Svoboda and Mainen, 1999) and contains two types of calcium releasing channels, the inositol-1,4,5-trisphosphate receptor (IP3) and the ryanodine receptor. Another report also suggests that the ryanodine receptor may cause ER calcium release because application of a ryanodine receptor

inhibitor, dantrolene, protects neurons from NMDA mediated excitotoxicity (Frandsen and Schousboe, 1992). Caffeine, which activates the ryanodine receptor did not cause CPEB4 nuclear accumulation probably because it did not cause sufficient ER calcium depletion and/or its well known pleiotropic effects. On the other hand, inhibition of the IP3 receptor with 2-aminoethoxydiphenyl borate (2-APB) blocked NMDA-induced CPEB4 nuclear accumulation, indicating that the IP3 receptor is of particular importance for causing CPEB4 to remain nuclear.

Mechanism for ER calcium depletion induced CPEB4 nuclear retention

The treatment of neurons with TG but not TM excludes ER stress per se as a possible mechanism for inducing CPEB4 nuclear accumulation. The retention of CPEB4 in the nucleus after BAPTA-AM incubation suggests that ER calcium depletion plays an inhibitory role in CPEB4 nuclear export. One key extant question is how does ER calcium depletion induce CPEB4 retention in the nucleus? Recent investigations of ER calcium homeostasis suggest that store operated calcium entry (SOCE) replenishes ER calcium levels after depletion. SOCE involves two protein families: the stromal interacting molecule (Stim) family and plasma membrane calcium channels, Orai. Stim proteins are located in the ER membrane and serve as ER lumen calcium level sensors (Roos et al., 2005; Zhang et al., 2005). Orai channel proteins interact with aggregated stim proteins and induce calcium influx when ER calcium is depleted (Feske et al.,

2006; Luik et al., 2006; Mercer et al., 2006; Peinelt et al., 2006; Prakriya et al., 2006). The influxed cytoplasmic calcium is then transported into the ER by the sarco/endoplasmic reticulum Ca^{2+}-ATPase (SERCA) system (Jousset et al., 2007). Whether calcium influxed through SOCE triggers CPEB4 nuclear retention upon ER calcium depletion and NMDA stimulation requires further investigation.

Materials and methods

Hippocampal neuron culture

The culture of primary rat hippocampal neurons was performed as described (Banker and Goslin, 1988) with a typical plating density of 1.8 x 10^4 cells/cm^2 cultured in Neurobasal media (Invitrogen) containing B27 supplement (B27 media) and glutamine (1 µg/ml). Cytosine arabinoside (Ara-C) (1 µ M) was added at DIV3 to prevent glial cell proliferation.

Lentiviral vector construction and virus production

Lentivirus expressing CPEB3 and CPEB4 were constructed by inserting myc-CPEB3 and myc-CPEB4 into the BamHI and XhoI sites of pFugw vector (Addgene). For virus production, 10 µ g of virus transfer vector that express various CPEBs, 7.5 µ g gag-pol expressing vector, psPAX2 (from Addgene) and 5 µ g VSV-G expressing vector, pMD2.G (from Addgene) were co-transfected into 1X10^7 293T cells plated in 10 cm culture dishes using Lipofectamine 2000 (Invitrogen). Three hours after transfection, the medium was replaced with Neurobasal medium containing B27 supplement (B27 media). Forty-eight hours after transfection, the medium was collected and passed through a 0.45 mm filter; the virus titer in the filtrate was calculated by serial dilution to determine the

minimum amount of virus that can infect 90% of neurons plated at 1.8 x 10^4 cells/cm as assayed by immunocytochemistry for the myc-tagged fusion proteins.

CPEB4 knockdown

Lentiviruses expressing shRNA against CPEB4 (pLL3.7-syn-KD2 and pLL3.7-syn-KD3) followed the procedure of (Huang et al., 2006). The primers for constructing pLL3.7-syn-KD2 were C4-KD2-F:

TGGCTGCAGCATGGAGAGATAGATTTCaagaGaATCTATCTCTCCATGCTG

CAGCCTTTTTTC and C4-KD2-R:

TCGAGAAAAAAGGCTGCAGCATGGAGAGATAGATTC

TCTTGAAATCTATCTCTCCATGCTGCAGCCA. The primers for constructing pLL3.7-syn-KD3 were C4-KD3-F:

TGGCTGCCTCATTTGGCGAATAATTTCaagaGaATTATTCGCC

AAATGAGGCAGCCTTTTTTC and C4-KD3-R:

TCGAGAAAAAAGGCTGCCTCATTTGGC

GAATAATTCTCTTGAAATTATTCGCCAAATGAGGCAGCCA. Lentivirus expressing shRNA was produced by transfecting 293T cell (1X10^6 cells/ml) with transfer vector together with packaging vectors, pSPAX2 and pMD2.G using lipofectamine 2000. Three hours after transfection, the cells were washed and cultured 48 hours after transfection, when the culture media was collected and filtered through a 0.2 mm syringe filter. The virus containing media was used

directly without concentration; the titer was determined as the minimal amount needed to infect more > 90% of cultured neurons.

Image acquisition and processing

A Nikon ECLIPSE E600 microscope is used to take fluorescence images; confocal images were acquired using a spinning disk confocal microscope (CSU10B, Solamere Technology Group) controlled by Metamorph software. Most of the images were taken using Plan Flour objective lens with 20 fold magnification and numerical aperture (N.A.) of 0.5. Cool charged CCD camera is made by Diagnostic instruments Inc (RT color). Images were taken and further processed using software SPOT version 3.5.8. Where indicated, fluorescence intensity was quantified using Image J software (NIH).

Antibodies and immunohistochemistry

CPEB4 antibody was produced as described (Huang et al., 2006); HA (16B12) and myc (9E10) monoclonal antibodies were produced as ascites fluid (Covance), and CHOP antibody was purchased from Santa Cruz Biotechnology. A TUNEL assay kit was purchased from MBL international. For CPEB4 immunostaining, cells were fixed in 2% paraformaldehyde/PBS/4% sucrose for 20 min and then blocked in 10% BSA for 20 min before overnight incubation with affinity purified CPEB4 antibody at 4^{o}C. Secondary antibody (Alexa 595 conjugated goat anti-rabbit and Alexa 488 conjugated goat anti-mouse), application and washing were performed as described (Molecular Probe). For

some experiments, neurons treated with TTX or TTX plus NMDA were collected and probed for CPEB4 and actin on western blots.

Middle cerebral artery occlusion (MCAO) and oxygen glucose deprivation (OGD)

MCAO was performed as described (van Leyen et al., 2006), except that MCAO was extended to 90 min and reperfusion to 24 hours before sacrifice. For OGD, MEM media is purged with nitrogen for 20 minutes to remove oxygen from solution. Gas purged media was placed in an anaerobic chamber for 30 mins to equilibrate pH. DIV14 hippocampal neurons were then cultured in oxygen purged, glucose-deficient MEM media in anaerobic chamber with an air mixture of 0.5% oxygen, 10% carbon dioxide and 89.5% nitrogen for 1 hour. The cells were then moved to normal neurobasal medium with B27 and cultured under standard conditions for various times before fixation.

In vitro nuclear import assay

HeLa cells grown on Lab-Tek Chamber Slides were permeabilized by digitonin (40mg/ml) in TB buffer (20 mM HEPES, pH7.4, 110 mM KOAc, 2 mM $Mg(OAc)_2$, 2 mM DTT, 1 mM EGTA and protease inhibitor) for 5 min on ice. The cells were then washed with TB buffer plus BSA (10 mg/ml) twice. After the second wash, the import reaction mixture was added (2ul 100 mg/ml BSA, 8 ml HeLa cytosol with ATP regeneration system, 2 ml GST-CPEB4RBD and 8 ml TB buffer). The ATP regeneration system contained 1 mM ATP, 5 mM phosphocreatine and 20

units/ml creatine phosphokinase. Permeabilized HeLa cells were incubated in a nuclear import reaction for 20 min at 25 ^{o}C; the cells were then washed with cold TB buffer before fixation with 4% formaldehyde/PBS for 10 mins. The fixed cells were stained with anti-GST antibody to detect nuclear import substrate and counterstained with DAPI.

Pharmacological treatment of primary neuron culture

Freshly prepared glutamate (100 μM), NMDA (100 μM), AMPA (300 μM), DHPG (100 μM) or ionomycin (5 μM) were applied to DIV16 hippocampal neurons for 1 hr before fixation and immunostaining. In some experiments, APV (2-amino-5-phosphonovaleric acid, 20 μM), Ant-AIP-II (Calbiochem, 10 μM), EGTA (2mM) were added to the cells 20 min before NMDA. BAPTA-AM (Calbiochem, 50 μM) was added to cultures for 20 min and then replaced with culture media for 40 min. Thapsigargin (Calbiochem, 2 mM stock) and tunicamycin (Calbiochem, 5 mg/ml 1000X stock) were suspended in DMSO and added to cultures. 2-aminoethoxydiphenyl borate (2-APB, 20 μM) was added to neurons 45 mins before NMDA.

Sucrose Gradients

Brain tissue from two month-old mice was washed once in 1X PBS, homogenized in 2 ml of 0.8 M sucrose and centrifuged at 10, 000 rpm for 10 min. 1.5 ml of the supernatant was subsequently removed and layered on 2.0 M sucrose in an SW41 centrifuge tube. 2.25 of 1.3 M, 1.95 M and 2.5 M sucrose

were layered on top of the brain lysates, which was followed by centrifugation at 40K for 5 h. An 18- gauge needle was used to pierce the bottom of the tube and 1 ml fractions were collected; 200 μl of each fraction were removed to a clean microcentrifuge. 2.5 volumes of 100% ethanol was added and the tubes were stored overnight at -20°C. The precipitates were collected by centrifugation and with 70% ethanol. The pellets were suspended in 100 μl of 1X SDS sample and analyzed by western blotting for CPEB4 (antibody dilution of 1:1000) or PDI (antibody dilution of 1:750, Santa Cruz).

Immuno Electron Microscopy

CPEB4 enriched fractions were pooled and diluted 5-fold in homogenization buffer (HB) (20 mM Tris-HCl, pH 7.5, 2 mM $MgCl_2$, 50 mM KCl, 250 mM sucrose, 1 mM phenylmethylsulfonyl fluoride). Pooled fractions were then centrifuged for 1h at 36K and the pellet washed once with 1X PBS. Pellets were then incubated with CPEB4 antibody (1:500) for 1 h at room temperature. Pellets were then washed twice with 1X PBS and blocked for 15 minutes with 5% BSA/PBS. Subsequently, the pellets were incubated with 10 nm goat anti-rabbit gold-conjugated antibody (1:25, Tedpella) for 1h at room temperature. The pellets were then washed three times 5 minutes each with 1X PBS and fixed with 2.5% glutaraldehyde in 0.1 M phosphate buffer pH 8.0.

Measurement of intracellular Ca2+

Neurons were plated at a density of $0.5x10^5$ cells/well in a 96 well dish and maintained in neurobasal medium containing B27. DIV16 hippocampal neurons were loaded with 1 μM Fluo-3/AM, a Ca2+-sensitive fluorescent probe (Invitrogen), containing 0.02% Pluronic F-127 (Molecular Probes) in Hank's buffered salt solution for 30 minutes at 37°C. The plates were gently washed with buffer and incubated for another 30 minutes at 37°C to permit de-esterification of intracellular Fluo-3/AM. The fluorescence of Fluo-3 is a measure of the Ca2+ concentration and was determined using a POLARstar Optima fluorescence plate reader (BMG Labtech) equipped with 485/10 nm excitation filter and a 520/10 nm emission filter. After dye loading, neurons were treated with various reagents (see Figure 3.11 for a complete list) and the relative fluorescence intensity was determined.

Measurement of ER calcium

ER calcium measurements were carried out using the ER targeted cameleon construct, D1ER (Palmer et al., 2004). Primary hippocampal neurons (DIV 12) were transfected with 1.6 mg of the pD1ER using Lipofectamine 2000 and maintained in Neurobasal medium. Four days after transfection, the appropriate pharmacological agent (see Figure 3.12) was added to the neurons and fluorescence resonance energy transfer (FRET) from the donor fluorophore CFP (441/485 nm excitation/emission) to the acceptor fluorophore YFP (441/550 nm excitation/emission) was measured. The magnitude of FRET signal is

proportional to the amount of calcium in the ER. Cells were imaged on Olympus IX 70 Inverted Light Microscope. To calibrate the relative FRET signal, R_{min} was obtained by treating the cells with 3 mM EGTA and 2 μM ionomycin and the FRET signal from untreated cells was set as R_{max}. Fluorescence images were background corrected. The emission ratio (FRET/CFP) was quantified before and after treatment of the neurons and percent calcium change was calculated by setting R_{min} as -100% change and R_{max} as 0% change. See Figure 3.12 for an illustration of the FRET assay.

Plasmid constructions

CPEB4 internal serial deletion was done by PCR using pcDNA-mycCPEB4 as template and various primer sets in PCR reactions using Pfu Turbo for amplification. Primers used to generate different deletion mutants are: for D1, C4-D1-R, CCCGTAATCCCCCATATGGGAT and C4-D1-F, GGTCAGGAAGCTGGAATACTG, for D2, C4-D2-R, TGGACTTGGGGAAAGCTGCTG and C4-D2-F, AATAATGGTGCTCTCTTGTTTC, for D3, C4-D3-R, AGCTGAAGCGCCAGGGACCCCTC and C4-D3-F, CCTTTGAAGAAAAATTTCGC, for 8

D4, C4-D4-R, TGAGATTGAGTTCAGGGGTG and C4-D4-F, GGGTCACCTCACTGCTTCAC, for D5, C4-D5-R, CAGACCACTATGAAGAGGTTG and C4-D5-F,

ATCAAGGATAAACCAGTGCAG, for D6, C4-D6-R, GGTTGGACTTGATACACACAG and C4-D6-F, ATAGATAAACGGGTGGAGGT, for D7, C4-D7-R, CTCTCCATGCTGCAGCTGAAC and C4-D7-F, TAAAGGATAACTGCAGTGCTC. PCR products were passed through a DyeEx column (Qiagen) to remove free nucleotide before digested by DpnI to remove template plasmid then ligated overnight in the presence of T4 PNK (Polynucleotide Kinase) by T4 DNA ligase. Selected clones were verified by sequencing. N-EGFP (NLS-MS2-EGFP) plasmid was constructed by inserting BamHI-NotI (NotI site filled in by T4 DNA polymerase) fragment from pG14-MS2-GFP into pEGFP-N3 (Clontech) digested by (EcoRI site filled in by T4 DNA polymerase). For minimal NES domain determination, various primers were used in PCR reactions to amplify different regions of CPEB4 and inserted between PstI and KpnI sites of pNLS-MS2-EGFP. Primers used to amplify various regions are: for N-EGFP-268, C4-218PstI, GGCCCTGCAGTCAATAATGGTGCTCTCTTG and C4-486KpnI, GGCCGGTACCTTCCACTCTCTCCCCATTCTG; for N-EGFP-145: C4-486KpnI, GGCCGGTACCTTCCACTCTCTCCCCATTCTG and C4-341PstI, GGCCCTGCAGTCGGTGGAATAACACCCCTGAAC; for N-EGFP-110: C4-486KpnI, GGCCGGTACCTTCCACTCTCTCCCCATTCTG and C4-376PstN, GGGCCCCTGCAGGAACGCCCCAGGACGTTTG; for N-EGFP-83: C4-424KpnC, GGGCCCGGTACCGTTTAGACGACCTTTAATGG and C4-341PstI, GGCCCTGCAGTCGGTGGAATAACACCCCTGAAC; for N-EGFP-48: C4-

424KpnC, GGGCCCGGTACCGTTTAGACGACCTTTAATGG and C4-376PstN, GGGCCCCTGCAGGAACGCCCCAGGACGTTTG. NESm of CPEB4 were generated by site directed mutagenesis using primers, L387-391AF, 9

CGTTTGACATGCACTCAGCAGAGAGCTCAGCAATTGACATAATGAGAGC and L387-391AR,

GCTCTCATTATGTCAATTGCTGAGCTCTCTGCTGAGTGCATGTCAAACG, in a 50 µl PCR reaction contained 2.5 units *Pfu*Turbo (Stratagene) a reaction as directed by user manual. PCR cycling condition for both serial internal deletion and site directed mutagenesis is the same as described below: 95oC for 30 sec. followed by 16 cycles of 95 ºC for 30 sec, 55 ºC for 1min, 68 ºC for 12 min. then ended in 68 ºC for 5 min

Acknowledgements

We thank Lan Xu for advice on the *in vitro* nuclear import assay, Oswald Steward for providing rat brain sections, and Melissa Jungnickel and Keith Sutton for help with the calcium fluorescence assays. We also thank the UMass Medical School imaging facility and the electron microscopy core facility, Robert Singer for the N-EGFP-MS2 plasmid, Roger Tsien for the Cameleon D1ER plasmid, Arthur Mercurio for the use of his hypoxia chamber, and Rachel Groppo for reading the manuscript. This work was supported by grants from the NIH (GM46779 and HD37267). AC-M was supported by 3 R01 GM046779-19S1. Core support from the Diabetes and Endocrinology Research Center Program Project (DK32520) is gratefully acknowledged.

CHAPTER IV

DISCUSSION AND CONCLUSIONS

In this thesis, I have focused on the role of cytoplasmic polyadenylation in mitochondrial activity and neuronal function and survival. CPEB has earlier been shown to be involved in oocyte maturation, senescence, neuronal plasticity, learning and memory. This study explores novel regulatory roles of CPEB and CPEB4 in cellular physiology.

The role of cytoplasmic polyadenylation binding protein CPEB in mitochondrial function and neuronal growth and branching was elucidated in chapter II. The CPEB KO mice have various defects in oocyte and sperm development, learning and memory defects (Richter, 2007). One additional area of CPEB influence is in control of senescence. Mouse embryonic fibroblasts (MEFs) and human foreskin fibroblasts deficient in CPEB can successfully bypass senescence (Burns and Richter, 2008; Groisman et al., 2006), whereas WT MEFs and WT human fibroblasts cannot bypass senescence and exit the cell cycle after passage 6. This senescence bypass is mediated by p53 in mouse and human cells and additionally requires myc in mouse fibroblasts (Burns and Richter, 2008; Groisman et al., 2006; Groppo and Richter). In addition to its role

in senescence, p53 has also been shown to be important for regulating mitochondrial function and thereby implicating CPEB in mitochondrial regulation (Matoba et al., 2006); in fact CPEB deficient human fibroblasts show reduced mitochondrial mass and function (Burns and Richter, 2008). I have uncovered that CPEB KO mice also display brain-specific mitochondrial dysfunction phenotype. CPEB is important for cytoplasmic polyadenylation induced translation of a mitochondrial protein NDUFV2, which is part of the ETC complex I. CPEB KO mice thus have defects in ETC complex I amount and activity, and exhibit reduced mitochondrial oxygen consumption and ATP production without affecting mitochondrial amounts. This reduction in mitochondrial ATP production is not compensated by increased glycolysis (as happens in Warburg effect) leading to reduction in overall ATP levels. CPEB regulates the translation of NDUFV2 by binding to the CPE elements in the 3'UTR of NDUFV2. These results show an important role for translational control in regulating mitochondrial function. A consequence of this impaired mitochondrial function is the loss of growth and branching in CPEB KO neurons. Hippocampal neurons cultured from CPEB KO mouse brains show reduced dendritic branches and reduced length of the branches. These defects can be rescued either by ectopic expression of NDUFV2 or by increasing ATP levels using the high energy substrate phosphocreatine showing the importance of mitochondrial function in regulating neuronal growth.

In chapter III, I focused on the nucleo-cytoplasmic shuttling of cytoplasmic polyadenylation binding protein 4 (CPEB4) and its effects on neuronal function. CPEB4 is predominantly expressed in brain and is found to localize mostly to the cell body of neurons (Huang et al., 2006; Theis et al., 2003). A small portion of CPEB4 protein also localizes to synaptic regions and cofractionates with the post synaptic density (Huang et al., 2006). To investigate whether this localization changes upon stimulation, neurons were treated with N-methyl D-aspartate (NMDA). Surprisingly, CPEB4 localized to nucleus upon NMDA treatment. Other neuronal stimulators such as glutamate and 2-amino-3-(3-hydroxy-5-methyl-isoxazol-4-yl)propanoic acid (AMPA) but not dihydroxyphenylglycine (DHPG) also produce the same nuclear localization of CPEB4 suggesting that stimulation of ionotropic glutamatergic receptors leads to nuclear localization of CPEB4. These neuronal stimulators cause changes in cellular ionic balance and thus propagate their signals; cytoplasmic calcium levels as well as ER calcium levels change during stimulation. I found that ER calcium depletion and not cytoplasmic calcium increase plays a bigger role in mediating CPEB4 nuclear localization. Although CPEB4 does not have a clear nuclear localization signal in its sequence, the nuclear export signal was identified to be between residues 341-424. This nuclear localization probably affords protection against apoptosis during stress conditions such as ischemia or oxygen glucose deprivation. Neurons lacking CPEB4 do not survive beyond day 8 in culture highlighting the importance of CPEB4 in neuronal function.

CPEB and mitochondria function

Mitochondria are important for cell survival and function. This is exemplified by the fact that mitochondrial oxidative phosphorylation defects are one of the most common inborn errors of metabolism (Kirby and Thorburn, 2008). In this thesis, CPEB was shown to play a role in regulating mitochondrial function specifically through its effect on ETC complex I, thus highlighting the importance of CPEB in body homeostasis. I observed these mitochondrial defects in hippocampus as well as in the cortex. Additional analysis on specific areas of the brain need to be undertaken to see if there is any brain region specific dysfunctions. Hippocampal and purkinje cerebellar neurons have high metabolic rates and glucose utilization and they might be the most affected regions. I have focused on the hippocampus, but studies on purkinje neurons will prove useful. Purkinje neurons are also known to be highly branched and it is possible that the neuronal branching in this area of the brain is also affected in the CPEB KO brain.

Defects in one subunit of an ETC complex have been shown to have damaging consequences for the cell. Hoefs *et al*. (2008) showed that mutation in an ETC complex I component NDUFA2 can cause reduced complex I function and lead to Leigh disease (Hoefs et al., 2008). Mutation in another complex I protein NDUFA1 gene has been linked to Leigh disease, myotonic epilepsy and developmental delay and this patient showed reduced levels of complex I

(Fernandez-Moreira et al., 2007). A 4 bp deletion in the NDUFV2 gene is associated with early-onset hypertrophic cardiomyopathy and encephalopathy. Patients with this mutation had a significant complex I deficiency. These studies indicate that mutation or defect in a single subunit of this complex can dramatically affect the amount and functioning of the entire complex. This could manifest as a disease in human body if the dysfunction is severe. Apart from Leigh disease and encephalopathy, mitochondrial defect is known to be associated with many neurodegenerative disease such as Parkinson's, Alzheimer's and Huntington's diseases and Amyotrophic Lateral Sclerosis (reviewed in (Lin and Beal, 2006).

The master energy sensor in the cell is 5' AMP activated protein kinase, a serine/threonine protein kinase, which maintains the energy status at the cellular as well as systemic level. It is upregulated by an increase in AMP/ATP ratio in the cell. Once activated, it shuts down anabolic processes and upregulates catabolic processes in order to conserve existing energy and acquire extra energy. It regulates the uptake of glucose, lipogenesis, fatty acid oxidation, glycolysis and many other metabolic processes. AMPK also phosphorylates Raptor, dissociating the mTOR complex and thereby inhibiting protein synthesis. Thus, AMPK activation down-regulates general protein synthesis. It will be interesting to check the level of activation of AMPK in the CPEB KO mice brain as well as in the rest of the tissues. The reduced ATP levels in CPEB KO should activate AMPK which would then inhibit general protein synthesis. Additionally,

CPEB KO also has inhibition of CPEB-mediated translation control activation. This is intriguing and experiments on AMPK will shed more light on this complexity.

The bioenergetic defects in CPEB KO mice are due to reduced translation of the complex I component NDUFV2; these defects can be rescued by ectopic expression of NDUFV2. Although NDUFV2 rescues the complex I defect, ATP deficiency and the neuron growth defect, the rescue is not complete, suggesting that there might be other players in this pathway. One plausible alternative mechanism could involve other proteins in complex I itself. Complex I contains 45 proteins of which 4 were shown to be unaffected by CPEB. Expression of the remaining 41 subunits was not tested in this work. There might be CPEB-dependent expression of one or more of those complex I subunits, albeit indirectly because their mRNAs do not possess CPE sequences in their 3'UTRs. In a 2-Dimensional electrophoresis separation analysis of complex I proteins from WT and CPEB KO brains followed by mass spectrometry based identification of proteins, only NDUFV2 protein level was found to be reduced in CPEB KO brain (data not shown). Moreover, NDUFV2 mRNA contains CPE sequence in its 3'UTR. Therefore, I focused the study on NDUFV2. Another plausible explanation for incomplete rescue by NDUFV2 could involve ETC complex II. CPEB KO mice also showed a minor deficiency in ETC complex II activity which also impacts the overall ATP production independent of complex I. NDUFV2 might rescue complex I function but has no effect on complex II activity

and therefore even after NDUFV2 ectopic expression, ATP levels are not restored to WT levels. Complex II, also known as succinate dehydrogenase (SDH), has 4 subunits – SDHA, SDHB, SDHC and SDHD. None of these 4 mRNAs have CPEs in their 3' UTRs, suggesting that CPEB does not play a role in mediating their translation activation. CPEB is computationally predicted to bind to about 20% of all brain mRNAs, but we do not know what its direct targets are. High throughput approaches such as identification of the entire set of CPEB bound mRNAs will help address this question and provide more insights into the role of CPEB. I would predict that many nuclear encoded mitochondrial genes have CPEs and are probably regulated by CPEB. Once we know the entire repertoire of CPEB bound targets, we can better understand the role of CPEB in mitochondrial function.

NDUFV2 is an important component of complex I. It is one of the 14 core subunits which make up the minimal structural unit required for the enzyme's function. NDUFV2 is highly conserved through evolution. Complex I assembly proceeds through multiple steps and NDUFV2 joins in one of the last steps of the assembly pathway. In the absence of NDUFV2 the whole complex I falls apart and is not assembled properly. This explains why loss of a single subunit NDUFV2 leads to reduction of complex I in CPEB KO.

Whether the regulation of NDUFV2 mRNA happens in the cell body and/or dendrites remains to be investigated. CPEB has been shown to regulate

transport of CPE-containing RNA in neurons (Huang et al., 2003). It is likely that CPEB transports NDUFV2 mRNA to dendrites by binding to its CPE element and the regulation of the translation of NDUFV2 occurs in dendrites, since CPEB as well as mitochondria are known to localize to dendrites. It will be interesting to investigate this further as this will shed light on the localization of this process.

This phenomenon of mitochondrial regulation by CPEB might be even more dramatic under conditions where the demand for energy is enormous such as in intense neuronal activity. Upon stimulation of neurons with stimulus such as NMDA, CPEB gets phosphorylated and activated and mediates translational enhancement of its targets (Huang et al., 2002). I envision that the above described phenomenon of mitochondrial regulation by CPEB becomes especially important during increased activity of brain; the brain requires enhanced ATP production upon stimulation which is supplied by increasing the mitochondrial activity which is produced by CPEB mediated increase in NDUFV2 translation and thus enhanced mitochondrial complex I production. It has been shown that neuronal stimulation by potassium chloride (KCl) can induce GA-binding protein, which is a transcription factor that binds to guanine and adenine rich sites in DNA and is required for expression of mitochondrial ETC complex IV proteins (Zhang and Wong-Riley, 2000). A CPEB-mediated increase in mitochondrial biogenesis could be an additional mechanism for activity-dependent increases in energy levels. This model can be tested by stimulating CPEB KO neurons with various

neurotransmitters and measuring increase in mitochondrial protein synthesis in WT versus CPEB KO neurons.

Mitochondrial dysfunction is also associated with many neurodegenerative diseases particularly Parkinson's and Alzheimer's diseases. Of special importance to this study is Parkinson's disease because complex I has been implicated in its pathogenesis. It will be interesting to study if there are any neurodegenerative phenotypes in the CPEB KO mice. Although the mouse is not an ideal model system to study these diseases at the organismal level, many of the molecular phenotypes observed in patients with these diseases are also found in mouse models. These studies need to be performed in aged mice. The CPEB KO mice may show some molecular degeneration phenotypes upon staining with markers such as tyrosine hydroxylase which stains dopaminergic neurons. Parkinson's disease is caused by degeneration of dopaminergic neurons in the substantia nigra region of the brain.

CPEB and neuronal growth

Neuronal growth is regulated by various factors such as netrin, NGF, Brain derived neurotrophic factor (BDNF) and neurotropins. Many of these growth and differentiation regulators act through cAMP signaling (Murray et al., 2009). CPEB was shown to be involved in regulating neuronal growth in *Xenopus* occyte retinal neurons (Bestman and Cline, 2008, 2009). In this thesis, I have uncovered the role of CPEB in regulating dendritic growth and branching in cultured mouse

hippocampal neurons as well as in mouse hippocampal neurons *in vivo*. Thus, CPEB plays an important role in neuronal growth. CPEB knockout mice exhibit synaptic plasticity as well as learning and memory defects, possibly due to its effect on neuronal branching and growth (Alarcon et al., 2004; Berger-Sweeney et al., 2006; Tay and Richter, 2001; Zearfoss et al., 2008). CPEB KO neurons are less branched and probably less connected to other neurons and cells in their surroundings.

Defect in neuronal branching can be rescued by chronic treatment of neurons with phosphocreatine, which is a high energy substrate. Upon entering the cells, phosphocreatine donates its high energy phosphate to ADP to form ATP thus increasing the ATP levels in a reaction catalyzed by creatine kinase. We surmise this is the mechanism by which phosphocreatine rescues neuronal branching defect. But it is possible that there are other mechanisms at play. For instance, creatine is known to activate signaling pathways like Akt/PKB leading to cellular modifications and signaling which might lead to the observed changes in dendrite growth and morphogenesis (Ceddia and Sweeney, 2004; Deldicque et al., 2007).

Significance of CPEB4

Many proteins such as transport receptors and adaptors, steroid hormone receptors, transcription factors, cell cycle regulators and RNA-binding proteins are known to shuttle between the nucleus and cytoplasm. Heterogeneous

nuclear ribonucleoproteins (hnRNPs) were the first RNA binding proteins to be discovered to shuttle between nucleus and cytoplasm (Dreyfuss et al., 1993). Initially RNA-binding proteins were thought to just transport mRNA into cytoplasm, but many studies have shown that these proteins also control the activities of the bound mRNAs in the cytoplasm (Shyu and Wilkinson, 2000). Many RNA-binding proteins such as hnRNPA1, hnRNP K, Sex lethal (SXL), bicoid and HuD are known to shuttle between cytoplasm and nucleus (Gama-Carvalho and Carmo-Fonseca, 2001). CPEB was previously shown to shuttle between the nucleus and cytoplasm and was shown to regulate alternate splicing of collagen 9a1 mRNA (Lin et al., 2010). CPEB4 now also joins this list of shuttling proteins as detailed in this thesis. It accumulates in the nucleus upon NMDA excitotoxicity and affords protection from apoptosis but the exact mechanism of how it protects the neurons is not clear. It has been demonstrated that the extra synaptic NMDA NR2B receptors play a major role in mediating excitotoxicity. Perturbing synaptic localization of NR2A NMDARs did not have an effect on the toxicity by exogenous NMDA suggesting the importance of extra synaptic receptors (Sattler et al., 2000). These extra synaptic receptors are present in the cell body of the neurons and are thought to form clusters, through their interaction with PSD-95 proteins. The extra synaptic receptors are activated by bath glutamate exposure or ischemia and they shut off the CREB pathway, which in turn causes loss of mitochondrial membrane potential and cell death by inducing apoptosis (Hardingham et al., 2002). Perhaps CPEB4 interferes in this

pathway and thus prevents apoptosis? To demonstrate whether the synaptic NR2A receptors or the extra synaptic NR2B receptors play the major role, inhibitors such as ifenprodil (which specifically inhibits NR2B) can be utilized. Further studies need to also focus on the neuroprotective role of CPEB4. Does CPEB4 also afford such protection to other cells apart from neurons? What other conditions will result in nuclear accumulation of CPEB4? These are some unresolved questions and will need to be addressed in future studies.

CaM kinase II has been shown here to play a role in the nuclear localization of CPEB4 through the use of CaMKII inhibitory peptide AIPII (Ishida et al., 1995). CaM kinases are serine/threonine protein kinases that are regulated by calcium and calmodulin. CaMKII is capable of phophorylating substrates such as AMPA receptors, synapsin I, tyrosine hydroxylase, L-type Ca^{2+} channels, and MAP-2 (microtubule associated protein 2) (Colbran and Brown, 2004). CaMKII is the major PSD protein whose amounts in PSD double upon activation. The level of CaMKII in the PSD affects LTP and hippocampal dependent learning. The NMDA receptor contributes to this synaptic localization of CaMKII by binding to it. Targeting to NMDA receptors is responsible for the calcium linked translocation of CamKII to synapses (Schulman, 2004). In our results, we found that CaM kinase inhibition leads to loss of CPEB4 nuclear localization upon NMDA application.

In a high throughput whole genome approach, Ortiz-Zapater *et al*. identified the set of RNAs bound by CPEB4 using RNA-immunoprecipitation followed by microarray (Ortiz-Zapater et al., 2012). Knowing the mRNAs bound by CPEB4 will give us some insight into its function. One of the significant categories of mRNAs identified in that study is cellular functions relevant to apoptosis and cell death; these mRNAs could be involved in mediating CPEB4 afforded neuroprotection against apoptosis. A large majority of the bound mRNAs are related to general translation factors and ribosomal proteins, thus suggesting a role for CPEB4 in translation control of all mRNAs. Interestingly, there are many calcium regulatory genes such as *commd5* (copper metabolism domain containing gene 5), tpm1 (tropomyosin 1) in the list of mRNAs bound by CPEB4. Commd5 protein expression is negatively regulated by extracellular calcium concentration and Tpm1 is involved in calcium dependent regulation of muscle contraction. Exploring the functions of these mRNAs will provide useful hints for elucidating CPEB4 function.

Importance of CPEB family proteins

In this thesis and as detailed in the literature, the importance of CPEB family proteins is being recognized for their critical role in cellular function. The founding member CPEB was originally discovered in *Xenopus*, but now CPEB family

proteins have been demonstrated to be present in many organisms and play important roles in cell physiology. These proteins perform their functions by regulating mRNA translation, which go on to fine tune various processes in the cell. It will be really beneficial to identify the entire repertoire of mRNA bound by these RNA binding proteins. High throughput analysis such as Hits-CLIP (High throughput sequencing of tags obtained upon cross linking and immunoprecipitation) can be performed in order to understand the function of these proteins and their interacting mRNAs. Hits-CLIP involves cross linking the protein to their interacting mRNAs and immunoprecipitation of the cross linked complexes followed by sequencing of these mRNAs tags obtained (Licatalosi et al., 2008). Knowledge of the mRNAs bound to CPEB1-4 can help us better understand their role in cellular functions.

Conclusions

CPEB plays an important role in oogenesis, cell division, senescence, neuronal synaptic plasticity, learning and memory. Such pleiotropism places CPEB in an important stature in the cell. Recently, CPEB has been shown to be related to three similar proteins (CPEB2-4), which together constitute the CPEB family. This thesis describes research into role of CPEB in mitochondrial function, its implications in neuronal growth and branching 173and explores the causes and consequences of nucleo-cytoplasmic shuttling of CPEB4. These two proteins are also important for neuronal growth, function and survival. Thus, CPEB family proteins are vital regulators of cellular physiology.

BIBLIOGRAPHY

Alarcon, J.M., Hodgman, R., Theis, M., Huang, Y.S., Kandel, E.R., and Richter, J.D. (2004). Selective modulation of some forms of schaffer collateral-CA1 synaptic plasticity in mice with a disruption of the CPEB-1 gene. Learning & memory (Cold Spring Harbor, N.Y *11*, 318-327.

Alexandrov, I.M., Ivshina, M., Jung, D.Y., Friedline, R., Ko, H.J., Xu, M., O'Sullivan-Murphy, B., Bortell, R., Huang, Y.T., Urano, F., et al. Cytoplasmic Polyadenylation Element Binding Protein Deficiency Stimulates PTEN and Stat3 mRNA Translation and Induces Hepatic Insulin Resistance. PLoS genetics *8*, e1002457.

Banker, G., and Goslin, K. (1988). Developments in neuronal cell culture. Nature *336*, 185-186.

Barnard, D.C., Ryan, K., Manley, J.L., and Richter, J.D. (2004). Symplekin and xGLD-2 are required for CPEB-mediated cytoplasmic polyadenylation. Cell *119*, 641-651.

Berger-Sweeney, J., Zearfoss, N.R., and Richter, J.D. (2006). Reduced extinction of hippocampal-dependent memories in CPEB knockout mice. Learning & memory (Cold Spring Harbor, N.Y *13*, 4-7.

Bestman, J.E., and Cline, H.T. (2008). The RNA binding protein CPEB regulates dendrite morphogenesis and neuronal circuit assembly in vivo. Proceedings of the National Academy of Sciences of the United States of America *105*, 20494-20499.

Bestman, J.E., and Cline, H.T. (2009). The Relationship between Dendritic Branch Dynamics and CPEB-Labeled RNP Granules Captured in Vivo. Frontiers in neural circuits *3*, 10.

Birch-Machin, M.A., and Turnbull, D.M. (2001). Assaying mitochondrial respiratory complex activity in mitochondria isolated from human cells and tissues. Methods in cell biology *65*, 97-117.

Burns, D.M., and Richter, J.D. (2008). CPEB regulation of human cellular senescence, energy metabolism, and p53 mRNA translation. Genes & development *22*, 3449-3460.

Cao, G., Clark, R.S., Pei, W., Yin, W., Zhang, F., Sun, F.Y., Graham, S.H., and Chen, J. (2003). Translocation of apoptosis-inducing factor in vulnerable neurons after transient cerebral ischemia and in neuronal cultures after oxygen-glucose deprivation. J Cereb Blood Flow Metab *23*, 1137-1150.

Cao, Q., Kim, J.H., and Richter, J.D. (2006). CDK1 and calcineurin regulate Maskin association with eIF4E and translational control of cell cycle progression. Nature structural & molecular biology *13*, 1128-1134.

Ceddia, R.B., and Sweeney, G. (2004). Creatine supplementation increases glucose oxidation and AMPK phosphorylation and reduces lactate production in L6 rat skeletal muscle cells. The Journal of physiology *555*, 409-421.

Chacinska, A., Koehler, C.M., Milenkovic, D., Lithgow, T., and Pfanner, N. (2009). Importing mitochondrial proteins: machineries and mechanisms. Cell *138*, 628-644.

Chan, D.C. (2006). Mitochondrial fusion and fission in mammals. Annual review of cell and developmental biology *22*, 79-99.

Chang, L.H., Shimizu, H., Abiko, H., Swanson, R.A., Faden, A.I., James, T.L., and Weinstein, P.R. (1992). Effect of dichloroacetate on recovery of brain lactate,

phosphorus energy metabolites, and glutamate during reperfusion after complete cerebral ischemia in rats. J Cereb Blood Flow Metab *12*, 1030-1038.

Chen, H., and Chan, D.C. (2006). Critical dependence of neurons on mitochondrial dynamics. Current opinion in cell biology *18*, 453-459.

Chen, M., Zhang, J., and Manley, J.L. (2010). Turning on a fuel switch of cancer: hnRNP proteins regulate alternative splicing of pyruvate kinase mRNA. Cancer research *70*, 8977-8980.

Chen, P.J., and Huang, Y.S. (2012). CPEB2-eEF2 interaction impedes HIF-1alpha RNA translation. The EMBO journal *31*, 959-971.

Chen, X.J., and Butow, R.A. (2005). The organization and inheritance of the mitochondrial genome. Nature reviews. Genetics *6*, 815-825.

Choi, D.W., and Rothman, S.M. (1990). The role of glutamate neurotoxicity in hypoxic-ischemic neuronal death. Annu Rev Neurosci *13*, 171-182.

Christofk, H.R., Vander Heiden, M.G., Harris, M.H., Ramanathan, A., Gerszten, R.E., Wei, R., Fleming, M.D., Schreiber, S.L., and Cantley, L.C. (2008). The M2

splice isoform of pyruvate kinase is important for cancer metabolism and tumour growth. Nature *452*, 230-233.

Colbran, R.J., and Brown, A.M. (2004). Calcium/calmodulin-dependent protein kinase II and synaptic plasticity. Current opinion in neurobiology *14*, 318-327.

Colgan, D.F., and Manley, J.L. (1997). Mechanism and regulation of mRNA polyadenylation. Genes & development *11*, 2755-2766.

Corpet, F. (1988). Multiple sequence alignment with hierarchical clustering. Nucleic Acids Res *16*, 10881-10890.

Dang, C.V. (2012). Links between metabolism and cancer. Genes & development *26*, 877-890.

Daugas, E., Susin, S.A., Zamzami, N., Ferri, K.F., Irinopoulou, T., Larochette, N., Prevost, M.C., Leber, B., Andrews, D., Penninger, J., et al. (2000). Mitochondrio-nuclear translocation of AIF in apoptosis and necrosis. Faseb J *14*, 729-739.

David, C.J., Chen, M., Assanah, M., Canoll, P., and Manley, J.L. (2010). HnRNP proteins controlled by c-Myc deregulate pyruvate kinase mRNA splicing in cancer. Nature *463*, 364-368.

Deldicque, L., Theisen, D., Bertrand, L., Hespel, P., Hue, L., and Francaux, M. (2007). Creatine enhances differentiation of myogenic C2C12 cells by activating both p38 and Akt/PKB pathways. American journal of physiology *293*, C1263-1271.

Delettre, C., Lenaers, G., Griffoin, J.M., Gigarel, N., Lorenzo, C., Belenguer, P., Pelloquin, L., Grosgeorge, J., Turc-Carel, C., Perret, E., et al. (2000). Nuclear gene OPA1, encoding a mitochondrial dynamin-related protein, is mutated in dominant optic atrophy. Nature genetics *26*, 207-210.

Demaurex, N., and Frieden, M. (2003). Measurements of the free luminal ER Ca(2+) concentration with targeted "cameleon" fluorescent proteins. Cell Calcium *34*, 109-119.

Distelmaier, F., Koopman, W.J., van den Heuvel, L.P., Rodenburg, R.J., Mayatepek, E., Willems, P.H., and Smeitink, J.A. (2009). Mitochondrial complex I deficiency: from organelle dysfunction to clinical disease. Brain *132*, 833-842.

Dreyfuss, G., Matunis, M.J., Pinol-Roma, S., and Burd, C.G. (1993). hnRNP proteins and the biogenesis of mRNA. Annual review of biochemistry *62*, 289-321.

Du, L., and Richter, J.D. (2005). Activity-dependent polyadenylation in neurons. RNA (New York, N.Y *11*, 1340-1347.

Ellis, C.E., Murphy, E.J., Mitchell, D.C., Golovko, M.Y., Scaglia, F., Barcelo-Coblijn, G.C., and Nussbaum, R.L. (2005). Mitochondrial lipid abnormality and electron transport chain impairment in mice lacking alpha-synuclein. Molecular and cellular biology *25*, 10190-10201.

Emptage, N., Bliss, T.V., and Fine, A. (1999). Single synaptic events evoke NMDA receptor-mediated release of calcium from internal stores in hippocampal dendritic spines. Neuron *22*, 115-124.

Fernandez-Moreira, D., Ugalde, C., Smeets, R., Rodenburg, R.J., Lopez-Laso, E., Ruiz-Falco, M.L., Briones, P., Martin, M.A., Smeitink, J.A., and Arenas, J. (2007). X-linked NDUFA1 gene mutations associated with mitochondrial encephalomyopathy. Annals of neurology *61*, 73-83.

Ferrari, F., Mercaldo, V., Piccoli, G., Sala, C., Cannata, S., Achsel, T., and Bagni, C. (2007). The fragile X mental retardation protein-RNP granules show an mGluR-dependent localization in the post-synaptic spines. Mol Cell Neurosci *34*, 343-354.

Feske, S., Gwack, Y., Prakriya, M., Srikanth, S., Puppel, S.H., Tanasa, B., Hogan, P.G., Lewis, R.S., Daly, M., and Rao, A. (2006). A mutation in Orai1 causes immune deficiency by abrogating CRAC channel function. Nature *441*, 179-185.

Forster, M.J., Dubey, A., Dawson, K.M., Stutts, W.A., Lal, H., and Sohal, R.S. (1996). Age-related losses of cognitive function and motor skills in mice are associated with oxidative protein damage in the brain. Proceedings of the National Academy of Sciences of the United States of America *93*, 4765-4769.

Fox, C.A., Sheets, M.D., and Wickens, M.P. (1989). Poly(A) addition during maturation of frog oocytes: distinct nuclear and cytoplasmic activities and regulation by the sequence UUUUUAU. Genes & development *3*, 2151-2162.

Frandsen, A., and Schousboe, A. (1992). Mobilization of dantrolene-sensitive intracellular calcium pools is involved in the cytotoxicity induced by quisqualate and N-methyl-D-aspartate but not by 2-amino-3-(3-hydroxy-5-methylisoxazol-4-yl)propionate and kainate in cultured cerebral cortical neurons. Proc Natl Acad Sci U S A *89*, 2590-2594.

Gama-Carvalho, M., and Carmo-Fonseca, M. (2001). The rules and roles of nucleocytoplasmic shuttling proteins. FEBS letters *498*, 157-163.

Ge, S., Goh, E.L., Sailor, K.A., Kitabatake, Y., Ming, G.L., and Song, H. (2006). GABA regulates synaptic integration of newly generated neurons in the adult brain. Nature *439*, 589-593.

Groisman, I., Huang, Y.S., Mendez, R., Cao, Q., Theurkauf, W., and Richter, J.D. (2000). CPEB, maskin, and cyclin B1 mRNA at the mitotic apparatus: implications for local translational control of cell division. Cell *103*, 435-447.

Groisman, I., Ivshina, M., Marin, V., Kennedy, N.J., Davis, R.J., and Richter, J.D. (2006). Control of cellular senescence by CPEB. Genes & development *20*, 2701-2712.

Groisman, I., Jung, M.Y., Sarkissian, M., Cao, Q., and Richter, J.D. (2002). Translational control of the embryonic cell cycle. Cell *109*, 473-483.

Groppo, R., and Richter, J.D. CPEB control of NF-kappaB nuclear localization and interleukin-6 production mediates cellular senescence. Molecular and cellular biology *31*, 2707-2714.

Groppo, R., and Richter, J.D. (2009). Translational control from head to tail. Current opinion in cell biology *21*, 444-451.

Hagele, S., Kuhn, U., Boning, M., and Katschinski, D.M. (2009). Cytoplasmic polyadenylation-element-binding protein (CPEB)1 and 2 bind to the HIF-1alpha mRNA 3'-UTR and modulate HIF-1alpha protein expression. The Biochemical journal *417*, 235-246.

Hardingham, G.E., Fukunaga, Y., and Bading, H. (2002). Extrasynaptic NMDARs oppose synaptic NMDARs by triggering CREB shut-off and cell death pathways. Nature neuroscience *5*, 405-414.

Hock, M.B., and Kralli, A. (2009). Transcriptional control of mitochondrial biogenesis and function. Annual review of physiology *71*, 177-203.

Hoefs, S.J., Dieteren, C.E., Distelmaier, F., Janssen, R.J., Epplen, A., Swarts, H.G., Forkink, M., Rodenburg, R.J., Nijtmans, L.G., Willems, P.H., et al. (2008). NDUFA2 complex I mutation leads to Leigh disease. American journal of human genetics *82*, 1306-1315.

Hofmann, I., Schnolzer, M., Kaufmann, I., and Franke, W.W. (2002). Symplekin, a constitutive protein of karyo- and cytoplasmic particles involved in mRNA biogenesis in Xenopus laevis oocytes. Mol Biol Cell *13*, 1665-1676.

Hollenbeck, P.J. (2005). Mitochondria and neurotransmission: evacuating the synapse. Neuron *47*, 331-333.

Hu, B.R., Martone, M.E., Jones, Y.Z., and Liu, C.L. (2000). Protein aggregation after transient cerebral ischemia. J Neurosci *20*, 3191-3199.

Huang, Y.S., Carson, J.H., Barbarese, E., and Richter, J.D. (2003). Facilitation of dendritic mRNA transport by CPEB. Genes & development *17*, 638-653.

Huang, Y.S., Jung, M.Y., Sarkissian, M., and Richter, J.D. (2002). N-methyl-D-aspartate receptor signaling results in Aurora kinase-catalyzed CPEB phosphorylation and alpha CaMKII mRNA polyadenylation at synapses. Embo J *21*, 2139-2148.

Huang, Y.S., Kan, M.C., Lin, C.L., and Richter, J.D. (2006). CPEB3 and CPEB4 in neurons: analysis of RNA-binding specificity and translational control of AMPA receptor GluR2 mRNA. The EMBO journal *25*, 4865-4876.

Huang, Y.S., and Richter, J.D. (2007). Analysis of mRNA translation in cultured hippocampal neurons. Methods in enzymology *431*, 143-162.

Hudmon, A., and Schulman, H. (2002). Neuronal CA2+/calmodulin-dependent protein kinase II: the role of structure and autoregulation in cellular function. Annu Rev Biochem *71*, 473-510.

Igea, A., and Mendez, R. (2010). Meiosis requires a translational positive loop where CPEB1 ensues its replacement by CPEB4. The EMBO journal *29*, 2182-2193.

Ishida, A., Kameshita, I., Okuno, S., Kitani, T., and Fujisawa, H. (1995). A novel highly specific and potent inhibitor of calmodulin-dependent protein kinase II. Biochemical and biophysical research communications *212*, 806-812.

Ishida, A., Shigeri, Y., Tatsu, Y., Uegaki, K., Kameshita, I., Okuno, S., Kitani, T., Yumoto, N., and Fujisawa, H. (1998). Critical amino acid residues of AIP, a highly specific inhibitory peptide of calmodulin-dependent protein kinase II. FEBS letters *427*, 115-118.

Ishihara, N., Nomura, M., Jofuku, A., Kato, H., Suzuki, S.O., Masuda, K., Otera, H., Nakanishi, Y., Nonaka, I., Goto, Y., et al. (2009). Mitochondrial fission factor Drp1 is essential for embryonic development and synapse formation in mice. Nature cell biology *11*, 958-966.

Johnson, D.T., Harris, R.A., French, S., Blair, P.V., You, J., Bemis, K.G., Wang, M., and Balaban, R.S. (2007). Tissue heterogeneity of the mammalian mitochondrial proteome. American journal of physiology *292*, C689-697.

Jousset, H., Frieden, M., and Demaurex, N. (2007). STIM1 knockdown reveals that store-operated Ca2+ channels located close to sarco/endoplasmic Ca2+ ATPases (SERCA) pumps silently refill the endoplasmic reticulum. J Biol Chem *282*, 11456-11464.

Kann, O., and Kovacs, R. (2007). Mitochondria and neuronal activity. American journal of physiology *292*, C641-657.

Keleman, K., Kruttner, S., Alenius, M., and Dickson, B.J. (2007). Function of the Drosophila CPEB protein Orb2 in long-term courtship memory. Nature neuroscience *10*, 1587-1593.

Kim, J.H., and Richter, J.D. (2006). Opposing polymerase-deadenylase activities regulate cytoplasmic polyadenylation. Molecular cell *24*, 173-183.

Kim, J.H., and Richter, J.D. (2007). RINGO/cdk1 and CPEB mediate poly(A) tail stabilization and translational regulation by ePAB. Genes & development *21*, 2571-2579.

Kirby, D.M., and Thorburn, D.R. (2008). Approaches to finding the molecular basis of mitochondrial oxidative phosphorylation disorders. Twin research and human genetics : the official journal of the International Society for Twin Studies *11*, 395-411.

Koc, E.C., and Koc, H. (2012). Regulation of mammalian mitochondrial translation by post-translational modifications. Biochimica et biophysica acta *1819*, 1055-1066.

Koopman, W.J., Nijtmans, L.G., Dieteren, C.E., Roestenberg, P., Valsecchi, F., Smeitink, J.A., and Willems, P.H. (2010). Mammalian mitochondrial complex I: biogenesis, regulation, and reactive oxygen species generation. Antioxidants & redox signaling *12*, 1431-1470.

Kudo, N., Matsumori, N., Taoka, H., Fujiwara, D., Schreiner, E.P., Wolff, B., Yoshida, M., and Horinouchi, S. (1999). Leptomycin B inactivates CRM1/exportin 1 by covalent modification at a cysteine residue in the central conserved region. Proceedings of the National Academy of Sciences of the United States of America *96*, 9112-9117.

Kunz, W.S. (2003). Different metabolic properties of mitochondrial oxidative phosphorylation in different cell types--important implications for mitochondrial cytopathies. Experimental physiology *88*, 149-154.

Kurihara, Y., Tokuriki, M., Myojin, R., Hori, T., Kuroiwa, A., Matsuda, Y., Sakurai, T., Kimura, M., Hecht, N.B., and Uesugi, S. (2003). CPEB2, a novel putative translational regulator in mouse haploid germ cells. Biology of reproduction *69*, 261-268.

Kuznetsov, A.V., Hermann, M., Saks, V., Hengster, P., and Margreiter, R. (2009). The cell-type specificity of mitochondrial dynamics. The international journal of biochemistry & cell biology *41*, 1928-1939.

Lazarou, M., Thorburn, D.R., Ryan, M.T., and McKenzie, M. (2009). Assembly of mitochondrial complex I and defects in disease. Biochimica et biophysica acta *1793*, 78-88.

Levine, A.J., and Puzio-Kuter, A.M. The control of the metabolic switch in cancers by oncogenes and tumor suppressor genes. Science (New York, N.Y *330*, 1340-1344.

Levine, A.J., and Puzio-Kuter, A.M. (2010). The control of the metabolic switch in cancers by oncogenes and tumor suppressor genes. Science (New York, N.Y *330*, 1340-1344.

Li, Z., and Graham, B.H. (2012). Measurement of mitochondrial oxygen consumption using a Clark electrode. Methods in molecular biology *837*, 63-72.

Li, Z., Okamoto, K., Hayashi, Y., and Sheng, M. (2004). The importance of dendritic mitochondria in the morphogenesis and plasticity of spines and synapses. Cell *119*, 873-887.

Licatalosi, D.D., Mele, A., Fak, J.J., Ule, J., Kayikci, M., Chi, S.W., Clark, T.A., Schweitzer, A.C., Blume, J.E., Wang, X., et al. (2008). HITS-CLIP yields genome-wide insights into brain alternative RNA processing. Nature *456*, 464-469.

Lin, A.C., Tan, C.L., Lin, C.L., Strochlic, L., Huang, Y.S., Richter, J.D., and Holt, C.E. (2009). Cytoplasmic polyadenylation and cytoplasmic polyadenylation element-dependent mRNA regulation are involved in Xenopus retinal axon development. Neural development *4*, 8.

Lin, C.L., Evans, V., Shen, S., Xing, Y., and Richter, J.D. (2010). The nuclear experience of CPEB: implications for RNA processing and translational control. Rna *16*, 338-348.

Lin, J., Handschin, C., and Spiegelman, B.M. (2005). Metabolic control through the PGC-1 family of transcription coactivators. Cell metabolism *1*, 361-370.

Lin, M.T., and Beal, M.F. (2006). Mitochondrial dysfunction and oxidative stress in neurodegenerative diseases. Nature *443*, 787-795.

Loeffen, J., Smeitink, J., Triepels, R., Smeets, R., Schuelke, M., Sengers, R., Trijbels, F., Hamel, B., Mullaart, R., and van den Heuvel, L. (1998). The first nuclear-encoded complex I mutation in a patient with Leigh syndrome. American journal of human genetics *63*, 1598-1608.

Luik, R.M., Wu, M.M., Buchanan, J., and Lewis, R.S. (2006). The elementary unit of store-operated Ca2+ entry: local activation of CRAC channels by STIM1 at ER-plasma membrane junctions. The Journal of cell biology *174*, 815-825.

Macchi, P., Brownawell, A.M., Grunewald, B., DesGroseillers, L., Macara, I.G., and Kiebler, M.A. (2004). The brain-specific double-stranded RNA-binding

protein Staufen2: nucleolar accumulation and isoform-specific exportin-5-dependent export. The Journal of biological chemistry *279*, 31440-31444.

Majumdar, A., Cesario, W.C., White-Grindley, E., Jiang, H., Ren, F., Khan, M.R., Li, L., Choi, E.M., Kannan, K., Guo, F., et al. (2012). Critical role of amyloid-like oligomers of Drosophila Orb2 in the persistence of memory. Cell *148*, 515-529.

Mandel, C.R., Kaneko, S., Zhang, H., Gebauer, D., Vethantham, V., Manley, J.L., and Tong, L. (2006). Polyadenylation factor CPSF-73 is the pre-mRNA 3'-end-processing endonuclease. Nature *444*, 953-956.

Matoba, S., Kang, J.G., Patino, W.D., Wragg, A., Boehm, M., Gavrilova, O., Hurley, P.J., Bunz, F., and Hwang, P.M. (2006). p53 regulates mitochondrial respiration. Science (New York, N.Y *312*, 1650-1653.

Mendez, R., Hake, L.E., Andresson, T., Littlepage, L.E., Ruderman, J.V., and Richter, J.D. (2000). Phosphorylation of CPE binding factor by Eg2 regulates translation of c-mos mRNA. Nature *404*, 302-307.

Mendez, R., and Richter, J.D. (2001). Translational control by CPEB: a means to the end. Nature reviews. Molecular cell biology *2*, 521-529.

Mercer, J.C., Dehaven, W.I., Smyth, J.T., Wedel, B., Boyles, R.R., Bird, G.S., and Putney, J.W., Jr. (2006). Large store-operated calcium selective currents due to co-expression of Orai1 or Orai2 with the intracellular calcium sensor, Stim1. The Journal of biological chemistry *281*, 24979-24990.

Merrick, W.C. (1992). Mechanism and regulation of eukaryotic protein synthesis. Microbiological reviews *56*, 291-315.

Mironov, S.L. (2009). Complexity of mitochondrial dynamics in neurons and its control by ADP produced during synaptic activity. The international journal of biochemistry & cell biology *41*, 2005-2014.

Morgan, M., Iaconcig, A., and Muro, A.F. (2010). CPEB2, CPEB3 and CPEB4 are coordinately regulated by miRNAs recognizing conserved binding sites in paralog positions of their 3'-UTRs. Nucleic acids research *38*, 7698-7710.

Morimoto, N., Oida, Y., Shimazawa, M., Miura, M., Kudo, T., Imaizumi, K., and Hara, H. (2007). Involvement of endoplasmic reticulum stress after middle cerebral artery occlusion in mice. Neuroscience *147*, 957-967.

Morris, R.L., and Hollenbeck, P.J. (1993). The regulation of bidirectional mitochondrial transport is coordinated with axonal outgrowth. Journal of cell science *104 (Pt 3)*, 917-927.

Murray, A.J., Tucker, S.J., and Shewan, D.A. (2009). cAMP-dependent axon guidance is distinctly regulated by Epac and protein kinase A. J Neurosci *29*, 15434-15444.

Nagaoka, K., Udagawa, T., and Richter, J.D. (2012). CPEB-mediated ZO-1 mRNA localization is required for epithelial tight-junction assembly and cell polarity. Nature communications *3*, 675.

Nicholls, D.G., and Budd, S.L. (2000). Mitochondria and neuronal survival. Physiological reviews *80*, 315-360.

Niimura, M., Takagi, N., Takagi, K., Mizutani, R., Ishihara, N., Matsumoto, K., Funakoshi, H., Nakamura, T., and Takeo, S. (2006). Prevention of apoptosis-inducing factor translocation is a possible mechanism for protective effects of hepatocyte growth factor against neuronal cell death in the hippocampus after transient forebrain ischemia. J Cereb Blood Flow Metab *26*, 1354-1365.

Nishi, K., Yoshida, M., Fujiwara, D., Nishikawa, M., Horinouchi, S., and Beppu, T. (1994). Leptomycin B targets a regulatory cascade of crm1, a fission yeast nuclear protein, involved in control of higher order chromosome structure and gene expression. The Journal of biological chemistry *269*, 6320-6324.

Novoa, I., Gallego, J., Ferreira, P.G., and Mendez, R. (2010). Mitotic cell-cycle progression is regulated by CPEB1 and CPEB4-dependent translational control. Nature cell biology *12*, 447-456.

Ortiz-Zapater, E., Pineda, D., Martinez-Bosch, N., Fernandez-Miranda, G., Iglesias, M., Alameda, F., Moreno, M., Eliscovich, C., Eyras, E., Real, F.X., et al. (2012). Key contribution of CPEB4-mediated translational control to cancer progression. Nature medicine *18*, 83-90.

Pagliarini, D.J., Calvo, S.E., Chang, B., Sheth, S.A., Vafai, S.B., Ong, S.E., Walford, G.A., Sugiana, C., Boneh, A., Chen, W.K., et al. (2008). A mitochondrial protein compendium elucidates complex I disease biology. Cell *134*, 112-123.

Palmer, A.E., Jin, C., Reed, J.C., and Tsien, R.Y. (2004). Bcl-2-mediated alterations in endoplasmic reticulum Ca2+ analyzed with an improved genetically encoded fluorescent sensor. Proceedings of the National Academy of Sciences of the United States of America *101*, 17404-17409.

Paschen, W., Hotop, S., and Aufenberg, C. (2003). Loading neurons with BAPTA-AM activates xbp1 processing indicative of induction of endoplasmic reticulum stress. Cell calcium *33*, 83-89.

Pavlopoulos, E., Trifilieff, P., Chevaleyre, V., Fioriti, L., Zairis, S., Pagano, A., Malleret, G., and Kandel, E.R. (2011). Neuralized1 activates CPEB3: a function for nonproteolytic ubiquitin in synaptic plasticity and memory storage. Cell *147*, 1369-1383.

Peinelt, C., Vig, M., Koomoa, D.L., Beck, A., Nadler, M.J., Koblan-Huberson, M., Lis, A., Fleig, A., Penner, R., and Kinet, J.P. (2006). Amplification of CRAC current by STIM1 and CRACM1 (Orai1). Nature cell biology *8*, 771-773.

Peng, S.C., Lai, Y.T., Huang, H.Y., Huang, H.D., and Huang, Y.S. (2010). A novel role of CPEB3 in regulating EGFR gene transcription via association with Stat5b in neurons. Nucleic acids research *38*, 7446-7457.

Peritz, T., Zeng, F., Kannanayakal, T.J., Kilk, K., Eiriksdottir, E., Langel, U., and Eberwine, J. (2006). Immunoprecipitation of mRNA-protein complexes. Nature protocols *1*, 577-580.

Petosa, C., Schoehn, G., Askjaer, P., Bauer, U., Moulin, M., Steuerwald, U., Soler-Lopez, M., Baudin, F., Mattaj, I.W., and Muller, C.W. (2004). Architecture of CRM1/Exportin1 suggests how cooperativity is achieved during formation of a nuclear export complex. Molecular cell *16*, 761-775.

Pieczenik, S.R., and Neustadt, J. (2007). Mitochondrial dysfunction and molecular pathways of disease. Experimental and molecular pathology *83*, 84-92.

Plesnila, N., Zhu, C., Culmsee, C., Groger, M., Moskowitz, M.A., and Blomgren, K. (2004). Nuclear translocation of apoptosis-inducing factor after focal cerebral ischemia. J Cereb Blood Flow Metab *24*, 458-466.

Plum, F. (1983). What causes infarction in ischemic brain?: The Robert Wartenberg Lecture. Neurology *33*, 222-233.

Prakriya, M., Feske, S., Gwack, Y., Srikanth, S., Rao, A., and Hogan, P.G. (2006). Orai1 is an essential pore subunit of the CRAC channel. Nature *443*, 230-233.

Raichle, M.E., and Gusnard, D.A. (2002). Appraising the brain's energy budget. Proceedings of the National Academy of Sciences of the United States of America *99*, 10237-10239.

Richter, J.D. (2007). CPEB: a life in translation. Trends in biochemical sciences *32*, 279-285.

Roos, J., DiGregorio, P.J., Yeromin, A.V., Ohlsen, K., Lioudyno, M., Zhang, S., Safrina, O., Kozak, J.A., Wagner, S.L., Cahalan, M.D., et al. (2005). STIM1, an essential and conserved component of store-operated Ca2+ channel function. The Journal of cell biology *169*, 435-445.

Rose, C.R., and Konnerth, A. (2001). Stores not just for storage. intracellular calcium release and synaptic plasticity. Neuron *31*, 519-522.

Rossi, D.J., Oshima, T., and Attwell, D. (2000). Glutamate release in severe brain ischaemia is mainly by reversed uptake. Nature *403*, 316-321.

Salehi-Ashtiani, K., Luptak, A., Litovchick, A., and Szostak, J.W. (2006). A genomewide search for ribozymes reveals an HDV-like sequence in the human CPEB3 gene. Science (New York, N.Y *313*, 1788-1792.

Sattler, R., Xiong, Z., Lu, W.Y., MacDonald, J.F., and Tymianski, M. (2000). Distinct roles of synaptic and extrasynaptic NMDA receptors in excitotoxicity. J Neurosci *20*, 22-33.

Scarpulla, R.C. (2008). Nuclear control of respiratory chain expression by nuclear respiratory factors and PGC-1-related coactivator. Annals of the New York Academy of Sciences *1147*, 321-334.

Schmeing, T.M., and Ramakrishnan, V. (2009). What recent ribosome structures have revealed about the mechanism of translation. Nature *461*, 1234-1242.

Schulman, H. (2004). Activity-dependent regulation of calcium/calmodulin-dependent protein kinase II localization. J Neurosci *24*, 8399-8403.

Sheng, Z.H., and Cai, Q. (2012). Mitochondrial transport in neurons: impact on synaptic homeostasis and neurodegeneration. Nature reviews *13*, 77-93.

Shi, Y., Di Giammartino, D.C., Taylor, D., Sarkeshik, A., Rice, W.J., Yates, J.R., 3rd, Frank, J., and Manley, J.L. (2009). Molecular architecture of the human pre-mRNA 3' processing complex. Molecular cell *33*, 365-376.

Shoubridge, E.A. (2012). Supersizing the mitochondrial respiratory chain. Cell metabolism *15*, 271-272.

Shyu, A.B., and Wilkinson, M.F. (2000). The double lives of shuttling mRNA binding proteins. Cell *102*, 135-138.

Si, K., Giustetto, M., Etkin, A., Hsu, R., Janisiewicz, A.M., Miniaci, M.C., Kim, J.H., Zhu, H., and Kandel, E.R. (2003a). A neuronal isoform of CPEB regulates local protein synthesis and stabilizes synapse-specific long-term facilitation in aplysia. Cell *115*, 893-904.

Si, K., Lindquist, S., and Kandel, E.R. (2003b). A neuronal isoform of the aplysia CPEB has prion-like properties. Cell *115*, 879-891.

Sonenberg, N., and Hinnebusch, A.G. (2007). New modes of translational control in development, behavior, and disease. Molecular cell *28*, 721-729.

Sonenberg, N., and Hinnebusch, A.G. (2009). Regulation of translation initiation in eukaryotes: mechanisms and biological targets. Cell *136*, 731-745.

Stebbins-Boaz, B., Cao, Q., de Moor, C.H., Mendez, R., and Richter, J.D. (1999). Maskin is a CPEB-associated factor that transiently interacts with eIF-4E. Molecular cell *4*, 1017-1027.

Steward, O., Wallace, C.S., Lyford, G.L., and Worley, P.F. (1998). Synaptic activation causes the mRNA for the IEG Arc to localize selectively near activated postsynaptic sites on dendrites. Neuron *21*, 741-751.

Stowers, R.S., Megeath, L.J., Gorska-Andrzejak, J., Meinertzhagen, I.A., and Schwarz, T.L. (2002). Axonal transport of mitochondria to synapses depends on milton, a novel Drosophila protein. Neuron *36*, 1063-1077.

Susin, S.A., Lorenzo, H.K., Zamzami, N., Marzo, I., Snow, B.E., Brothers, G.M., Mangion, J., Jacotot, E., Costantini, P., Loeffler, M., et al. (1999). Molecular characterization of mitochondrial apoptosis-inducing factor. Nature *397*, 441-446.
Svoboda, K., and Mainen, Z.F. (1999). Synaptic [Ca2+]: intracellular stores spill their guts. Neuron *22*, 427-430.

Szymczak, A.L., Workman, C.J., Wang, Y., Vignali, K.M., Dilioglou, S., Vanin, E.F., and Vignali, D.A. (2004). Correction of multi-gene deficiency in vivo using a single 'self-cleaving' 2A peptide-based retroviral vector. Nature biotechnology *22*, 589-594.

Tay, J., and Richter, J.D. (2001). Germ cell differentiation and synaptonemal complex formation are disrupted in CPEB knockout mice. Developmental cell *1*, 201-213.

Theis, M., Si, K., and Kandel, E.R. (2003). Two previously undescribed members of the mouse CPEB family of genes and their inducible expression in the principal cell layers of the hippocampus. Proceedings of the National Academy of Sciences of the United States of America *100*, 9602-9607.

Tymianski, M., Charlton, M.P., Carlen, P.L., and Tator, C.H. (1993a). Source specificity of early calcium neurotoxicity in cultured embryonic spinal neurons. J Neurosci *13*, 2085-2104.

Tymianski, M., Wallace, M.C., Spigelman, I., Uno, M., Carlen, P.L., Tator, C.H., and Charlton, M.P. (1993b). Cell-permeant Ca2+ chelators reduce early excitotoxic and ischemic neuronal injury in vitro and in vivo. Neuron *11*, 221-235.

Udagawa, T., Swanger, S.A., Takeuchi, K., Kim, J.H., Nalavadi, V., Shin, J., Lorenz, L.J., Zukin, R.S., Bassell, G.J., and Richter, J.D. (2012). Bidirectional control of mRNA translation and synaptic plasticity by the cytoplasmic polyadenylation complex. Molecular cell *47*, 253-266.

van Leyen, K., Kim, H.Y., Lee, S.R., Jin, G., Arai, K., and Lo, E.H. (2006). Baicalein and 12/15-lipoxygenase in the ischemic brain. Stroke; a journal of cerebral circulation *37*, 3014-3018.

Van Remmen, H., and Richardson, A. (2001). Oxidative damage to mitochondria and aging. Experimental gerontology *36*, 957-968.

Vander Heiden, M.G., Cantley, L.C., and Thompson, C.B. (2009). Understanding the Warburg effect: the metabolic requirements of cell proliferation. Science (New York, N.Y *324*, 1029-1033.

Wang, C.F., and Huang, Y.S. (2012). Calpain 2 activated through N-methyl-D-aspartic acid receptor signaling cleaves CPEB3 and abrogates CPEB3-repressed translation in neurons. Molecular and cellular biology *32*, 3321-3332.

Watterson, D.M., Mirzoeva, S., Guo, L., Whyte, A., Bourguignon, J.J., Hibert, M., Haiech, J., and Van Eldik, L.J. (2001). Ligand modulation of glial activation: cell permeable, small molecule inhibitors of serine-threonine protein kinases can block induction of interleukin 1 beta and nitric oxide synthase II. Neurochemistry international *39*, 459-468.

Weeber, E.J., Levy, M., Sampson, M.J., Anflous, K., Armstrong, D.L., Brown, S.E., Sweatt, J.D., and Craigen, W.J. (2002). The role of mitochondrial porins and the permeability transition pore in learning and synaptic plasticity. The Journal of biological chemistry *277*, 18891-18897.

Wells, D.G., Dong, X., Quinlan, E.M., Huang, Y.S., Bear, M.F., Richter, J.D., and Fallon, J.R. (2001). A role for the cytoplasmic polyadenylation element in NMDA receptor-regulated mRNA translation in neurons. J Neurosci *21*, 9541-9548.

Wittig, I., Braun, H.P., and Schagger, H. (2006). Blue native PAGE. Nature protocols *1*, 418-428.

Wu, L., Wells, D., Tay, J., Mendis, D., Abbott, M.A., Barnitt, A., Quinlan, E., Heynen, A., Fallon, J.R., and Richter, J.D. (1998). CPEB-mediated cytoplasmic polyadenylation and the regulation of experience-dependent translation of alpha-CaMKII mRNA at synapses. Neuron *21*, 1129-1139.

Zearfoss, N.R., Alarcon, J.M., Trifilieff, P., Kandel, E., and Richter, J.D. (2008). A molecular circuit composed of CPEB-1 and c-Jun controls growth hormone-mediated synaptic plasticity in the mouse hippocampus. J Neurosci *28*, 8502-8509.

Zhang, C., and Wong-Riley, M.T. (2000). Depolarizing stimulation upregulates GA-binding protein in neurons: a transcription factor involved in the bigenomic expression of cytochrome oxidase subunits. The European journal of neuroscience *12*, 1013-1023.

Zhang, S.L., Yu, Y., Roos, J., Kozak, J.A., Deerinck, T.J., Ellisman, M.H., Stauderman, K.A., and Cahalan, M.D. (2005). STIM1 is a Ca2+ sensor that activates CRAC channels and migrates from the Ca2+ store to the plasma membrane. Nature *437*, 902-905.

Zhao, H., Yenari, M.A., Cheng, D., Barreto-Chang, O.L., Sapolsky, R.M., and Steinberg, G.K. (2004). Bcl-2 transfection via herpes simplex virus blocks apoptosis-inducing factor translocation after focal ischemia in the rat. J Cereb Blood Flow Metab *24*, 681-692.

Zhao, J., Hyman, L., and Moore, C. (1999). Formation of mRNA 3' ends in eukaryotes: mechanism, regulation, and interrelationships with other steps in mRNA synthesis. Microbiology and molecular biology reviews : MMBR *63*, 405-445.

Zhu, C., Qiu, L., Wang, X., Hallin, U., Cande, C., Kroemer, G., Hagberg, H., and Blomgren, K. (2003). Involvement of apoptosis-inducing factor in neuronal death

after hypoxia-ischemia in the neonatal rat brain. Journal of neurochemistry *86*, 306-317.

Zuchner, S., Mersiyanova, I.V., Muglia, M., Bissar-Tadmouri, N., Rochelle, J., Dadali, E.L., Zappia, M., Nelis, E., Patitucci, A., Senderek, J., et al. (2004). Mutations in the mitochondrial GTPase mitofusin 2 cause Charcot-Marie-Tooth neuropathy type 2A. Nature genetics *36*, 449-451.